

University of Windsor

Scholarship at UWindor

Electronic Theses and Dissertations

Theses, Dissertations, and Major Papers

1994

A study of the mafic and ultramafic rocks in the Queensborough area, eastern Ontario.

Michael John. Harris
University of Windsor

Follow this and additional works at: <https://scholar.uwindsor.ca/etd>

Recommended Citation

Harris, Michael John., "A study of the mafic and ultramafic rocks in the Queensborough area, eastern Ontario." (1994). *Electronic Theses and Dissertations*. 805.
<https://scholar.uwindsor.ca/etd/805>

This online database contains the full-text of PhD dissertations and Masters' theses of University of Windsor students from 1954 forward. These documents are made available for personal study and research purposes only, in accordance with the Canadian Copyright Act and the Creative Commons license—CC BY-NC-ND (Attribution, Non-Commercial, No Derivative Works). Under this license, works must always be attributed to the copyright holder (original author), cannot be used for any commercial purposes, and may not be altered. Any other use would require the permission of the copyright holder. Students may inquire about withdrawing their dissertation and/or thesis from this database. For additional inquiries, please contact the repository administrator via email (scholarship@uwindsor.ca) or by telephone at 519-253-3000ext. 3208.



National Library
of Canada

Acquisitions and
Bibliographic Services Branch

395 Wellington Street
Ottawa, Ontario
K1A 0N4

Bibliothèque nationale
du Canada

Direction des acquisitions et
des services bibliographiques

395, rue Wellington
Ottawa (Ontario)
K1A 0N4

Your file - Votre référence

Our file - Notre référence

NOTICE

The quality of this microform is heavily dependent upon the quality of the original thesis submitted for microfilming. Every effort has been made to ensure the highest quality of reproduction possible.

If pages are missing, contact the university which granted the degree.

Some pages may have indistinct print especially if the original pages were typed with a poor typewriter ribbon or if the university sent us an inferior photocopy.

Reproduction in full or in part of this microform is governed by the Canadian Copyright Act, R.S.C. 1970, c. C-30, and subsequent amendments.

AVIS

La qualité de cette microforme dépend grandement de la qualité de la thèse soumise au microfilmage. Nous avons tout fait pour assurer une qualité supérieure de reproduction.

S'il manque des pages, veuillez communiquer avec l'université qui a conféré le grade.

La qualité d'impression de certaines pages peut laisser à désirer, surtout si les pages originales ont été dactylographiées à l'aide d'un ruban usé ou si l'université nous a fait parvenir une photocopie de qualité inférieure.

La reproduction, même partielle, de cette microforme est soumise à la Loi canadienne sur le droit d'auteur, SRC 1970, c. C-30, et ses amendements subséquents.

Canada

**A STUDY OF THE MAFIC AND ULTRAMAFIC ROCKS
IN THE QUEENSBOROUGH AREA, EASTERN ONTARIO**

by

Michael John Harris

**A thesis submitted to the
Faculty of Graduate Studies and Research
through the Department of Geology
in partial fulfilment of the requirements for
the Degree of Master of Science at the
University of Windsor**

Windsor, Ontario, Canada

1994

© 1994 Michael John Harris



National Library
of Canada

Acquisitions and
Bibliographic Services Branch

395 Wellington Street
Ottawa, Ontario
K1A 0N4

Bibliothèque nationale
du Canada

Direction des acquisitions et
des services bibliographiques

395, rue Wellington
Ottawa (Ontario)
K1A 0N4

Your file Votre référence

Our file Notre référence

THE AUTHOR HAS GRANTED AN
IRREVOCABLE NON-EXCLUSIVE
LICENCE ALLOWING THE NATIONAL
LIBRARY OF CANADA TO
REPRODUCE, LOAN, DISTRIBUTE OR
SELL COPIES OF HIS/HER THESIS BY
ANY MEANS AND IN ANY FORM OR
FORMAT, MAKING THIS THESIS
AVAILABLE TO INTERESTED
PERSONS.

L'AUTEUR A ACCORDE UNE LICENCE
IRREVOCABLE ET NON EXCLUSIVE
PERMETTANT A LA BIBLIOTHEQUE
NATIONALE DU CANADA DE
REPRODUIRE, PRETER, DISTRIBUER
OU VENDRE DES COPIES DE SA
THESE DE QUELQUE MANIERE ET
SOUS QUELQUE FORME QUE CE SOIT
POUR METTRE DES EXEMPLAIRES DE
CETTE THESE A LA DISPOSITION DES
PERSONNE INTERESSEES.

THE AUTHOR RETAINS OWNERSHIP
OF THE COPYRIGHT IN HIS/HER
THESIS. NEITHER THE THESIS NOR
SUBSTANTIAL EXTRACTS FROM IT
MAY BE PRINTED OR OTHERWISE
REPRODUCED WITHOUT HIS/HER
PERMISSION.

L'AUTEUR CONSERVE LA PROPRIETE
DU DROIT D'AUTEUR QUI PROTEGE
SA THESE. NI LA THESE NI DES
EXTRAITS SUBSTANTIELS DE CELLE-
CI NE DOIVENT ETRE IMPRIMES OU
AUTREMENT REPRODUITS SANS SON
AUTORISATION.

ISBN 0-612-01403-7

Canada

Name MICHAEL JOHN HARRIS

Dissertation Abstracts International is arranged by broad, general subject categories. Please select the one subject which most nearly describes the content of your dissertation. Enter the corresponding four-digit code in the spaces provided.

GEOLOGY

SUBJECT TERM

0372 U·M·I
SUBJECT CODE

Subject Categories

THE HUMANITIES AND SOCIAL SCIENCES

COMMUNICATIONS AND THE ARTS
Architecture 0729
Art History 0377
Cinema 0900
Dance 0378
Fine Arts 0357
Information Science 0723
Journalism 0391
Library Science 0399
Mass Communications 0708
Music 0413
Speech Communication 0459
Theater 0465

EDUCATION
General 0515
Administration 0514
Adult and Continuing 0516
Agricultural 0517
Art 0273
Bilingual and Multicultural 0282
Business 0688
Community College 0275
Curriculum and Instruction 0727
Early Childhood 0518
Elementary 0524
Finance 0277
Guidance and Counseling 0519
Health 0680
Higher 0745
History of 0520
Home Economics 0278
Industrial 0521
Language and Literature 0279
Mathematics 0280
Music 0522
Philosophy of 0998
Physical 0523

Psychology 0525
Reading 0535
Religious 0527
Sciences 0714
Secondary 0533
Social Sciences 0534
Sociology of 0340
Special 0529
Teacher Training 0530
Technology 0710
Tests and Measurements 0288
Vocational 0747

LANGUAGE, LITERATURE AND LINGUISTICS

Language 0679
Ancient 0289
Linguistics 0290
Modern 0291
Literature 0401
General 0294
Classical 0295
Comparative 0297
Medieval 0298
Modern 0316
African 0591
American 0305
Asian 0352
Canadian (English) 0355
Canadian (French) 0593
English 0311
Germanic 0312
Latin American 0315
Middle Eastern 0313
Romance 0314
Slavic and East European

PHILOSOPHY, RELIGION AND THEOLOGY

Philosophy 0422
Religion 0318
General 0321
Biblical Studies 0319
Clergy 0320
History of 0322
Philosophy of 0469
Theology 0323

SOCIAL SCIENCES

American Studies 0323
Anthropology 0324
Archaeology 0326
Cultural 0327
Physical 0310
Business Administration 0272
General 0770
Accounting 0454
Banking 0338
Management 0385
Marketing 0501
Canadian Studies 0503
Economics 0505
General 0508
Agricultural 0509
Commerce-Business 0510
Finance 0511
History 0358
Labor 0366
Theory 0351
Folklore 0578
Geography 0366
Gerontology 0351
History 0578

Ancient 0579
Medieval 0581
Modern 0582
Black 0328
African 0331
Asia, Australia and Oceania 0332
Canadian 0334
European 0335
Latin American 0336
Middle Eastern 0337
United States 0585
History of Science 0398
Law 0615
Political Science 0616
General 0617
International Law and Relations 0814
Public Administration 0452
Recreation 0626
Social Work 0627
Sociology 0938
General 0631
Criminology and Penology 0628
Demography 0629
Ethnic and Racial Studies 0630
Individual and Family Studies 0700
Industrial and Labor Relations 0344
Public and Social Welfare 0709
Social Structure and Development 0999
Theory and Methods 0453
Transportation 0453
Urban and Regional Planning 0453
Women's Studies

THE SCIENCES AND ENGINEERING

BIOLOGICAL SCIENCES

Agriculture 0473
General 0285
Agronomy 0475
Animal Culture and Nutrition 0476
Animal Pathology 0359
Food Science and Technology 0478
Forestry and Wildlife 0479
Plant Culture 0480
Plant Pathology 0817
Plant Physiology 0777
Range Management 0746
Wood Technology 0306
Biology 0287
General 0308
Anatomy 0309
Biostatistics 0379
Botany 0329
Cell 0353
Ecology 0369
Entomology 0793
Genetics 0410
Limnology 0307
Microbiology 0317
Molecular 0416
Neuroscience 0433
Oceanography 0821
Physiology 0778
Radiation 0472
Veterinary Science 0786
Zoology 0760
Biophysics 0786
General 0760
Medical

EARTH SCIENCES

Biogeochemistry 0425
Geochemistry 0996

Geodesy 0370
Geology 0372
Geophysics 0373
Hydrology 0388
Mineralogy 0411
Paleobotany 0345
Paleoecology 0426
Paleontology 0418
Paleozoology 0985
Palynology 0427
Physical Geography 0368
Physical Oceanography 0415

HEALTH AND ENVIRONMENTAL SCIENCES

Environmental Sciences 0768
Health Sciences 0566
General 0300
Audiology 0992
Chemotherapy 0567
Dentistry 0350
Education 0769
Hospital Management 0758
Human Development 0982
Immunology 0564
Medicine and Surgery 0347
Mental Health 0569
Nursing 0570
Obstetrics and Gynecology 0380
Occupational Health and Therapy 0354
Ophthalmology 0381
Pathology 0571
Pharmacology 0419
Pharmacy 0572
Physical Therapy 0382
Public Health 0573
Radiology 0574
Recreation 0575

Speech Pathology 0460
Toxicology 0383
Home Economics 0386

PHYSICAL SCIENCES

Pure Sciences
Chemistry 0485
General 0749
Agricultural 0486
Analytical 0487
Biochemistry 0488
Inorganic 0738
Nuclear 0490
Organic 0491
Pharmaceutical 0494
Physical 0495
Polymer 0754
Radiation 0405
Mathematics 0605
Physics 0986
General 0606
Acoustics 0608
Astronomy and Astrophysics 0748
Atmospheric Science 0607
Atomic 0798
Electronics and Electricity 0759
Elementary Particles and High Energy 0609
Fluid and Plasma 0610
Molecular 0752
Nuclear 0756
Optics 0611
Radiation 0463
Solid State 0346
Statistics 0984

Applied Sciences

Applied Mechanics 0346
Computer Science 0984

Engineering
General 0537
Aerospace 0538
Agricultural 0539
Automotive 0540
Biomedical 0541
Chemical 0542
Civil 0543
Electronics and Electrical 0544
Heat and Thermodynamics 0348
Hydraulic 0545
Industrial 0546
Marine 0547
Materials Science 0794
Mechanical 0548
Metallurgy 0743
Mining 0551
Nuclear 0552
Packaging 0549
Petroleum 0765
Sanitary and Municipal 0554
System Science 0790
Geotechnology 0428
Operations Research 0796
Plastics Technology 0795
Textile Technology 0994

PSYCHOLOGY

General 0621
Behavioral 0384
Clinical 0622
Developmental 0620
Experimental 0623
Industrial 0624
Personality 0625
Physiological 0989
Psychobiology 0349
Psychometrics 0632
Social 0451



Abstract

The amphibolite-ultramafic belt in the southern Grimsthorpe Domain, eastern Ontario, is interpreted to be part of a Mesoproterozoic ophiolite sequence, herein named the Queensborough Ophiolite Complex. The Queensborough Ophiolite Complex is bounded to the east by the intrusive contact of the Elzevir Tonalite Batholith, to the west by the Queensborough Fault Zone (new name proposed herein) and to the south by the Moira Lake Fault Zone. The rock succession comprises up to 800 m thick of ultramafic rocks consisting of assemblages of serpentine, talc, chlorite, carbonate, anthophyllite, and actinolite/tremolite. Structurally overlying (up dip of) the ultramafic rocks is a belt of amphibolite rocks at least three kilometres thick, and consists mostly of meta-gabbros with very minor mafic meta-volcanics and unsystematically distributed mafic dykes. The meta-volcanics are fine-grained, massive actinolite-plagioclase rocks, and may show pillow structures. The meta-gabbros are coarse- to medium-grained, massive to sheared rocks, and comprise mostly of actinolite/tremolite and plagioclase. The mafic dykes are fine- to coarse-grained, actinolite-plagioclase rocks, generally having biotite in their mineralogy. The dykes have two distinct textures; a massive to lineated texture, or a feather-amphibolite texture. Most samples were chemically analyzed either by standard X-Ray Fluorescence techniques, or standard Inductively Coupled Plasma - Mass Spectrometry techniques. Chemically, the mafic rocks of the Queensborough Ophiolite Complex show fractional crystallization patterns indicative of olivine, plagioclase, orthopyroxene and clinopyroxene. The nearby presence of the large Elzevir Tonalite batholith suggest the Queensborough Complex was formed in a back-arc basin. The lack of any subduction component in the meta-volcanic chemistry suggests the basin was associated with a young subduction zone. The Queensborough Ophiolite Complex can be compared to the more modern Eastern Papua Ophiolite Complex and the Yakuno Ophiolite on the basis of rock succession and chemistry. The geologic interpretations of the Belmont and Grimsthorpe Domains are modelled to have a similar tectonic evolution as the Tyrrhenian Sea.

Acknowledgements

I am very grateful for the extensive amount of time and patience Dr. T.E. Smith spent on this project. His overall knowledge, and interest in furthering studies in eastern Ontario made this an extremely gratifying project.

The Ontario Geological Survey, and specifically Drs. G. DiPrisco and R.M. Easton supplied some of the data through projects which I was involved with. Their information on the Grimsthorpe Domain is invaluable.

Antun Knitl and Ingrid Churchill are thanked for their time and expertise in the petrographic and geochemistry labs.

And to all others who have made this project possible, I extend my gratitude, thank you.

TABLE OF CONTENTS

Approval Page	ii
Abstract	iii
Acknowledgements	iv
Table of Contents	v
List of Figures	vii
List of Tables	ix
List of Abbreviations	x
Chapter 1 - Introduction	
1.1 - Regional Geology	1
1.2 - Tectonics of the Central Metasedimentary Belt	5
1.3 - Objectives	9
Chapter 2 - Previous Work	
2.1 - Geology of the Central Metasedimentary Belt	10
2.2 - Previous Geologic Interpretations of the Queensborough Area	19
Chapter 3 - Field Relations and Petrography	
3.1 - Boundaries of the southern part of the Grimsthorpe Domain	24
3.2 - General Geology of the southern Grimsthorpe Domain	28
3.3 - Petrography	30
3.4 - Mafic Meta-volcanic Suite	30
3.5 - Meta-gabbro Suite	34
3.6 - Ultramafic Suite	38
3.7 - Chlorite Schists	45
3.8 - Mafic Dykes	46
3.9 - Felsic Dykes	49
3.10 - Metasediments	50
3.11 - New Geologic Interpretations of the Queensborough Area	52

Chapter 4 - Geochemistry	
4.1 - Introduction	60
4.2 - Chemical Alteration	60
4.3 - Major Element Data	71
4.4 - Trace Element Data	77
4.5 - Petrogenesis	83
4.6 - Summary of Chemistry	87
Chapter 5 - Discussion and Conclusions	
5.1 - The Queensborough Ophiolite Complex	89
5.2 - Tectonic Models	94
5.3 - Conclusions	98
References	100
Appendix A - Sample Locations and Rock Types	107
Appendix B - Modal Mineralogy	112
Appendix C - Major and Trace Element Geochemistry	123
Vita Auctoris	134

List of Figures

Figure 1 - Location of the study area	2
Figure 2 - Subdivisions of the Grenville Province	2
Figure 3 - Subdivisions of the Grenville Province in Ontario	3
Figure 4 - Subdivisions of the Central Metasedimentary Belt in Ontario	6
Figure 5 - Local geology of the Queensborough area	20
Figure 6 - Major structural features of the Queensborough area	25
Figure 7 - Sampling locations of the Queensborough area	31
Figure 8 - Cross-section of an idealized ophiolite sequence	57
Figure 9 - Log molecular proportion plots with K_2O	63
Figure 10 - Log molecular proportion plots with Na_2O	66
Figure 11 - Molecular proportion plots for ultramafic samples	69
Figure 12 - Major element variation diagrams versus MgO	72
Figure 13 - Jensen cation plot for meta-volcanic samples	74
Figure 14 - Trace element variation diagrams versus MgO	78
Figure 15 - TiO_2 vs. Zr and Y vs. Zr plots	82
Figure 16 - MgO-FeO sail diagram of Hanson and Langmuir	84

Figure 17 - Nb-Zr, TiO ₂ -Zr and Y-Zr plots for mineral fractionation trends	86
Figure 18 - Cr-Y and Cr-TiO ₂ plots to discriminate between MORB and back-arc ophiolites	92
Figure 19 - Multi-element plots of Saunders and Tarney	93
Figure 20 - Cross-section of the Tyrrhenian Sea	97

List of Tables

Table 1 - Summary of the main characteristics of the terranes and domains of the Central Metasedimentary Belt	12
Table 2 - Summary of the characteristic features of the plutonic suites of the Central Metasedimentary Belt	14
Table 3 - Principle features of peridotite-gabbro complexes	53
Table 4 - Average trace element ratios for selective volcanics and dykes from the Belmont Domain and the mafic dykes of the Queensborough Complex	81
Table 5 - Average chemistry of peridotites from the Tyrrhenian Sea and ultramafics of the Queensborough Complex	96

List of Abbreviations

cm	centimetres
CS	chlorite schists
FD	felsic dykes
Ga	billion years ago
HCl	hydrochloric acid
km	kilometres
m	metres
Ma	million years ago
MB	marbles
MD	mafic dykes
MG	meta-gabbros
mm	millimetres
MOR	mid-ocean ridge
MORB	mid-ocean ridge basalts
MS	meta-sediments
MV	meta-volcanics
ppm	parts per million
SSZ	supra-subduction zone
UM	ultramafics
UTM	Universal Transverse Mercator (Grid)
wt. %	weight percent

Chapter 1 - Introduction

This study was carried out in the Queensborough area which lies in eastern Ontario, approximately 170 km southwest of Ottawa and 180 km northeast of Toronto (Figure 1). The village of Queensborough is situated in the center of the area, at 44°36'N and 77°25'W. The field area encompasses approximately 220 km², of which about 20% is rock outcrop. The study is aimed at describing the geology and stratigraphy of the area and evaluating its tectonic significance within the Central Metasedimentary Belt (Figure 2).

1.1 - Regional Geology

The Queensborough area lies geologically within the Grenville Province, a large complex orogenic province that is divided into belts, terranes and domains. The Grenville Province records the tectonic evolution of the southeastern margin of Laurentia during the Mesoproterozoic [Easton, 1992]. In Ontario, the Grenville Province can be subdivided into two major divisions [Wynne-Edwards, 1972]; the Central Gneiss Belt and the Central Metasedimentary Belt (Figure 3). The Central Gneiss Belt is separated from the Paleoproterozoic and Archean rocks to the northwest by the Grenville Front. The Central Gneiss Belt and the Central Metasedimentary Belt are separated by the Central Metasedimentary Belt Boundary Zone, which is defined by a major shear zone trending northeast (Figure 3).

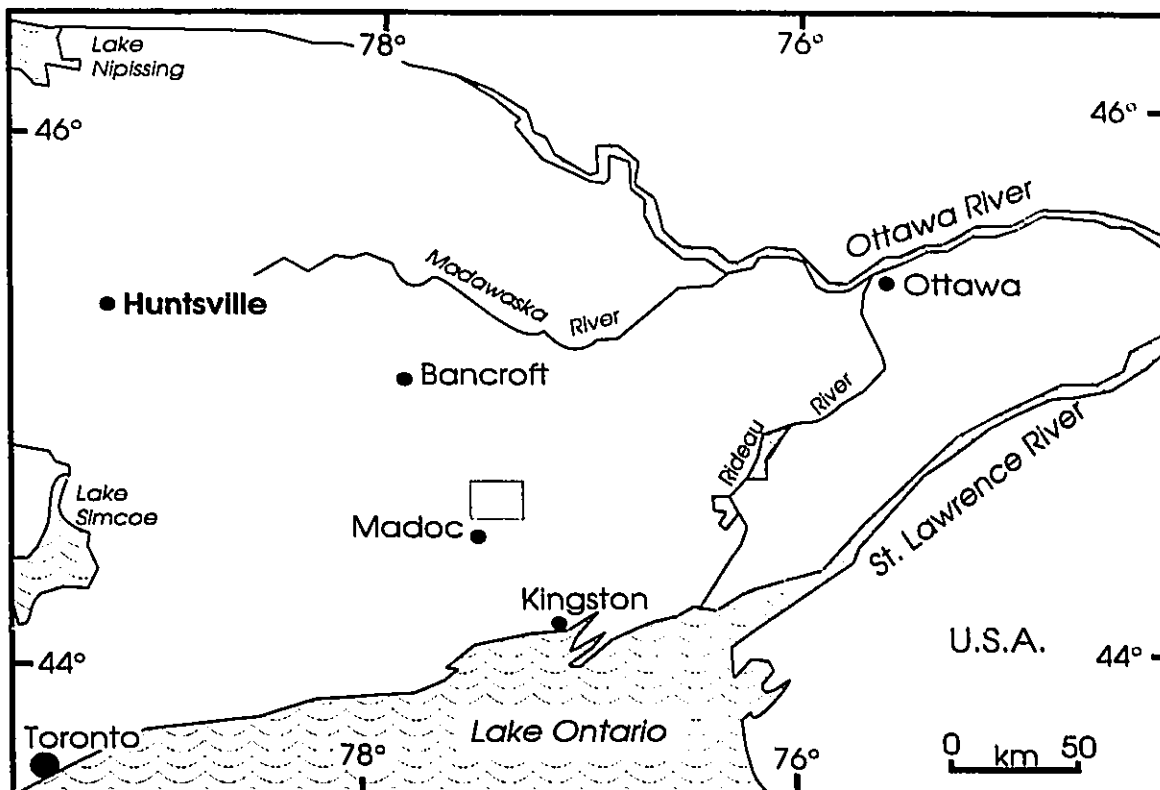


Figure 1 - Location of the Queensborough area, in eastern Ontario (shaded box northeast of Madoc) [after Meen, 1944].

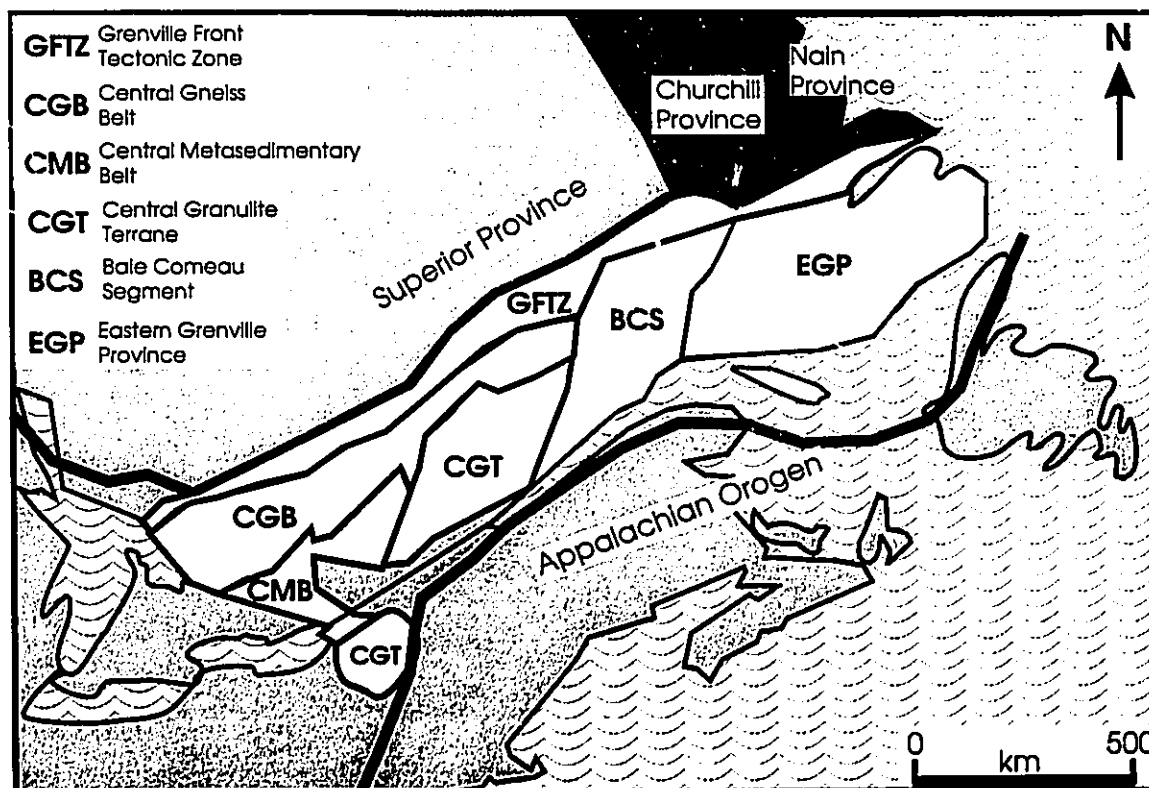


Figure 2 - The subdivisions of the Grenville Province. Boundaries are according to Wynne-Edwards [1972; after Moore, 1986].

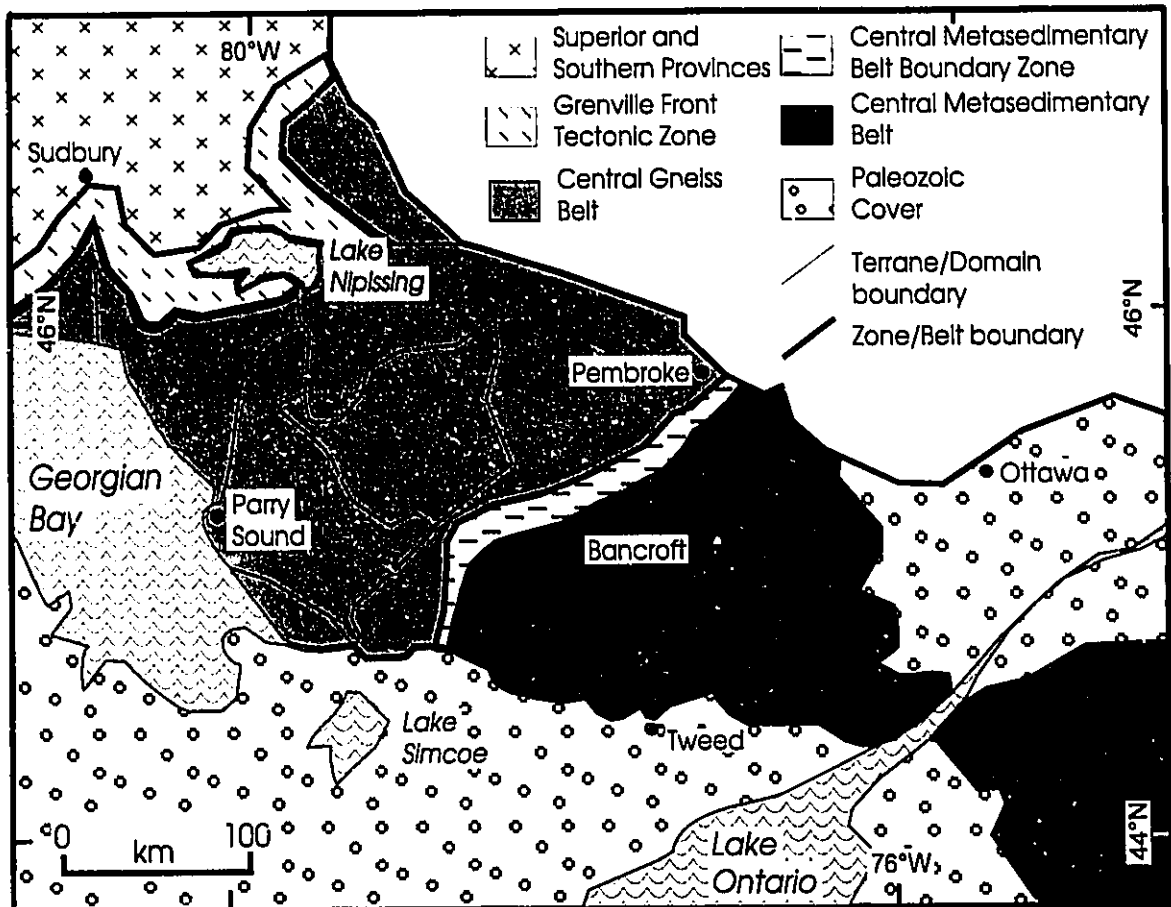


Figure 3 - Lithotectonic terranes and domains of the Grenville Province, Ontario [after Easton, 1992].

The Grenville Front [Derry, 1950] and the Grenville Front Tectonic Zone, which includes the Grenville Front Boundary Fault, extends for approximately 20 to 30 km east of the older Superior, Penokean and Southern Provinces (Figures 2 and 3), which are northwest of the Central Gneiss Belt. The Grenville Front Boundary Fault is a major shear zone several kilometres wide marked by northeast trending mylonites, with moderate to shallow, southeasterly dipping tectonic layering and southeasterly plunging mineral lineations. The Central Gneiss Belt (Figures 2 and 3), consists mainly of upper amphibolite- and local granulite-facies, quartzo-feldspathic orthogneisses with subordinate paragneiss. The dominant structural trend is northeast, however, northwest trends occur along Georgian Bay [Easton, 1992]. The Central Gneiss Belt consists of a variety of Archean to Mesoproterozoic crustal segments, all of which have been affected by the "Grenville Orogeny" [Easton, 1986]. Several distinctive lithotectonic terranes¹, some further subdivided into domains², have been identified within the Central Gneiss Belt [Culshaw *et al.* 1983; Davidson, 1986] (Figure 3).

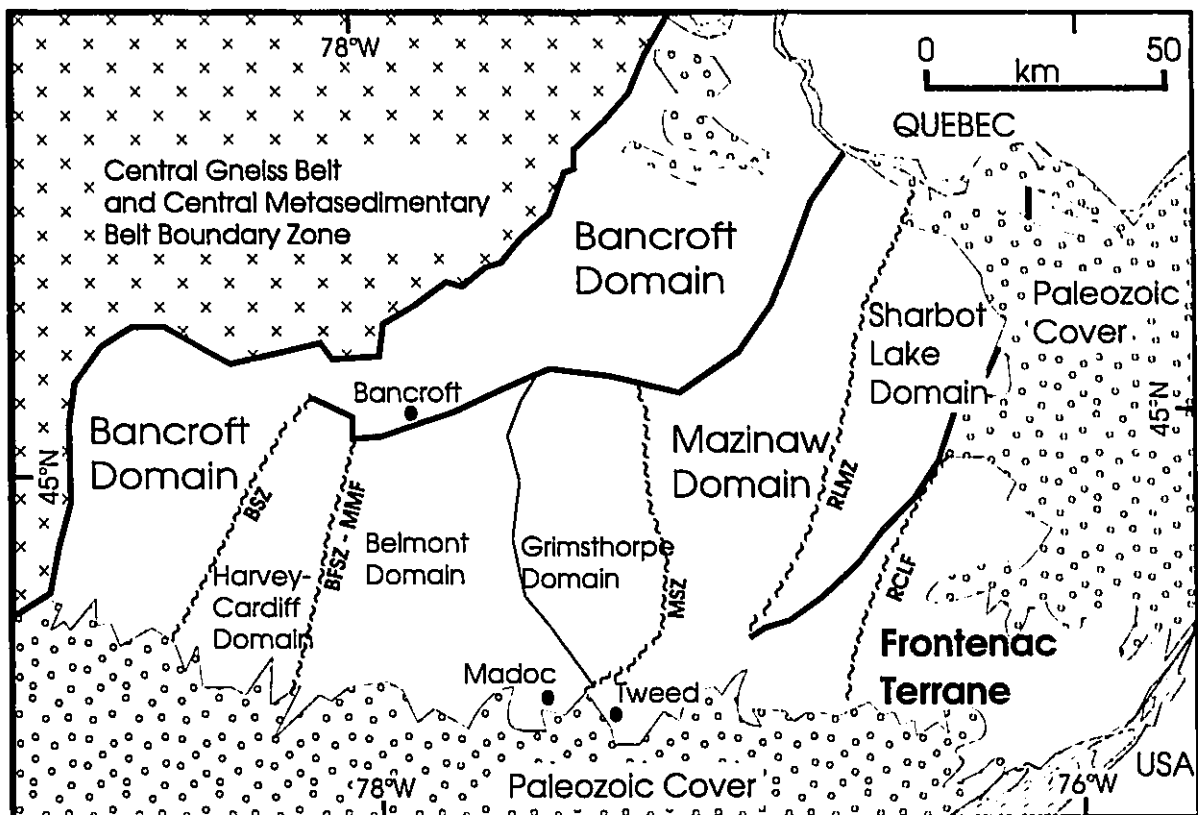
¹ A **terrane** is a fault-bounded package of strata that is allochthonous to, and has a geological history distinct from the adjacent geologic units. [Williams *et al.* 1992]

² A **domain** is a lithotectonic region distinguished from another by differences in rock assemblages, internal structures, metamorphic grade and geophysical signatures. (Davidson, 1986)

The Central Metasedimentary Belt Boundary Zone [Davidson *et al.* 1982, 1984; Hanmer, 1988] is a north to northeast trending zone of cataclastic and tectonically disrupted quartzo-feldspathic gneisses that separates the Central Gneiss Belt from the Central Metasedimentary Belt (Figure 3). The Central Metasedimentary Belt (Figures 2 and 3) represents a major Mesoproterozoic accumulation of marble, volcanic rocks and clastic metasedimentary rocks. These supracrustal rocks have been intruded by compositionally diverse, syntectonic, late tectonic and post-tectonic plutonic rocks; and the entire succession has been metamorphosed at grades varying from greenschist to granulite facies. The Central Metasedimentary Belt is divided into two terranes; the BEMS terrane (informal name) and the Frontenac Terrane. The BEMS terrane is further subdivided into the Bancroft, Harvey-Cardiff, Belmont, Grimsthorpe, Mazinaw and Sharbot Lake domains.

1.2 - Tectonics of the Central Metasedimentary Belt

The early development of the Central Metasedimentary Belt is difficult to establish. It is known that volcanic assemblages of 1300 to 1280 Ma exist in the Belmont and Grimsthorpe Domains (eg. the Tudor Formation), and that these volcanic rocks were intruded by 1270 Ma tonalites (eg. the Elzevir Tonalite) [Easton, 1992]. A younger (1260 to 1250 Ma) mafic-felsic volcanic assemblage and siliceous clastic and carbonate supracrustal



BSZ - Bancroft Shear Zone RLMZ - Robertson Lake Mylonite Zone
 MSZ - Mooroton Shear Zone RCLF - Rideau-Canoe Lake Fault
 BFSZ - MMF - Burleigh Falls Shear Zone - McArthurs Mills Fault

Figure 4 - Lithotectonic terranes and domains of the Central Metasedimentary Belt, in Ontario [after Easton, 1992].

assemblage overlies the older volcanic assemblage. This assemblage is also present in the Bancroft, Mazinaw and Sharbot Lake Domains [Easton, 1992], indicating that a 'superterrane' was present at that time. The presence of nepheline syenite, anorthosite, tonalite, and granite plutons within the four domains is further evidence of the amalgamation of the domains by 1250 to 1240 Ma. Disagreement exists, as to the tectonic conditions that were present at that time, specifically; was the Belmont and Grimsthorpe Domains orogenic or anorogenic? Furthermore, does oceanic crust exist, does an island arc (or arcs) exist, and if so where are they, and what about the possible existence of a back-arc basin and related arc sutures. There are four main plate tectonic models that are presently in use for this area of the Central Metasedimentary Belt.

The island arc model of Brown *et al.* [1975], is based upon four main points: a) relict oceanic lithosphere is preserved (Kaladar Complex in the terrain northeast of Madoc, Ontario); b) granitic to dioritic batholiths were intruded into the oceanic crustal material; c) platformal sediments were deposited unconformably over oceanic crust; and d) the basement and cover then became involved in intense regional deformation and metamorphism. Although some of the original data is now disputed (eg. the Kaladar Complex southwest of Flinton, is no longer thought to be an ophiolite [Easton, 1992]), the theory is still invoked.

The second approach uses the geochemistry of the metavolcanic suites in the Belmont Domain to suggest that the volcanic rocks were emplaced in association with rifting of continental crust. The rifting may be related to a back-arc environment, or may be the result of attenuated continental crust associated with development of a continental margin arc. [Condie and Moore, 1977; Bartlett, 1983; Holm *et al.* 1986; Smith and Holm, 1987, 1990a, 1990b].

Condie [1982] pointed out that the Central Metasedimentary Belt is similar in many respects to Archean greenstone belts and may therefore have a similar origin. He argued that Archean greenstone belts and comparable Proterozoic belts were formed in cratonic rifts produced by upwelling asthenosphere or mantle plumes, and that they are not associated with convergent plate boundaries.

Lumbers *et al.* [1990] noted that the voluminous, mantle-derived tholeiitic basalts of the Hastings sequence and the closely associated calc-alkalic magmatism are also typical features of Archean greenstone belts, agreeing with Condie [1982]. Lumbers *et al.* [1990] suggests that the Central Metasedimentary Belt may have formed within a rift developed by necking of the lithosphere in response to asthenospheric motions or by thinning of the lithosphere over a mantle plume. These authors were more specific than Condie, placing the Grenville Orogeny at 1240-1180 Ma, with

extension-related plutonism at 1090 Ma followed by a pegmatitic tectonothermal event at 1070-1020 Ma.

1.3 - Objectives

Field descriptions and reconnaissance mapping, petrography, and geochemistry are used to establish the stratigraphic sequence and local tectonic regime of the Queensborough area. In addition, the significance of the geology of the Grimsthorpe Domain with respect to the geologic history of the Central Metasedimentary Belt will be discussed.

Chapter 2 - Previous Work

2.1 - Geology of the Central Metasedimentary Belt

The Central Metasedimentary Belt of Ontario has previously been divided into five terranes. With recent geologic work in the area, and changes in the terminology and definitions, the Central Metasedimentary Belt is now considered to comprise two terranes; the BEMS terrane (informal name) and the Frontenac Terrane.

The BEMS terrane consists of six domains; the Bancroft, Mazinaw and Sharbot Lake that extend northwards into Quebec; and the Harvey-Cardiff, Belmont and Grimsthorpe, which with Bancroft and Mazinaw, are overlain by Paleozoic strata to the south (Figure 4). The Bancroft Domain lies east and south of the Central Gneiss Belt and the Central Metasedimentary Belt Boundary Zone. The Harvey-Cardiff Domain lies south and east of the Bancroft Domain. The Belmont Domain lies east of Harvey-Cardiff and south of Bancroft. The Grimsthorpe Domain lies east of Belmont, and south of Bancroft. The Mazinaw Domain lies east of the Grimsthorpe and Bancroft Domains. The Sharbot Lake Domain lies east and north of the Mazinaw Domain. The Frontenac Terrane lies east of the Mazinaw and Sharbot Lake Domains, and extends westward into New York, U.S.A., where it is called the Adirondack Lowlands (Figure 4).

The two terranes are distinguished from one another by differences in rock types and/or geologic and structural histories, and are separated by

faults or shear zones (see footnotes on page 4). The geological history of each of these terranes is very complex. Table 1 summarizes the rock types, chemical suites, age of volcanism and/or sedimentation, metamorphic conditions and potential basement of the terranes and domains.

The Bancroft Domain boundary with the Central Metasedimentary Belt Boundary Zone is taken as the northern and western limits of the major marble belts found in the Bancroft Domain [Easton, 1992]. The boundary between the Bancroft and Harvey-Cardiff Domains is along the Bancroft Shear Zone [Carlson *et al.* 1990], and is defined by a thin zone of marble mylonites. Further north, between the Bancroft and Mazinaw Domains, the northern lithologic boundary of the Abinger Granite of the Mazinaw Domain separates the abundant thin sheets of metaplutonic rocks (probable thrust nappes; [Easton, 1992]) of the Bancroft Domain from the more typical elongate pluton patterns of the Mazinaw Domain, and thus is the boundary contact [Easton, 1992]. The Harvey-Cardiff Domain is separated from the Belmont Domain by the Burleigh Fault in the south, and the McArthurs Mills shear zone to the north [Easton, 1992]. The Belmont Domain is separated from the Grimsthorpe Domain by the Queensborough Fault Zone (see section 3-1). The boundary between the Grimsthorpe and Mazinaw Domains is along the Mooroton Shear Zone, a zone of straight gneisses 150 m wide, trending north-south along the Skootamatta River [Easton, 1990]. The eastern boundary of the Mazinaw Domain with the Sharbot Lake

Table 1 - Summary of the main characteristics of the terranes and domains of the Central Metasedimentary Belt [after Easton, 1992].

Name	Major Supracrustal Rock Types	Volcanic Geochemical Affinities
Bancroft Domain	calcite and dolomite marbles, quartz arenite, quartzofeldspathic gneiss, minor para-amphibolite	volcaniclastic rocks only, alkali basalt and calc-alkalic
Harvey-Cardiff Domain	mafic and felsic metavolcanic rocks, metawackes, metapelite, turbidites, calcite and dolomite marbles	bimodal tholeiitic basalt-dacite-rhyolite
Belmont Domain	mafic, intermediate, and felsic metavolcanic and volcaniclastic rocks, siliceous clastic rocks, deep and shallow water calcite and dolomite marbles containing stromatolites	80% bimodal tholeiitic basalt-dacite-rhyolite, minor calc-alkalic andesite, andesite-rhyolite
Grimsthorpe Domain	mafic metavolcanic and volcaniclastic rocks	tholeiitic
Mazinaw Domain	mafic, intermediate and felsic metavolcanic and volcaniclastic rocks, siliceous clastic rocks, deep and shallow water calcite and dolomite marbles containing stromatolites, unconformably overlain by conglomerate, arenite, pelite, schist and marbles	calc-alkalic andesite-rhyolite, minor tholeiitic basalt
Sharbot Lake Domain	mafic volcanic rocks, minor volcaniclastic and siliceous clastic rocks, dominantly calcite and dolomite marbles, stromatolites	tholeiitic
Frontenac Terrane	paragneiss, quartzofeldspathic gneiss, calcite and dolomite marbles, quartz arenite	no volcanic rocks present

Age of Volcanism and/or Sedimentation	Major Plutonic Suites Present * see Table 2	Metamorphic Conditions	Potential Basement
> 1400 Ma < 1250 Ma	Dysart, nepheline syenite, Killer Creek, Elzevir, Lavant, Methuen, Skootamatta, fenite- carbonatite-granite pegmatite	middle to upper amphibolite-facies	tonalitic, ca. 1350 Ma or older
> 1300 Ma < 1250 Ma	Elzevir, Methuen, fenite- carbonatite-granite pegmatite	middle to upper amphibolite facies	unknown
> 1300 Ma < 1260 Ma	nepheline syenite, Elzevir, Lavant, Methuen, Skootamatta	upper greenschist to lower amphibolite facies	unknown
> 1350 Ma < 1250 Ma	Killer Creek, Elzevir, Skootamatta	upper greenschist to lower amphibolite facies	gabbroic <1290 Ma, represented by the Canniff Complex
> 1300 Ma < 1250 Ma unconformity 1150 Ma sed.	anorthosite, Killer Creek, Elzevir, Methuen, granite pegmatite	lower to upper amphibolite facies	Grimsthorpe domain-type basement to supracrustal rocks
> 1300 Ma < 1250 Ma	Lavant, Methuen, Skootamatta?	lower greenschist to middle amphibolite facies	unknown
> 1800 Ma < 1180 Ma	anorthosite, Gananoque, Skootamatta, granite pegmatite	granulite facies	> 1400 Ma, possibly as old as 1800 Ma granitic to grano-dioritic

Table 2 - Summary of plutonic suites in the Central Metasedimentary Belt (after Easton, 1992).

Rock Suite and Age Range (Ma)	Rock Types
Fenite-carbonatite-granite pegmatite 1070 - 1040	"fenite" or "skarn" assemblages, calcite apatite veins, carbonatite, pegmatitic granite, granitic pegmatite
Skootamatta Suite monzonite-diorite 1090 - 1075	potassic monzonite and syenite, biotite diorite, minor granite, nepheline-normative monzodiorite, peridotite, lamprophyre
Gananoque Suite syenite-monzonite 1180 - 1160	potassic syenite and monzonite, minor syeno-granite, monzogranite, biotite diorite, gabbro
Methuen Suite alaskite 1250 - 1240	alaskite, minor alkalic feldspar syenite-albite granite, syenogranite, aplite
Lavant Suite diorite-gabbro 1250 - 1240	diorite, gabbro, minor quartz diorite, tonalite, granodiorite, albite syenite and granite, pyroxenite
Elzevir Suite tonalite 1280 - 1270	tonalite, granodiorite, trondhjemite, minor diorite, albite granite
Killer Creek Suite gabbro 1300 - 1275	gabbro, melanocratic gabbro, anorthositic gabbro, hornblendite, minor anorthosite
Canniff Complex gabbro < 1290	protomylonitic gabbro and gabbroic mylonite altered to talc, serpentine, carbonate assemblages
anorthosite 1280 - 1250	oligoclase to labradorite anorthosite, minor gabbro, diorite, tonalite, quartz syenite, syenite
nepheline syenite 1280 - 1250	nepheline syenite, urtite, malignite, nepheline-normative diorite and gabbro, albite syenite, nepheline diorite, gabbro
Dysart Suite early tonalite 1370 - 1340	tonalite, trondhjemite, granodiorite

Domain is along the Robertson Lake Mylonite Zone, a thin zone of mylonites which have been traced for over 90 km. These mylonites represent a low-angle thrust fault, along which the Sharbot Lake Domain has been thrust westward over the Mazinaw Domain [Easton, 1988a, 1988b]. Only the western boundary of the Frontenac Terrane with the Mazinaw and Sharbot Lake Domains is seen in Ontario. The boundary is along the Rideau-Canoe Lake Fault, an extensional mylonite zone [Easton, 1992].

The Bancroft Domain (Figure 4) is defined as a carbonate basin [Moore, 1982], with a facies variation from west to east in the southern part of the domain. The western edge of the terrane is considered to have a near-shore facies, with a dolomite-quartzite association, and sabkha deposits [Haynes, 1986], which are characteristically shallow-water, shore-line environment deposits. These shallow-water units vary eastward into a far-shore-slope facies environment consisting of distal volcanoclastics with interbedded clastic and calcitic marbles. The presence of abundant arenite, stromatolites, and lack of carbonate turbidites are all consistent with a platformal, shallow water environment within the southern part of the Bancroft Domain.

The Harvey-Cardiff Domain has been interpreted to be a somewhat deeper water, and more volcanic and tectonically active basin as compared to the Bancroft Domain [Easton, 1992]. This interpretation is supported by

the presence of more volcanic rocks and less mature metasediments (eg. metawackes and turbiditic metacarbonates).

The Belmont Domain is viewed as comprising a series of volcanic islands, with volcanoclastic aprons generally as turbidite fans [Easton, 1992]. Carbonates are present in two regimes; 1) as shallow-water platformal sequences adjacent to the volcanic centres, and 2) as distal deposits from the volcanic centres, such as carbonate turbidites, but still close enough to interfinger with the volcanoclastic detritus [Easton, 1992]. Geochemical data and plutonic and sedimentary rocks associated with the volcanic sequences suggest a tectonic environment of attenuated continental crust in an ensialic back-arc basin [Holm *et al.* 1986; Smith and Holm, 1987, 1990a].

The Grimsthorpe Domain is composed of about sixty-five percent plutonic rocks of a wide compositional range, with supracrustal rocks comprising the remainder. Recently, Easton and Ford [in prep.] and Easton [1992] have suggested that the stratigraphic succession may be divided into a series of older flows and mafic intrusions (the Canniff Complex) that may represent an ophiolite succession, overlain by a younger volcanoclastic sequence (the Grimsthorpe Group). The whole sequence has been intruded by a series of ultramafic and mafic plutons, followed by intrusions of tonalitic plutons. Emplacement of post-tectonic syenitic plutons completes the magmatic succession.

The Mazinaw Domain (Figure 4) is composed of fifty-five percent meta-plutonic rocks, with the remainder being meta-sedimentary and meta-volcanic rocks in equal proportions. The lack of primary textures and structures in the Mazinaw Domain due to high metamorphic temperatures and intense deformation [Easton, 1992], makes stratigraphic correlation and identification of depositional and eruptive environments very difficult. Easton [1992] suggests that areas of volcanoclastic debris are interfingered with clastic and minor carbonate sediments around volcanic edifices.

The Sharbot Lake Domain (Figure 4) comprises mafic metavolcanic and carbonate rocks intruded by gabbroic, granodioritic and granitic plutons, and is lithologically similar to the Belmont and Grimsthorpe Domains. Easton [1992] suggests that the volcanism in the Sharbot Lake Domain occurred in an active carbonate basin. Eruptions of pillow lavas, massive flows and tuffs, which were later eroded into volcanoclastic debris or aprons around centres point to shallow water and subaerial volcanism. As volcanism decreased and eventually ceased, carbonate deposition increased, burying the volcanic piles. Dolomites and algal mats also define areas of shallow water in the domain.

The Frontenac Terrane (Figure 4) has long been discussed separately from the BEMS terrane (eg. Wynne-Edwards, 1972) due to its different lithologies and much higher metamorphic grade. The supracrustal sequence of the Frontenac differs from the other terrane in its lack of meta-volcanic

rocks, and abundance of quartzite units [Easton, 1992]. Easton [1992] describes the sedimentary succession of the Frontenac Terrane to suggest a platformal environment, with the deeper shelf to the west and northwest, characterised by calcitic marbles. To the southeast, he describes a very shallow-water to a shoreline environment, characterised by dolomitic marbles and stromatolites. Evaporite units in the Adirondack Lowlands [deLorraine and Dill, 1982] further support this shallow-water to shoreline environment.

In summary, the Central Metasedimentary Belt in Ontario can be viewed as having shallow-water environments to the northwest (Bancroft Domain) and to the southeast (Frontenac Terrane/Adirondack Lowlands). The presence of platformal sediments as well as evaporite sequences are evidence for continental crust to be present. Moving across the Central Metasedimentary Belt, towards the Grimsthorpe Domain, deeper water rocks are observed systematically, including submarine volcanics and turbidites. The question arises, is how deep is the water? Can the Grimsthorpe Domain be oceanic crust, or is it attenuated or thinning continental crust? The presence or absence of oceanic crust makes a difference in the tectonic evolution of the Central Metasedimentary Belt. When this problem is solved, the number of tectonic models for the Central Metasedimentary Belt will decrease.

2.2 - Previous Geologic Interpretations of the Queensborough Area

The Queensborough area lies in the southern half of the Grimsthorpe Domain (Figures 4 and 5). The geology of this area has been recently mapped by DiPrisco [1989], who described the stratigraphic succession as comprising a belt of amphibolites that consists mainly as mafic metavolcanics, which are overlain by siliceous clastic and carbonate meta-sediments. These supracrustal rocks have been intruded by plutons of ultramafic, mafic, tonalitic and syenitic composition (Table 1; Figure 5).

This study focuses on the amphibolites and ultramafic rocks. Early maps of the area [Meen, 1944; Hewitt, 1968] showed this belt to comprise mafic meta-volcanics and related meta-volcaniclastics. Recent workers [eg. LeBaron *et al.* 1987; DiPrisco, 1989; Easton, 1992] have not contested these descriptions, but have each suggested a different interpretation for the mafic-ultramafic rock successions. Each of these interpretations leads to a different tectonic setting for the Grimsthorpe Domain.

LeBaron *et al.* [1987; 1989] studied the amphibolite-ultramafic belt to the west of the Elzevir Tonalite (Figure 5) to define the extent and nature of the talc-bearing bodies in the ultramafic rocks. They used field relationships and geochemical data to show that a range of systematically distributed rock types varying from ultramafic komatiite to tholeiitic basalt outcrop in the area. LeBaron *et al.* [1987] describe the stratigraphy as having a base of 5 to 200 m of ultramafic komatiite, occurring as flows and possibly sills,

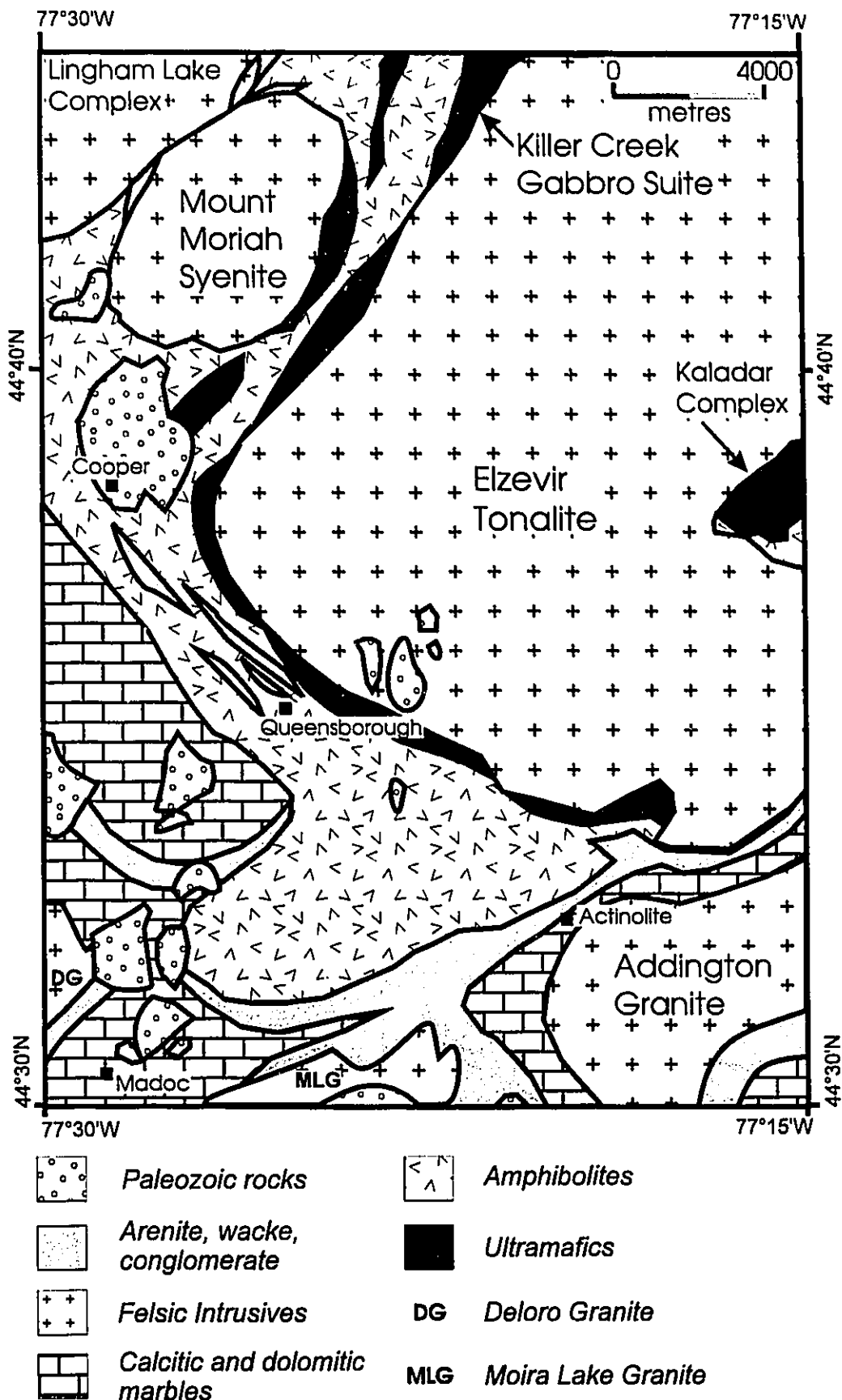


Figure 5 - Local Geology of the Queensborough area [after DiPrisco, 1989].

with the mineralogy consisting of actinolite-tremolite to serpentine-magnetite and talc-chlorite-carbonate-magnetite. There are brecciated zones within this unit that may be interpreted as original flow breccias. The ultramafic unit is overlain by 400 to 2000 m thick of komatiitic basalt occurring as meta-volcanic rocks and consisting mostly of actinolite with lesser amounts of hornblende and plagioclase. The top of the sequence comprises tholeiitic basalts, consisting of hornblende-amphibolites. Pillow lavas are preserved in some locations within these tholeiitic lavas. Mafic lapilli tuff and agglomerate (up to 20 m thick) with thin units of felsic tuff and rusty pyritic schists occur within the sequence.

DiPrisco [1989] re-interpreted the supracrustal rocks as mafic metavolcanics of the Tudor Formation [Lumbers, 1967] which were intruded by a number of ultramafic and mafic plutons. He suggested that many fine- to medium-grained sills intrude the volcanics, and are difficult to distinguish from the meta-volcanics. DiPrisco [1989] considers the ultramafic rocks along the Elzevir Tonalite (Figure 5) as part of the Killer Creek Gabbro Suite [Easton and Ford, 1990; formerly the Skootamatta Complex], not as komatiites as suggested by LeBaron *et al.* [1987]. The Killer Creek Gabbro Suite is a suite of coarse- to medium-grained gabbro, diorite and pyroxenite [DiPrisco, 1989]. The Suite is well preserved to the north of the Elzevir Tonalite. However, it is highly strained, layered to schistose and serpentized in the south where it consists of amphibole-plagioclase-rich

rocks. Relict coarse-grained gabbroic textures are still recognizable in some areas.

Most recently, Easton [1992] has described the ultramafic rocks as mafic to ultramafic protomylonitic meta-volcanic and intrusive rocks (the Canniff Complex), and considers them to be the oldest rocks in the Grimsthorpe Domain. The rocks are found in a thin band along the Elzevir Tonalite contact (Figure 5), and as clasts within the overlying younger metavolcanic and metavolcaniclastic rocks (the Grimsthorpe Group). Locally, the older units and clasts are altered to tremolite-talc-carbonate assemblages. Based on chemical data, Easton and Ford [in prep.] suggest that the mafic and ultramafic rocks of the Canniff Complex have an ocean floor affinity, and may be interpreted as the basement to the Grimsthorpe Domain.

Thus, LeBaron *et al.* [1987] suggest a complete volcanic sequence for the mafic-ultramafic rocks, from ultramafic komatiite to tholeiitic basalt. Komatiites are generally thought to have formed in thin continental to shallow-water oceanic crust, but are also generally restricted to Archean time [Hess, 1989]. DiPrisco [1989] believes the ultramafic rocks to be intrusive, related to the Killer Creek Gabbro Suite from north of the area. He considers the amphibolites to be meta-volcaniclastic rocks of the Tudor Formation. The Tudor volcanics to the west, in the Belmont Domain are suggested to be formed on an attenuated continental crust in an ensialic

back-arc basin. Easton [1992] suggests that the ultramafic rocks of the Canniff Complex are the oldest rocks in the Grimsthorpe Domain, and are overlain by the Tudor Volcanic sequence. The rocks of the Canniff Complex represent an intensely deformed (ie. promylonitic) sequence of ultramafic and mafic rocks which may represent part of an ophiolite sequence [Easton, 1992].

In recent studies [LeBaron *et al.* 1989; DiPrisco, 1989; Easton, 1992] the rock types present in the Grimsthorpe Domain have been interpreted variously as continental and oceanic crust. It is an objective of this study to solve this controversy and evaluate the tectonic significance of the Grimsthorpe Domain in relation to the Central Metasedimentary Belt.

Chapter 3 - Field Relations and Petrography

This chapter is divided into three sections. The first section will define the boundaries of the southern part of the Grimsthorpe Domain, which have not been clearly defined to date. The second section will describe in detail the petrography of the study area. The third section deals with the new geologic interpretations of the Queensborough area from the data in the second section.

3.1 - Boundaries of the southern part of the Grimsthorpe Domain

The only defined boundary of the Grimsthorpe Domain is the eastern boundary, where the Grimsthorpe is separated from the Mazinaw Domain by the Mooroton Shear Zone (see section 2.1).

The western boundary of the Grimsthorpe Domain with the Belmont Domain is marked by a fault zone which separates amphibolitic rocks of the Grimsthorpe from marbles in the Belmont [DiPrisco, 1989]. This fault, herein named the Queensborough Fault Zone¹ has a curved fault line, and strikes south to southeast (Figures 5 and 6). It is truncated in the south by

¹

The fault zone was unnamed previously, and since this zone now has tectonic significance being the western boundary of the Grimsthorpe Domain, it is proposed herein that the fault zone be named the Queensborough Fault Zone. The zone also has economic significance, as DiPrisco [1989] states that this fault zone was responsible for the gold mineralization in the Sophia Gold Mine, just west of Queensborough.

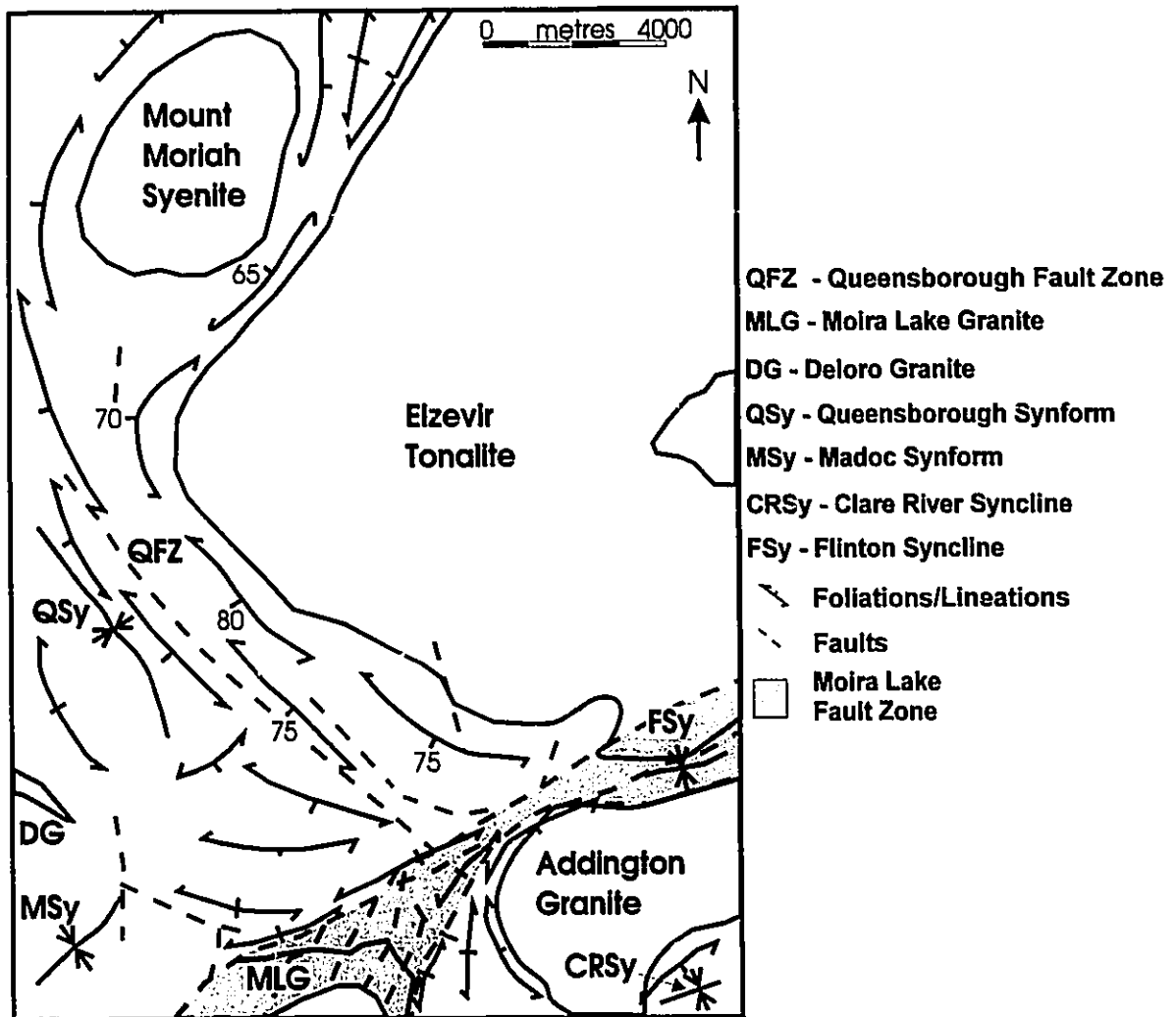


Figure 6 - Major structural elements in the Queensborough area, southern Grimsthorpe Domain [after DiPrisco, 1989].

the Moira Lake Fault Zone. There are three rock types immediately west of the Queensborough Fault Zone, that support the interpretation of the two domains being lithologically different. The marbles of the Belmont Domain follow the fault zone from south of Cooper southerly to Madoc (Figure 5), and do not occur anywhere in the Grimsthorpe Domain. These shallow-water, platform to turbiditic, calcitic and dolomitic marbles are generally medium- to coarse-grained and massive [Easton, 1992]. Outcrops near the Queensborough Fault Zone have finer grain sizes, and abundant secondary calcite and quartz veining. The marbles also become highly fractured and brecciated suggesting that the rocks have been deformed, most likely by the Queensborough Fault Zone. Further south, northeast of Madoc, are outcrops of mafic to felsic metavolcanic rocks (UTM 308000E, 4933600N) that are fine-grained, dark grey and massive to weakly lineated. One outcrop of fine-grained, grey felsic rock has coarser crystals (2 - 5 mm) of plagioclase, as well as a minor amount of lithic fragments and lapilli. The plagioclase crystals are subhedral, equidimensional, and disseminated throughout the rocks. This outcrop is best described as a meta-ashflow with lapilli, plagioclase phenoblasts, and lithic fragments. No ash-flows have been found in the Grimsthorpe Domain, thus supporting the lithological differences between the two domains. Further, there is a suite of felsic dykes which are characteristic of the Belmont Domain and do not occur in the Grimsthorpe Domain. In outcrop, the rocks are medium- to dark-grey,

fine-grained, and massive, with the width of the dykes ranging from 3 to 10 metres wide. The mineralogy consists of quartz (up to 20 modal percent), plagioclase (20 to 60 modal percent), actinolite/tremolite (up to 15 modal percent), carbonate (up to 30 modal percent), biotite, opaque minerals and chlorite (up to 15 modal percent) (Appendix B). The small amounts of quartz and biotite, and the presence of actinolite makes the mineralogy of the Belmont Domain felsic dykes different from those within the Grimsthorpe Domain (see section 3.9). The felsic dykes are very similar to others further west in the Belmont Domain [Gagnon, 1986; Smith and Holm, 1990a].

The southern boundary of the Grimsthorpe Domain is along the Moira Lake Fault Zone, which separates the Grimsthorpe from the Mazinaw Domain to the south and southeast (Figure 6). The fault zone is up to 1.5 kilometres wide and traceable up to 17 km in the map area (Figure 6). The highest strain occurs in the south, in the Moira Lake Granite, where the intrusive rocks and overlying meta-arenites and meta-wackes are mylonitized [DiPrisco, 1989]. This mylonite zone is up to 600 m wide and discontinuous. Although the fine-grained, pink to grey granitic rocks show no kinematic indicators, large scale block displacements suggest sinistral movement along northeast/north-northeast axes [DiPrisco, 1989]. (Throughout the Moira Lake Fault Zone are a series of northeast-trending faults and lineaments that have been left out of Figure 6 for clarity.)

The northern boundary of the Grimsthorpe Domain is delineated as the northern extent of the Weslemkoon Tonalite Batholith, which is outside of this study area. The northern boundary of the study area is approximately the 44°42'N latitude line, north of which access is limited.

3.2 - General Geology of the southern Grimsthorpe Domain

The meta-amphibolite and ultramafic rocks of this study (Figure 5) are surrounded by and intruded by a range of rock types. The eastern boundary of the amphibolite-ultramafic belt is the Elzevir Tonalite [1280-1270 Ma; Heaman, unpubl.], which is the largest pluton in the area, covering the northeast corner of the study area. The Killer Creek Gabbro Suite [Easton and Ford, 1990] lies in the north of the map area, along the western margin of the Elzevir Tonalite. In the northwest corner, the Lingham Lake Diorite-Gabbro Suite [Easton and Ford, 1990] and the Mount Moriah Syenite [DiPrisco, 1989] intrude the amphibolitic rocks. On the western side of the Queensborough Fault Zone, in the Belmont Domain, is a belt of steep westerly-dipping calcitic to dolomitic marbles. Along the southern margin of the amphibolites, a suite of meta-conglomerate, meta-arenites, and meta-wackes assigned to the Flinton Group [1128 ± 35 Ma, Boutcher *et al.*, 1965; DiPrisco, 1989; Wolff, 1982] overlie the contact between the amphibolites and the marbles. The meta-sediments are deformed by the Moira Lake Fault Zone (Figure 5). Several outliers of Middle Ordovician

sediments nonconformably overlie the Mesoproterozoic rocks. Pleistocene sediments are found throughout the area, but are generally restricted to topographic lows.

The map area in Figures 5 and 6 can be separated into two structural blocks, a northern section, and a southeastern section, separated by the Moira Lake Fault Zone. The southeastern section comprises rocks of the Mazinaw Domain, and is not of direct interest to this study.

Structurally, within the Grimsthorpe Domain, the area north of the Moira Lake Fault Zone to south of the Mount Moriah Syenite (Figures 5 and 6) is dominated by northwest structural trends. Around the Mount Moriah Syenite, structural trends strike north to northeast. The structural trends within the amphibolites and ultramafics parallel the intrusive contact of the Elzevir Tonalite (Figure 6). Two major synforms have been described in the western part of the study area, within the Belmont Domain. (Although originally named as synclines by Hewitt [1968], recent terminology and understanding of the local geology suggest the structures are better termed synforms.) Just north of Madoc in the Belmont Domain, is the Madoc Synform [Hewitt, 1968] (Figure 6), which trends and pitches northeast. Further north, and just northwest of Queensborough, is the Queensborough Synform [Hewitt, 1968] (Figure 6), which trends and pitches northwest. Amphibolite rocks are folded around the nose of the Queensborough Synform to the south, while the nose is occupied by silicified meta-

sediments and carbonates [DiPrisco, 1989]. The Flinton Syncline occurs in the southeast (Figure 6). It is fault bounded and shows no indication of unconformity with either the amphibolites or the marbles [DiPrisco, 1989]. The Flinton Syncline is occupied by rocks of the Flinton Group, consisting of stretched quartzose conglomerate, meta-quartz arenite, meta-wacke and calc-silicate paragneiss [DiPrisco, 1989].

3.3 - Petrography

Over 130 samples were collected throughout the area (Figure 7; Appendix A). The majority were collected along the north-northwest trending part of Hastings County Road 20, which cuts across strike of the amphibolite belt, allowing for a thick, representative sequence of strata to be collected (up to 5 km of thickness). Another large collection of samples is from south of the Elzevir Tonalite, where the ultramafics are best exposed. The rest of the samples were collected to represent the various lithologies and textures of all the rock types.

The rocks are divided into eight suites, based on mineralogy and textural criteria. The suites are; Mafic Metavolcanics (MV), Meta-Gabbros (MG), Ultramafics (UM), Chlorite Schists (CS), Mafic Dykes and Sills (MD), Felsic Dykes (FD), Meta-Sediments (MS), and Marbles (MB).

3.3 - Mafic Metavolcanic Suite

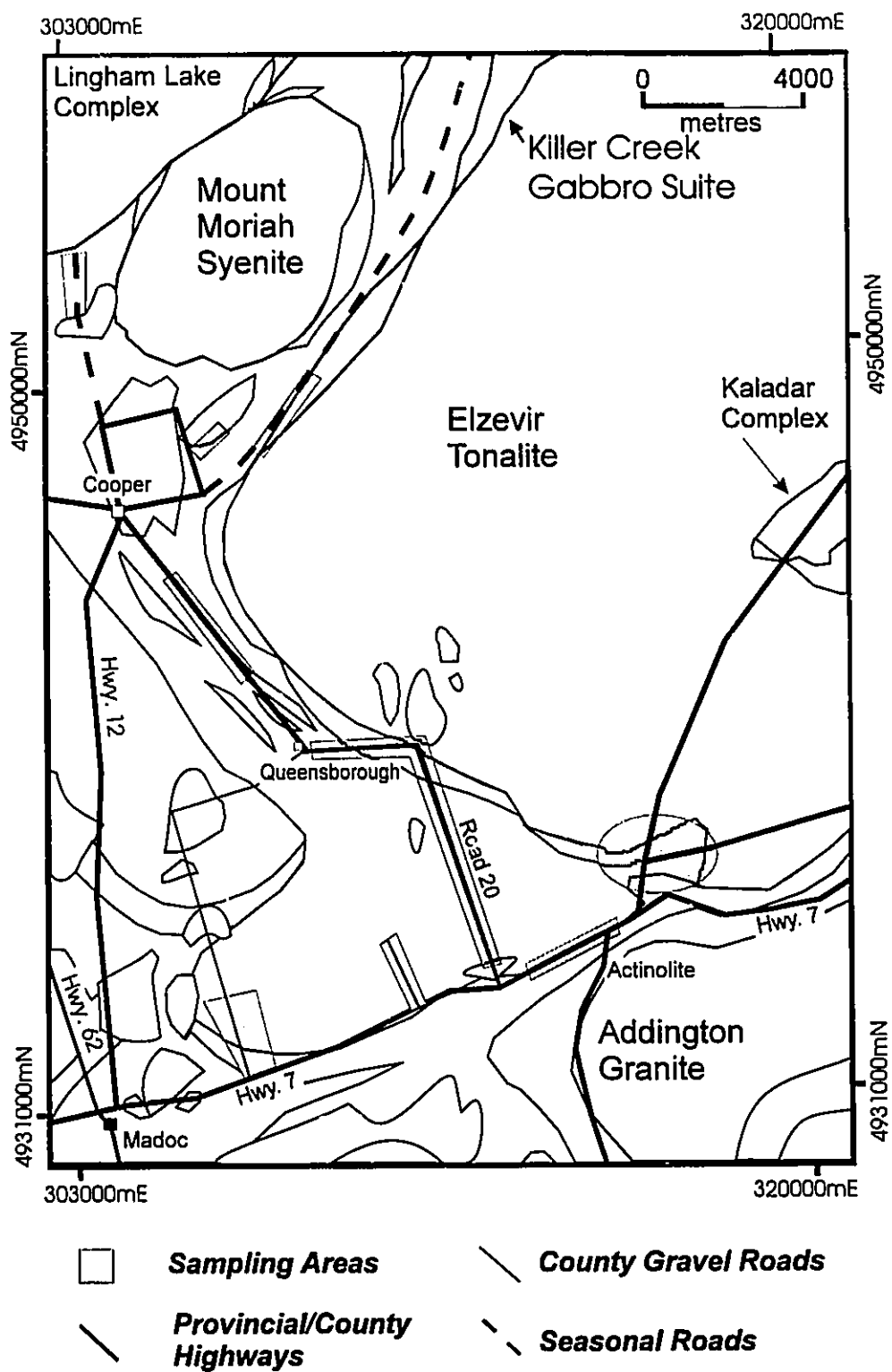


Figure 7 - Sample locations in the Queensborough area.

Previous workers in the area have referred to the belt of amphibolites (Figure 5) as the "Tudor Volcanics" [Lumbers, 1967; Hewitt, 1968], or as tholeiitic basalts with sections of mafic lapilli tuff and agglomerate [LeBaron *et al.*, 1987]. Recently, DiPrisco [1989] described the rocks as fine- to medium-grained, black to greenish amphibolites, being massive to strongly foliated and having fragmental and pillowed textures which are part of the Tudor Formation [Lumbers, 1967]. He added that many mafic and ultramafic plutonic rocks had intruded the volcanic sequence, which are not noted elsewhere in the Tudor Formation. Most recently, Easton [1992] divided the amphibolite strata into two successions; an older suite of tholeiitic flows and mafic intrusions (the Canniff Complex) which is overlain by a younger volcanoclastic sequence (the Grimsthorpe Group).

Field work for this study showed that the mafic metavolcanics were much less extensive in the area than previously described [eg. Hewitt, 1968; DiPrisco, 1989]. The meta-volcanic rocks were differentiated from the other mafic rocks (ie. meta-gabbros and mafic dykes) predominantly upon field relationships. There are very few localities in which unequivocal evidence indicative of a volcanic origin occurs. Such evidence includes; pillow lavas, amygdaloidal textures, or igneous layering that may depict a series of flows. There is one good outcrop of pillow lavas on Road 20 (UTM 312300E, 4936300N) where a three metre thick layer of pillows strikes 130° with a sub-vertical dip, and pillow tops point southwest. Individual

pillows range from 10 to 100 cm wide and 5 to 30 cm thick, with rusty selvages less than 1.0 cm thick. The pillowed rocks are dark green on the glaciated weathered surface, and dark grey on the fresh surface. The bed of pillows has meta-gabbroic rocks on both the top and bottom of the layer. Other meta-volcanic samples that are very similar to those meta-volcanic rocks of the Tudor Formation in the Belmont Domain [T.E. Smith, pers. comm., 1993] were collected from south of the Elzevir Tonalite, north of Actinolite (Figure 7). They are fine-grained, dark grey, massive, amphibole-plagioclase rocks. Outcrops of these samples are small (less than 3 m² in area), and do not possess a glaciated surface, and thus their identification is based upon petrography and not field relationships.

Mineralogically, the Grimsthorpe meta-volcanic samples are very simple, consisting of quartz, plagioclase, actinolite/tremolite, chlorite, oxides, sulphides, and carbonate (see Appendix B). Quartz is present as very fine- to fine-grained, anhedral, interstitial crystals, aggregates of crystals, or in veinlets with plagioclase and carbonate. Plagioclase occurs as interstitial, fine-grained, anhedral crystals, having simple to multiple twins. Actinolite and tremolite occur as very fine- to fine-grained, anhedral, equidimensional crystals to subhedral, blade-like and hexagonal cross-sectioned crystals. Elongate amphibole crystals define the rock lineation where present, and may contain inclusions of opaques and plagioclase. Carbonate occurs as very fine-grained, anhedral, interstitial crystals, in

veinlets with or without quartz, or as a pervasive alteration product of plagioclase and actinolite. Opaque minerals are very fine-grained, anhedral, equidimensional interstitial crystals, or fine-grained, subhedral, square/diamond cross-sectioned crystals or medium-grained, anhedral, skeletal crystals with plagioclase and actinolite inclusions. Chlorite is found as very fine-grained, subhedral flakes, or as pseudomorphs of actinolite.

Although consisting of metamorphic minerals, these mafic meta-volcanic rocks have field relationships (pillows) and petrologic features (fine-grained) that are comparable to original volcanic fabrics. The metavolcanic rocks, with their simple metamorphic mineralogy of actinolite/tremolite, quartz, plagioclase, chlorite, oxides, sulphides, and carbonates (probably calcite), most likely had pyroxene as the original mafic mineral, with plagioclase, and with or without quartz. With the lack of, or at least minimal amount of olivine, the meta-volcanics were probably tholeiites, as they are presently chemically classified (Chapter 4). The metamorphic assemblage chlorite + actinolite + quartz, indicates that the meta-volcanic rocks have been metamorphosed to low grade or greenschist facies [Winkler, 1979].

3.5 - Meta-Gabbro Suite

As described in section 2.2, most of the amphibolite rocks in the Grimsthorpe Domain were interpreted as mafic meta-volcanic rocks.

However, field relationships and petrography show that most of the rocks are of the meta-gabbro suite (Figure 5). In many areas the meta-gabbroic rocks are massive, medium- to coarse-grained, and shows no mineral alteration or deformation on a freshly broken surface. These rocks have a texture typical of many gabbros (ie. subhedral granular), although they consist of metamorphic minerals (eg. actinolite/tremolite, plagioclase, epidote, garnet). However, in individual outcrops, the meta-gabbros grade from the massive, coarse-grained amphibolite to very fine-grained, mylonitic amphibolites. These outcrops have zones of massive, medium- to coarse-grained meta-gabbroic blocks that are surrounded by dark green, fine-grained material. This amphibole-rich material may be lineated, or it may form a fabric around the massive gabbroic blocks. Where the rock is dominantly fine-grained material, folding may be present. The massive gabbroic blocks may be brecciated, and small pieces may show strain effects such as tails. These are characteristic features of rocks which have been deformed by shearing. Petrographically these sheared samples are fine-grained amphibolite and have been commonly misidentified as meta-volcanics in previous studies [eg. LeBaron *et al.*, 1987; DiPrisco, 1989].

The least deformed gabbroic rocks are massive, medium- to coarse-grained amphibolite, and consist of variable proportions of actinolite and plagioclase with minor magnetite, chlorite, and carbonate (eg. samples TD-26, TD-32; Appendix A). The rock has a distinctive weathered surface with

a medium green and dull white colour, while the fresh surface is dark-grey to greyish-black.

Within metres from the massive, undeformed gabbro, deformation and alteration is noticeable. The mineralogy does not change appreciably at initial stages of deformation, but the rocks do develop a weak lineation on the surface, defined by actinolite crystals (ie. sample TD-37; Appendix A). Grain size is reduced, and the colour of the weathered surface becomes darker green.

With increasing deformation, the outcrops develop a strong lineation, defined by actinolite. The weathered surface is a darker green colour, and grain size becomes seriate. Glaciated surfaces show anastomosing networks of thin shears, that give the rock a brecciated appearance. On freshly broken surfaces, the rock is dark-grey to greyish-black, with no indication of the thin shears, and the rock appears to be a massive, fine- to medium-grained amphibolite.

Rocks with the highest degree of deformation in the meta-gabbro suite show a strong lineation, and a weak foliation. The fresh surface shows the lineation well, and larger shears become visible. Quartz-calcite veinlets are abundant in these rocks, generally following the lineation direction. The grain size is generally fine-grained, although some actinolite crystals are still of medium-grain size.

Petrographically, the massive meta-gabbros comprise mostly of mixtures of plagioclase and actinolite. The actinolite crystals are generally individual euhedral prismatic crystals, having dimensions of <0.5 mm to 1.0 mm wide, and up to 4 mm long. Simple twins are common and a small proportion of actinolite crystals show partial alteration to chlorite. The plagioclase crystals occur as fine-grained, anhedral to subhedral, interstitial masses forming the matrix of the rock. Multiple twins and zoning are common, although difficult to see due to sericitic alteration of the crystals. Inclusions of actinolite are rare within the plagioclase. Opaque minerals are present as very fine-grained, subhedral, disseminated crystals, sometimes with a titanite rim. Carbonate occurs as fine- to very fine-grained, anhedral disseminated crystals. Chlorite occurs as very fine-grained crystals within actinolite crystals, as a pervasive alteration product (Appendix B; Group 1).

In the early stages of deformation, the actinolite and plagioclase crystals are commonly bent and fractured, and show undulatory extinction. The rock's lineation is defined by elongate actinolite and plagioclase crystals. Alteration of actinolite to chlorite is common, with some alteration to opaques and carbonate. Pervasive sericitic alteration of the plagioclase is very common. The amount of actinolite/tremolite, carbonate and chlorite is slightly increased, while quartz and plagioclase are decreased (Appendix B; Groups 2 and 3). In more strongly deformed samples, the actinolite crystals are well-aligned, and define the rock's lineation. Further, the actinolite is

highly deformed and altered as shown by fractured mineral terminations, bent crystals which show undulatory extinction and by having common chlorite and carbonate alteration products. Often chlorite and carbonate can be found as actinolite pseudomorphs. Plagioclase is less abundant, and affected by sericitic alteration. Quartz is less abundant to absent and the chlorite and carbonate content is increased (Appendix B; Group 4).

The coarse-grained, massive amphibolite rocks possess typical gabbroic textures, and the metamorphic mineral assemblage can be interpreted as having an original gabbroic mineralogy (ie. plagioclase, pyroxene). Field relationships and detailed petrography show that most of the fine-grained amphibolite rocks are also meta-gabbros. Thus the majority of the amphibolite belt along the western margin of the Grimsthorpe Domain may be classified as meta-gabbroic rocks.

3.6 - Ultramafic Suite

Rocks from the ultramafic suite were collected from three main areas; near the southern intrusive contact of the Elzevir Tonalite, northeast of the village of Actinolite; at the right-angled bend on Road 20 just east of Queensborough; and northeast of the village of Cooper (Figure 7). In general, the ultramafics are massive to well foliated, and consist of assemblages of actinolite, talc, serpentine, chlorite, plagioclase, opaque minerals and carbonate (Appendix B). The rocks range in colour from off-

white to light green and dark green. There are four common mineral assemblages in the suite; assemblage I being dominated by actinolite/tremolite, with or without plagioclase, and minor chlorite, carbonate, and opaque minerals. Assemblage II is predominantly tremolite, with talc, chlorite, carbonate and opaque minerals. Assemblage III is predominantly talc and carbonate, with subordinate chlorite, opaques and anthophyllite. Assemblage IV is predominantly antigorite and talc, with subordinate chrysotile, carbonate, chlorite, and opaques. Garnet, titanite and tremolite are present in trace amounts in the assemblage IV (Appendix B). Most of the ultramafic outcrops are small, covered with sand and clay, and generally only one of the above mineral assemblages occurs. One of the largest outcrops seen in the area is layered, having assemblages I, III, and IV present, as well as a layer of chlorite schist (see section 3.7) (samples KT-8 through KT-12; Appendix A). All the layers are less than one metre thick, and strike 120°, dipping to the south at 60°. There is a systematic sequence of rock types that can be identified extending southwards from the Elzevir Tonalite. The sequence consists of; fine-grained chlorite schist; assemblage IV, consisting mainly of antigorite, talc and carbonate; assemblage III, consisting of talc and carbonate; assemblage IV as above; assemblage III as above; and assemblage I, consisting mainly of tremolite and chlorite. This outcrop may indicate that the ultramafic suite

is compositionally layered, and the majority of the outcrops seen elsewhere are poorly exposed, and not large enough to see the layers.

Assemblage I is only found in the area south of the Elzevir Tonalite (Figure 7). The rocks are medium-grey to greenish-black, massive to weakly foliated and fine- to medium-grained. The mineralogy consists of tremolite mostly (15 - 80 modal percent), with minor actinolite, plagioclase (up to 15 modal percent), chlorite (10 - 55 modal percent), carbonate (up to 50 modal percent) and opaque minerals (up to 15 modal percent) (Appendix B; Assem. I). Tremolite and actinolite occur as fine- to medium-grained, subhedral prismatic crystals to anhedral, bent and broken crystals, some altering to chlorite. Plagioclase occurs as fine- to medium-grained (less than 5.0 mm), anhedral, interstitial crystals, with simple twins, and common alteration to carbonate. Chlorite occurs as fine-grained, subhedral flakes, which define the rock lineation where present. Chlorite may also be a pseudomorph of actinolite. The opaque minerals occur as very fine-grained, subhedral, equidimensional crystals, probably magnetite, or as medium-grained (less than 3.0 mm), patchy aggregates with minor actinolite and chlorite inclusions. Carbonate generally occurs as a pervasive alteration product of tremolite, although a few euhedral rhombohedral crystals are found interstitially within the matrix.

Assemblage II occurs mainly south of the Elzevir Tonalite and to a lesser extent to the east of Queensborough (UTM 311300E, 4939300N).

The rocks are fine- to medium-grained, massive, and greenish-grey to greenish-black. They comprise tremolite (10 to 65 modal percent), talc (5 to 10 modal percent), chlorite (5 to 40 modal percent), opaque minerals (up to 15 modal percent) and carbonate (5 to 50 modal percent) (Appendix B; Assem. II). The tremolite crystals are fine- to coarse-grained (less than 6.0 mm long), anhedral, bent and fractured, and have a high content of carbonate, chlorite and opaque minerals as selective alteration products, altering the tremolite crystals from the core out. Chlorite occurs as an alteration product of tremolite, but fine-grained, subhedral, interstitial flakes are also present. Carbonate can be found as fine-grained aggregates within the rock matrix of opaques, chlorite and talc, but more often occurs as an alteration product of tremolite. Opaque minerals are fine- to medium-grained (less than 3.0 mm), anhedral aggregates, sometimes with carbonate inclusions.

Assemblage III is found in all three of the sampling areas of the ultramafics (as above; Figure 7). The rocks are light-grey to dark greenish-grey in colour, fine- to medium-grained and porphyroblastic, and massive to weakly foliated. The mineralogy consists of talc (10 to 40 modal percent), carbonate (20 to 65 modal percent), chlorite and opaques (less than 10 modal percent) and anthophyllite (up to 65 modal percent) (Appendix B; Assem. III). Talc occurs as very fine- to medium-grained (less than 5.0 mm), anhedral to subhedral flakes, defining the foliation, where present. In

some instances, a pervasive foliation fabric is seen as the talc flakes are oriented around coarser carbonate crystals. Some talc crystals show effects of shearing, as they have been stretched, and have radial or uneven extinction patterns. Chlorite occurs as fine-grained, subhedral flakes, defining the foliation plane when one is present. The opaque minerals are very fine- to medium-grained (less than 3.0 mm), anhedral to subhedral, equidimensional crystals, sometimes occurring as 'chain aggregates' (up to 10 mm long) along the foliation planes. In all samples, some opaques are coarse enough to be porphyroblasts. Carbonate occurs as fine-grained, anhedral, interstitial matrix, or as medium-grained (less than 4.0 mm), euhedral, rhombohedral-shaped crystals. The rhombohedra do not effervesce readily with HCl and are probably dolomite. Anthophyllite occurs as medium- to coarse-grained (up to 10 mm long), subhedral, needle-like to blade-like crystals arranged in a radial pattern. They are differentiated from actinolite/tremolite by the crystal shape, brown colour in plane-polarised light, and straight extinction [Heinrich, 1965].

Rocks of assemblage IV were collected from south of the Elzevir Tonalite, and consist of massive, porphyroblastic rocks, having a fine-grained, light bluish-grey matrix of talc, carbonate, and chlorite, with medium- to coarse-grained, greenish-black, irregularly shaped blocks of serpentine. In one outcrop (sample KT-4; Appendix A) chrysotile veins up to 5 cm thick are found, but otherwise most of the serpentine present is of

the antigorite variety which occurs as irregular shaped blocks. The mineralogy of the rocks consists of antigorite (10 to 60 modal percent), talc (5 to 50 modal percent), carbonate (less than 30 modal percent), and chlorite and opaque minerals (less than 20 modal percent). Garnet, titanite, and tremolite are found in trace amounts (Appendix B; Assem. IV).

Antigorite occurs as large blocks (1.0 to 10 cm across), with no crystal form, but may have talc, chlorite and opaques as inclusions and/or alteration products. Talc occurs as fine- to medium-grained (less than 5.0 mm) subhedral flakes that are generally randomly oriented. Talc may form a pervasive foliation fabric around the antigorite blocks. Chlorite occurs as fine-grained, interstitial crystals, sometimes forming a pervasive foliation fabric around serpentine, along with the talc. Carbonate occurs as fine-grained crystals in the matrix with talc, as alteration products within the antigorite, or as very thin carbonate veinlets. Opaque minerals occur in the matrix as medium-grained (3.0 mm), irregular shaped crystals, or as microcrystalline inclusions within the antigorite blocks.

In summary, the ultramafic suite is composed of variable amounts of actinolite/tremolite, chlorite, serpentine and talc. This assemblage of minerals suggests the original mineralogy comprised pyroxene, olivine, and possibly amphibole. The four different mineral assemblages found in the ultramafic suite suggests that there were variations in their original mineralogy. Assemblage I comprises tremolite, plagioclase, chlorite,

carbonate (calcite) and opaque minerals. This assemblage is very similar to that of some of the meta-gabbros, and may be a more chemically altered meta-gabbro. Assemblage II consists of tremolite, talc, chlorite, opaques and carbonate (calcite and dolomite). The lack of quartz and plagioclase, and presence of talc is evidence that these rocks are ultramafic. Pyroxene was probably the most abundant original mafic mineral, with minor olivine and some oxides. This assemblage was probably derived from a pyroxenite. Assemblage III consists of talc, carbonate (dolomite), chlorite, opaques and anthophyllite probably had a mixture of pyroxene and olivine. These rocks probably were pyroxenites to peridotites. Assemblage IV, with the large blocks of serpentine, and a matrix of talc, carbonate (dolomite) and chlorite, was probably derived from a protolith in which olivine was abundant, with minor pyroxene and opaques. These rocks were probably peridotites, possibly with zones, pods or veins of dunite.

The ultramafic rocks have been given two different interpretations by previous workers, either extrusive or intrusive [eg. LeBaron *et al.*, 1987; DiPrisco, 1989]. The meta-ultramafic rocks are presently fine- to coarse-grained. Although metamorphism can cause mineral grain size growth, the low grade metamorphism (greenschist facies) as determined by the mineral assemblage of the ultramafic suite [Winkler, 1979] would not cause excessive grain size increase. Therefore, the original grain size was similar to the present grain size, and suggestive of an intrusive environment. The

ultramafic rocks are also layered and compositionally banded. These are not characteristics of komatiites, and thus the komatiite model as suggested by LeBaron *et al.*, [1987] is inappropriate and is not considered further in this study.

3.7 - Chlorite Schists

The chlorite schists occur in four localities within the ultramafic rocks described above (samples KT-11, KT-18; Appendix A; Figure 7) and appear to be zones of intense deformation. These schistose units are generally less than a metre wide, dark greenish-grey to greenish-black, fine- to very fine-grained and well foliated. They are made up of mixtures of quartz, plagioclase, opaque minerals, chlorite, and traces of carbonate, titanite, clinozoisite and talc (Appendix B). Quartz and plagioclase occur together as very fine-grained, anhedral crystals, generally in thin bands with plagioclase. The plagioclase may have simple twins and alters to carbonate. The opaque minerals form very fine-grained, anhedral crystals or fine- to medium-grained (less than 2.0 mm), subhedral, hexagonal cross-sectioned crystals with titanite and talc inclusions. Carbonate occurs as fine-grained, anhedral, interstitial crystals, or as an alteration product of plagioclase. Chlorite occurs as very fine- to medium-grained flakes (less than 3.0 mm), and defines the rock foliation. Crenulation cleavage is very prominent, and inclusions of opaques and titanite within the chlorite are common. Talc

occurs in trace amounts as fine-grained, anhedral crystals. Titanite occurs as very fine-grained, aggregates of crystals, often with the opaque minerals. Clinozoisite occurs in trace amounts as fine-grained, anhedral, prismatic crystals.

The chlorite schists occur as narrow units within the ultramafic suite. But the chlorite schists have only traces of actinolite, whereas some of the ultramafic rocks have abundant actinolite and tremolite. The change in mineralogy of the chlorite-rich units, specifically for the mafic minerals, suggests alteration under high fluid/rock ratio conditions. The fine-grained size and crenulation cleavage is indicative of ductile shear.

3.8 - Mafic Dykes

It can be very difficult to distinguish the mafic dykes from the meta-gabbros and meta-volcanics in the field. When outcrop size is large enough, cross-cutting relationships can be used. In other areas, where contacts are not visible or interpretable, changes in grain size or texture can be used. With small monolithologic outcrops, biotite is used as an indicator mineral of the mafic dykes, as biotite does not occur in the meta-gabbros or meta-volcanics.

The mafic dykes are distributed throughout the amphibolite belt, with samples collected from northeast of Actinolite; at many outcrops along County Road 20; and from a few outcrops along the road northwest of

Queensborough (Figure 7; Appendix A). The mafic dykes vary from fine-grained, massive units less than a metre wide, cutting across the host rock at steep angles (up to 90°), to coarse-grained dykes more than five metres wide, with an unknown cross-cutting angle due to small outcrop size. Some dykes may actually be sills, but with the limited exposure of some outcrops, the concordancy of the rock types cannot be proved.

The mafic dykes are characterized by two different textures; a fine- to coarse-grained, massive to lineated texture; and a "feather amphibolite" texture. Dykes with the latter texture have actinolite-porphyroblasts which are medium- to coarse-grained within a matrix of fine-grained, massive, plagioclase, quartz, chlorite and carbonate. The actinolite porphyroblasts are subhedral, with their terminations split to give a feathery appearance to the amphibole (samples TD-43, TD-44; Appendix A). In general, the mafic dykes are dark grey to greyish-black, massive to lineated, with seriate textures, having crystals up to 7.0 mm long. In thin section, the mineralogy comprises mixtures of; quartz, plagioclase, actinolite, biotite, chlorite, opaque minerals, carbonate, epidote, titanite and garnet (Appendix B). Quartz occurs as fine-grained, anhedral, interstitial crystals forming the matrix of the rocks with plagioclase, or occurring within veinlets with plagioclase. Plagioclase occurs as very fine- to medium-grained (less than 3.0 mm), anhedral, interstitial crystals with quartz in the matrix, or as subhedral, prismatic crystals. Simple and multiple twins are present. Many

plagioclase crystals have inclusions of actinolite and biotite, and are pervasively or selectively altered by sericitic mica. Actinolite is fine- to coarse-grained (up to 7.0 mm long), anhedral, equidimensional to subhedral, blade-like crystals. These elongate crystals define the lineation, when one is present. Abundant inclusions of plagioclase, quartz, carbonate and opaque minerals give some actinolite crystals a poikiloblastic texture. Chlorite pseudomorphs of actinolite are very common. The actinolite crystals are commonly deformed, and are characterised by bent and broken crystals, and radial extinction patterns. Brown biotite occurs as fine- to medium-grained (less than 4.0 mm in length), subhedral flakes, generally oriented parallel to the rock lineation. Opaque mineral inclusions are common in the biotite. Chlorite most often occurs as fine-grained, subhedral, blade-like flakes, disseminated throughout the section, or as pseudomorphs of actinolite. Chlorite may also occur as medium- to coarse-grained (up to 5.0 mm wide) subhedral flakes. Opaque minerals occur as fine-grained, anhedral, interstitial crystals disseminated throughout the section or replacing actinolite, and as medium-grained (3.0 mm), anhedral, skeletal crystals to subhedral, equidimensional square to rhombohedral cross-sectioned crystals. The larger opaque crystals have actinolite, plagioclase, and biotite inclusions. Carbonate occurs as fine-grained, anhedral, interstitial crystals within the rock matrix, or as veinlets. However, the carbonate is found more commonly occurring as a selective alteration

product on one set of twins of plagioclase, or altering actinolite from the rim of the crystal to the core. Carbonate pseudomorphs of actinolite are common. Clinozoisite, and more commonly epidote occur as fine-grained, anhedral, equidimensional crystals disseminated throughout the sections, or as epidote-rich zones. Titanite is rare, occurring as very fine- to fine-grained crystal aggregates, and can rim oxide minerals. Garnet is found in trace amounts as medium-grained (less than 4.0 mm), anhedral, elongate to fragmental crystals, having plagioclase, opaque or actinolite inclusions.

3.9 - Felsic Dykes

A few samples of felsic dykes were collected within two kilometres of the Elzevir Tonalite (sample KT-44; Appendix A). These dykes are 0.5 to 1.5 metres wide, medium- to dark-grey, massive to weakly lineated, fine- to medium-grained, and cut the foliation of the amphibolite host rocks at high angles. Thin sections show that they consist of 10 to 55 modal percent quartz, 10 to 75 modal percent plagioclase, 5 to 20 modal percent biotite, and chlorite, opaque minerals, carbonate and muscovite, (less than 20 modal percent) (Appendix B). The mineralogy and rock textures of the dykes are very similar to the rocks of the Elzevir pluton, and are believed to represent minor intrusions into the country rock [Connelly, 1986].

3.10 - Metasediments

The metasedimentary rocks are relatively easy to identify in the field because of compositional banding. Samples were collected in two areas; at the southern end of County Road 20, and along the road north of Queensborough (Figure 7). The metasediments collected north of Queensborough are within the Grimsthorpe Domain, but the samples from County Road 20 are on the northern edge of the Moira Lake Fault Zone, which defines the southern boundary of the Grimsthorpe Domain.

The samples collected at the southern end of Road 20 (samples KT-40, KT-41; Appendix A) are from outcrops that are banded, with bands being less than two centimetres thick, and alternate between dark and light colours, depending on differences in mafic mineral content. In thin section, the darker bands are rich in biotite, actinolite, epidote, and chlorite, while the lighter bands are rich in quartz, plagioclase and carbonate. The lighter bands have a brown weathered surface representative of the weathering of carbonate. Quartz pebbles are common throughout the outcrop, and are ellipsoidal, ranging 0.5 by 1.0 cm to 2.0 by 10 cm in cross-section. Boudinaged quartz veins are also present, with the boudins being slightly larger than the pebbles, and are usually separated by greater than 10 cm. Outcrops approximately 100 m to the south show pebbles to be even more flattened and stretched, suggesting that the Moira Lake Fault Zone is more intense to the south, along Highway 7 (Figure 6). These are very similar

rocks to those described by Wolff [1982] from the Bishops Corner Formation of the Flinton Group, just east of this study area. Thus, these deformed rocks are also part of the Flinton Group.

The other meta-sedimentary rock samples were collected north of Queensborough (UTM 305700E, 4942600N). The samples collected are fine- to medium-grained, banded, and dark grey. Bands consist of meta-wackes and meta-conglomerates. There are sulphide-rich bands throughout the succession. The mineralogy comprises actinolite (up to 60 modal percent), quartz (5 to 35 modal percent), plagioclase (10 to 40 modal percent), biotite (up to 25 modal percent), opaque minerals (up to 15 modal percent), carbonate (5 to 25 modal percent), chlorite (up to 10 modal percent), epidote (up to 5 modal percent), and muscovite (up to 10 modal percent) (Appendix B). The presence of meta-wackes and meta-conglomerates makes the unit similar to the Flinton Group described by Wolff [1982], and should be correlated with the Flinton Group.

The meta-sediments, now defined as Flinton Group rocks, are much younger than the amphibolite-ultramafic rocks, and thus are not relevant to the geologic interpretation of the Queensborough area at the time that the mafic and ultramafic rocks were formed.

3.11 - New Geologic Interpretations of the Queensborough Area

In summary, the recent field study in the Queensborough area suggests that the ultramafic-amphibolite belt of the Grimsthorpe Domain comprises ultramafic rocks along the western margin of the Elzevir Tonalite, followed by abundant meta-gabbros with unsystematically distributed mafic dykes and a few small outcrops of mafic meta-volcanics. The close spatial and temporal association of the meta-volcanics, meta-gabbros, mafic dykes, and ultramafics suggests that they were all emplaced during the same geologic event. Reconstruction suggests that a sequence of peridotites and pyroxenites are overlain by gabbros which intrude mafic pillow lavas. Jackson and Thayer [1972] suggests three models for such an emplacement of igneous rocks; 1) stratiform complexes; 2) concentric complexes; and 3) alpine complexes which includes ophiolite complexes (Table 3).

Stratiform complexes are found as intrusions into basaltic terranes and localized in Precambrian shields generally of Mesoproterozoic age, although they are most abundant in 2500 to 3500 Ma terranes. These are the only characteristics that may be common with the Queensborough area. Stratiform complexes are also characterised by sedimentary layering, strong contact metamorphism, and cyclic stratigraphy, none of which are present in the Queensborough area.

The Queensborough area has more common characteristics with the concentric complexes as compared with the stratiform complexes. These

Table 3 - Principal features of peridotite-gabbro complexes [Jackson *et al*, 1972].
Within the Alpine type; HST - Harzburgite sub-type; LST - Lherzolite sub-type.

	Stratiform	Concentric	Alpine
Characteristic Rock Types	Harzburgite, Orthopyroxenite, Websterite, Norite, Two-Pyroxene Gabbro, Anorthosite	Dunite, Wehrlite, Magnetite-Hornblende Pyroxenite, Two-Pyroxene Gabbro, Tonalite	HST: Harzburgite, Dunite LST: Spinel Lherzolite
Texture	Cumulus textures; apposition fabrics, seldom lineated	Cumulus textures; mush flow textures, apposition fabrics, commonly lineated	Tectonic fabrics (solid-flow textures), recrystallized textures, reequilibration textures
Structure			
A. Grain Orientation	Planar lamination	Lineate lamination	Foliation, lineation
B. Layers	Sedimentary in nature, mineral-graded layers; tabular; cyclic	Sedimentary, igneous, and metamorphic in nature, size graded layers, mush-flowage layers; sub-parallel to discordant; variable in layer repetition	Metamorphic and igneous in nature, solid flow layers; discordant; irregular repetition to absent
Cross-Cutting Structures	Rare "sandstone" dykes	Common mafic, ultramafic and pegmatitic dykes	Common mafic and ultramafic dykes
Structural Shape	Floored, tabular parallel to layers, funnel shaped	Cylindrical with roughly concentric map units	Very irregular, lensoid tectonic slices, diapiric cones

Cont..	Stratiform	Concentric	Alpine
Structural Setting	Intrusive into basaltic terranes; localized in Precambrian shields or basaltic terranes of any age	Intrusive into metamorphic country rocks; may be associated with granodiorite batholiths	Tectonic emplacements; fault contacts, serpentinite margins, brecciated borders, most are parts of ophiolite sequences
Age of Emplacement	Earliest Precambrian to Holocene; most abundant in 2500-3500 Ma. terranes	Pre-Devonian to middle Cretaceous	Late Precambrian to Tertiary; only one known older than 1200 Ma.
Mineralogy	Plagioclase, orthopyroxene, olivine, clinopyroxene, chromite	Clinopyroxene, olivine, plagioclase, hornblende, magnetite, orthopyroxene, chromite	HST: olivine, orthopyroxene, plagioclase, clinopyroxene, chromite LST: olivine, clinopyroxene, orthopyroxene, spinel, plagioclase, garnet, pargasite, phlogopite

characteristics include lineated to foliated grain textures, common cross-cutting mafic dykes and a structural setting, being associated with granodioritic batholiths (the Elzevir Tonalite). This last point may not be viable, as Elzevir-related dykes intrude the mafic rocks, making the mafic rocks older. Concentric complexes are further characterised by mush flow textures, concentric or cylindrical shapes and are generally pre-Devonian to middle Cretaceous, characteristics not present in the Queensborough area.

Alpine complexes have tectonic features of solid flow and recrystallization textures, foliated and lineated grain orientations, possible igneous and metamorphic layering, mafic and ultramafic cross-cutting dykes, an irregular structural shape, fault contacts, and possible serpentinite margins and brecciated borders, and are generally younger than the Mesoproterozoic. Most of these characteristics are shared with the Queensborough area. The age of emplacement may be a characteristic not shared, as the Queensborough area is intruded by the 1270 Ma Elzevir Batholith and Jackson and Thayer [1972] note that only one alpine complex was known to be older than 1200 Ma.

Thus, the best interpretation for the Queensborough succession is an alpine peridotite-gabbro complex. Ophiolite complexes generally fit into the alpine type gabbro-peridotite complex. An idealized ophiolite sequence consists of a basement of metamorphosed ultramafic rocks, ultramafic cumulates, cumulate gabbroic rocks, sheeted diabase-basaltic dykes, and

pillow lavas, usually overlain by cherts, argillites and limestones (Figure 8) [Hall, 1987]. Most of these units occur in the Queensborough area amphibolite-ultramafic belt with the exception of the sheeted dyke complex. There is a possibility that the sheeted dykes are present, but the lack of large exposures to properly map the intrusive contacts may preclude this observation. Furthermore, Williams and Malpas [1971] note that most of the sheeted dyke complexes that have been mapped are highly brecciated. They attribute this to cool ocean waters circulating through the dykes while the dykes are warm, causing quick cooling and brecciation. Thus, some of the brecciated zones in the Queensborough amphibolite rocks may be sheeted dykes. Therefore to a first order approximation, the Queensborough rock succession could be considered a partial ophiolite sequence.

In summary, the rock succession for the Queensborough area has up to 800 metres of ultramafic rocks, consisting of zones of pyroxenite and peridotite, and possibly dunite. Overlying the ultramafics, are meta-gabbros with mafic dykes that are at least three kilometres thick, and up to five kilometres thick which intrude pillowed basaltic meta-volcanic rocks. This rock succession is very similar to the idealized ophiolite, except for the possible absence of the sheeted dyke complex. This is not surprising as there are few places in the world where complete ophiolite sequences are present (eg. Semail, Newfoundland). Erosion has been extensive in the

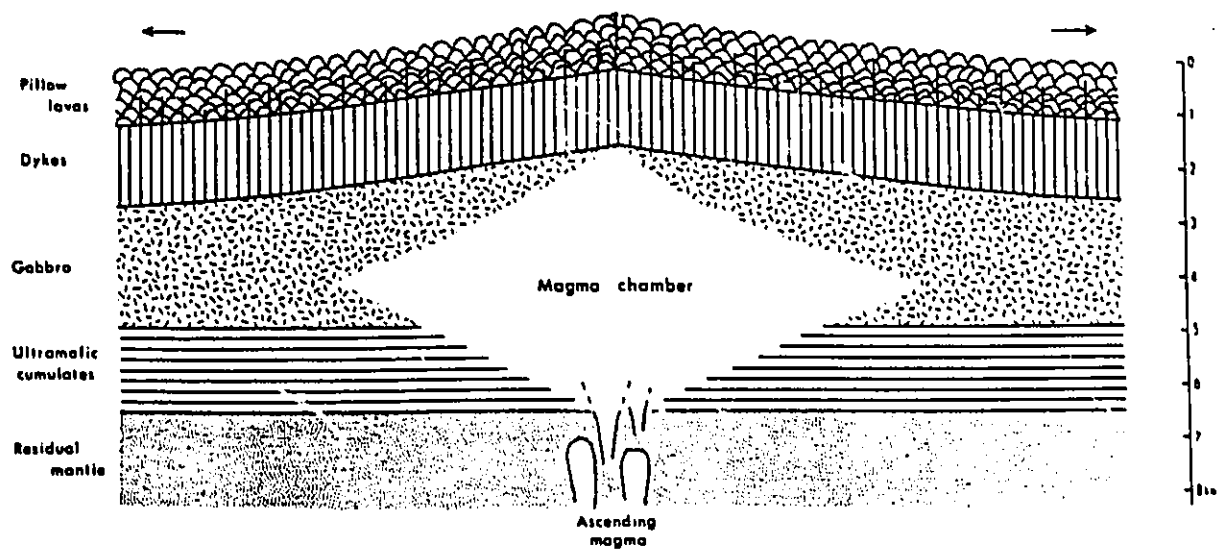


Figure 8 - An idealized cross-section through an oceanic spreading axis [from Hall, 1987].

Central Metasedimentary Belt, with estimates of over 20 km of rock being eroded away (eg. Moore, 1986; Davidson, 1986), more than enough to remove 2 to 6 km of pillows and sheeted dykes.

Thus, it is proposed, herein, that the belt of mafic and ultramafic rocks along the western side of the Elzevir Tonalite is a partial ophiolite sequence, and is herein named the Queensborough Ophiolite Complex.

The Queensborough Ophiolite Complex is completely metamorphosed and deformed, and is poorly exposed. Thus it cannot be mapped in detail and is therefore difficult to compare with more modern and well known ophiolite complexes. However, the Eastern Papua Ophiolite in New Guinea, which formed when a Paleogene island arc collided with continental crust of the Indo-Australian plate [Jaques and Robinson, 1977], has a rock succession [Davies, 1971] similar to that of the Queensborough complex. Similarly, the Yakuno Ophiolite in southwest Japan, also has a similar rock succession [Koide *et al.*, 1987], and similar major and normative chemistry of basalts and gabbros, with the Queensborough Complex. In both modern analogues, the sheeted dyke complex is absent. This is a feature atypical of ophiolite complexes formed in major ocean basins [Coleman, 1977]. Karig [1971] suggests that the complexes may be fragments of crust from a marginal basin, where oceanic crust forms in much less time, which may not allow for the intrusion of the sheeted dykes. The implication of a

marginal basin is comparable to the Belmont and Grimsthorpe Domains, as Smith and Holm [1987] interpret the Belmont Domain as a marginal basin.

Chapter 4 - Geochemistry

4.1 - Introduction

The major and trace element compositions of all samples collected during the 1987 field season were determined by standard X-Ray Fluorescence (XRF) techniques using a Phillips PW1410 X-ray spectrometer. Selected samples collected during the 1992 and 1993 field seasons were analyzed by standard Inductively Coupled Plasma - Mass Spectrometer (ICP-MS) techniques using a Fisons Instruments - VG PQe/Eclipse ICP-MS. The results and precision of these analyses are given in Appendix C.

4.2 - Chemical Alteration

All the rocks analyzed have been altered mineralogically and probably chemically during regional metamorphism. For instance, Smith and Holm (1990a, 1990b) have shown that similar meta-volcanic rocks, and associated dykes, of the neighbouring Belmont Domain have undergone increases in K_2O and Na_2O , and a decrease in CaO . They also suggest that the erratic distributions of Ba, Rb, Sr, and U indicate that their concentrations have been modified during metamorphism.

Beswick and Soucie [1978] have developed a method to identify the type and intensity of chemical alteration affecting volcanic rock suites during metasomatism and metamorphism. They show that unaltered

modern igneous rock suites all plot within well defined fields on log molecular ratio plots (LMPR plots) as predicted by Touminen [1964]. Two initial assumptions are used in this method; firstly, the altered rocks had original compositions which would have plotted within the trends defined by similar, but unaltered rock types; and secondly, Al_2O_3 has remained immobile during alteration as suggested by Carmichael [1969] and Fisher [1970].

The method involves plotting three components X, Y, and Z, on a graph that has axes of $\log X/Z$ versus $\log Y/Z$. Should there be any alteration to any of the components, the sample will not plot within the fields defined by the modern, unaltered suites. If alteration is present, and affects the X component, the sample will be shifted parallel to the X/Z axis. If the Y component is affected, the sample will be shifted parallel to the Y/Z axis. If the Z component is affected, the sample will be shifted along a line with a slope of 45° . If more than one of the three components are altered, the sample will plot along a vector that is the resultant of the two or three components. The further the sample plots from the modern field, the greater the intensity of alteration in the sample [Beswick and Soucie, 1978]. As more than one component can be altered, a single plot will not allow for a unique solution of the alteration taking effect, and thus a series of plots is necessary.

The Queensborough area meta-volcanic, meta-gabbroic and mafic dyke rocks described in Chapter 3 (from here on in called mafic rocks) are interpreted as being formed during the same igneous event (eg. formation of oceanic crust). They are all considered to be related by crystal-melt equilibria and thus originally should all lie within the fields shown in the Beswick and Soucie plots. They have also all been affected by the same metamorphic and tectonic events and should show the same types of alteration. The mafic rocks of the Queensborough Ophiolite Complex are plotted on LMPR plots (Figure 9), as well as composite samples of sea floor basalts (SFB) and Hawaiian tholeiite basalts (HTB) [Best, 1982] as examples of modern unaltered basalts.

In Figure 9A, all the meta-volcanics, most of the meta-gabbros and some of the mafic dykes lie within the field defined by the modern unaltered rocks from Beswick and Soucie [1978] and in between the SFB and HTB. These samples are considered to have a negligible amount of chemical alteration in SiO_2 , Al_2O_3 , and K_2O . A few meta-gabbros and mafic dykes lie to the upper right of the diagram, suggesting that K_2O may be depleted in those samples. Mafic dyke samples which lie to the lower left of the diagram may be diagnostic of samples which have undergone K_2O enrichment.

In Figure 9B, the majority of the mafic samples lie within the modern field, and in between the HTB and SFB. There are a few meta-gabbros and

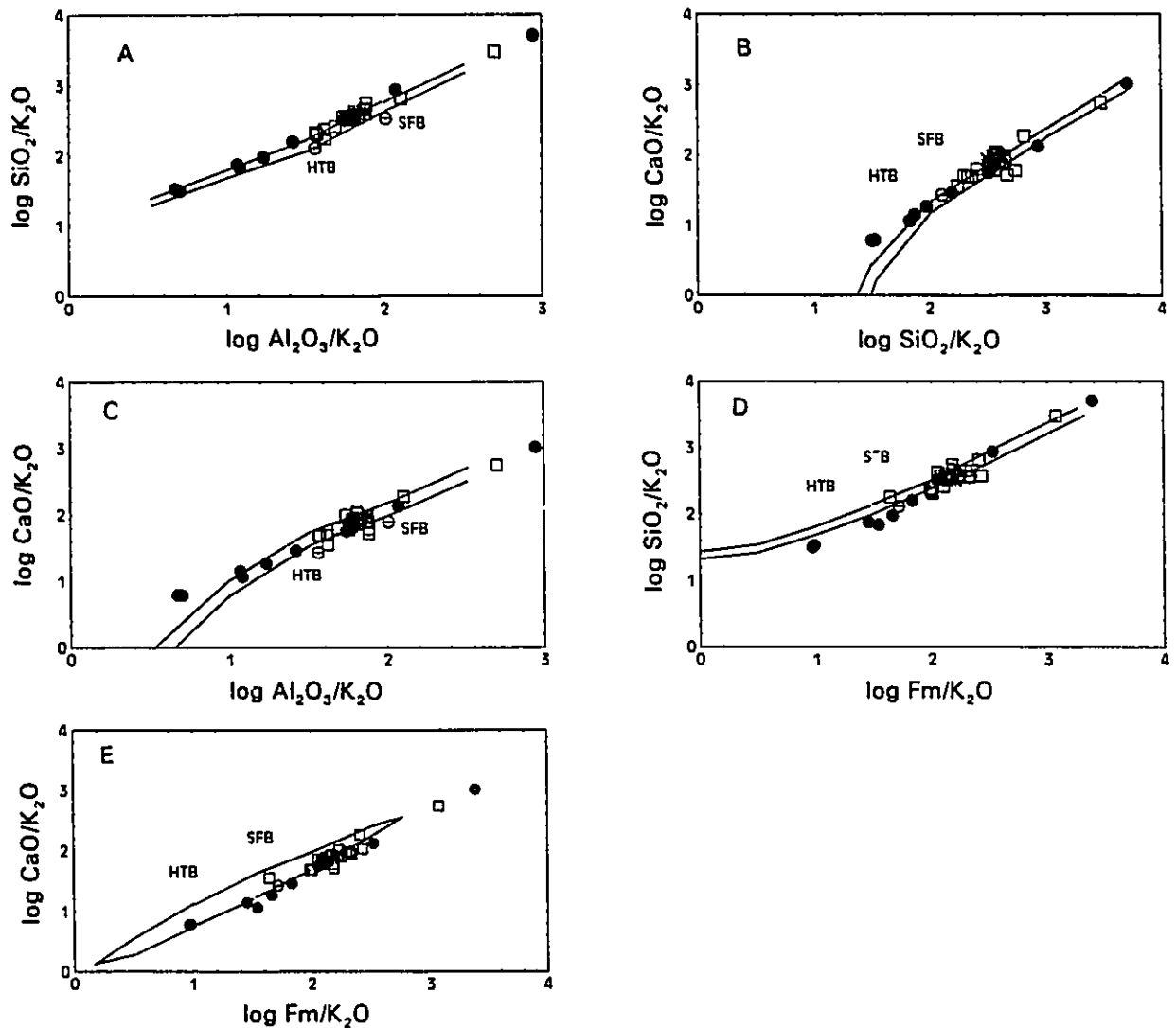


Figure 9 - Log Molecular Proportion Ratio plots normalized to K_2O from Beswick and Soucie [1978]. Symbols are; filled circles - mafic dykes; open squares - meta-gabbros; asteriks - meta-volcanics; circles with dash - average sea floor basalts (SFB) and Hawaiian tholeiitic basalts (HTB) [from Best, 1982].

mafic dykes which show K_2O depletion, and a few mafic dykes which show K_2O enrichment, as seen in Figure 9A. As well, in the lower left corner, two mafic dykes plot above the modern field, due to either SiO_2 depletion, or CaO or K_2O enrichment.

Figure 9C shows the same general pattern for the mafic samples as seen in Figures 9A and 9B. Most of the samples lie within the modern field, and in between the HTB and SFB. There are a few meta-gabbros and mafic dykes with K_2O depletion and a few mafic dykes with K_2O enrichment.

Figure 9C also shows two mafic dykes to plot above the modern field as seen in Figure 9B. In this plot, this may be due to either Al_2O_3 depletion, or CaO or K_2O enrichment. As Al_2O_3 is assumed to be immobile, CaO or K_2O must be enriched. In Figures 9B and 9C, as the origin is approached, the modern field curves downwards, leaving the 45° slope seen at the top of the curve. Extrapolation shows that the two mafic dykes plot along the 45° slope, and thus alteration can be attributed to K_2O , not CaO.

Figure 9D shows many of the mafic samples to lie along the bottom boundary of the modern field, but still between the HTB and SFB. This may suggest a minor amount of Fm^1 enrichment. Some meta-gabbroic and mafic dyke samples have K_2O depletion and some mafic dykes have K_2O enrichment. Figure 9E shows many of the mafic samples along the bottom

¹ Fm equals $MgO + MnO + FeO^*$ (in molecular weight percent).

boundary of the modern trend, but between the HTB and SFB samples. Similar to Figure 9D, the samples may be slightly enriched in Fm elements. The samples with K_2O depletion and enrichment are still present. As well, the two mafic dykes to the bottom right are within the modern field, supporting the earlier interpretation that K_2O and not CaO is enriched.

The majority of the mafic samples are relatively unmodified in SiO_2 , Al_2O_3 , Fm elements, CaO and K_2O . Some meta-gabbros and mafic dykes have K_2O depletion, while some mafic dykes have K_2O enrichment. This is consistently shown in all five diagrams. Figures 9D and 9E show many of the mafic samples to lie along the bottom boundary line of the modern unaltered field. This may be suggestive of Fm enrichment (increases in FeO , MgO and/or MnO) or it may be coincidental, as much of the original data from Beswick and Soucie [1978] lie along the same line.

Figure 10 is another LMPR plot, with Na_2O as the normalizing factor, instead of K_2O . All samples of the Queensborough Ophiolite Complex are plotted, with the composites of the Hawaiian tholeiite basalts and sea floor basalts. Fields for modern, unaltered volcanics are only available for Figures 10D and 10E, which show most of the meta-gabbros to lie along the top boundary, and the mafic dykes to lie along the bottom boundary. The meta-volcanics lie within the fields, although near the top right portions of the fields. The scatter from top right, to bottom left, relative to the sea floor basalts and Hawaiian tholeiite basalts indicate Na_2O alteration is present. In

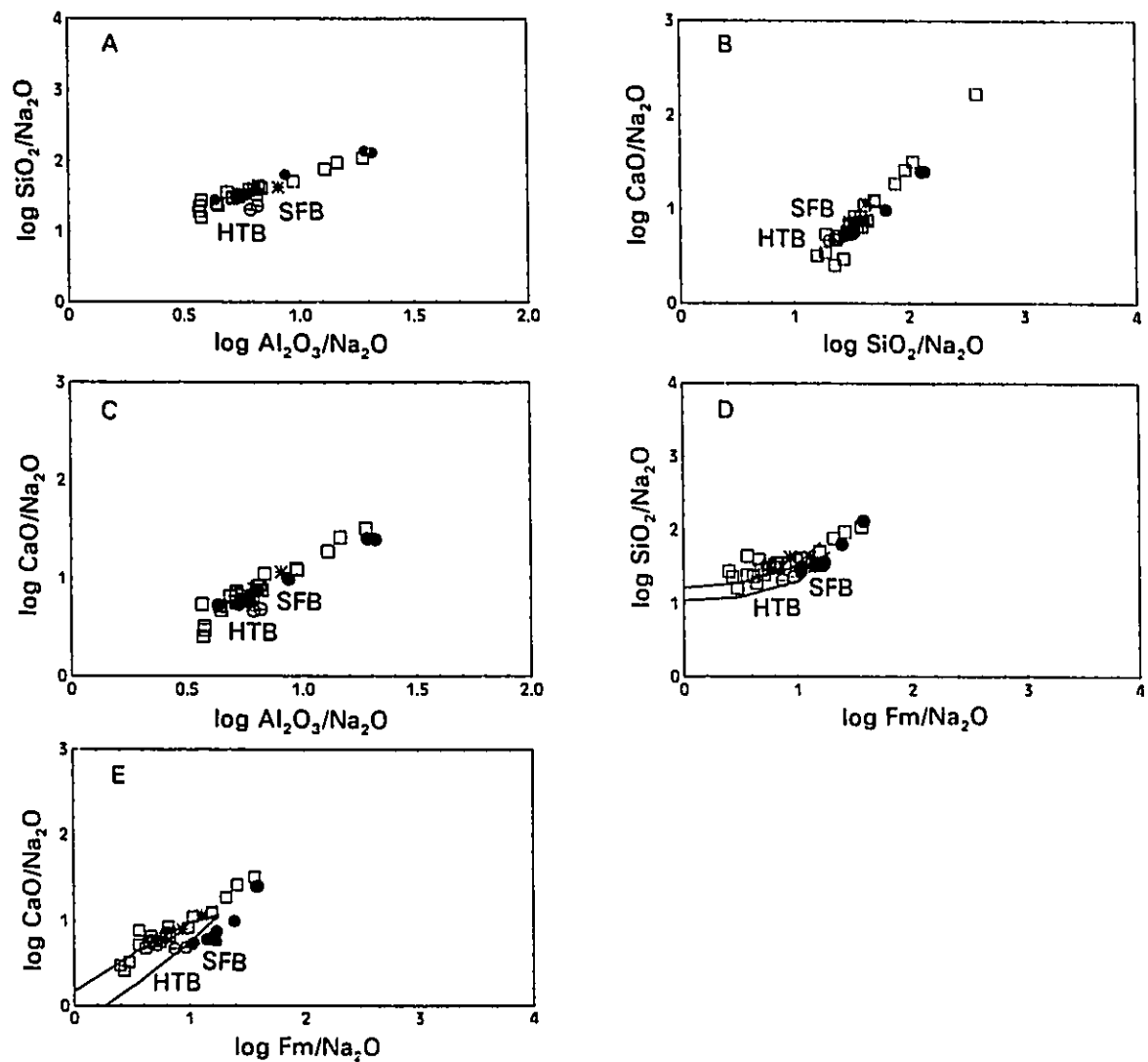


Figure 10 - Log Molecular Proportion Ratio plots normalized to Na_2O from Beswick and Soucie [1978]. Symbols as in Figure 9.

Figures 10A to 10C, the mafic samples show linear trends, with little variation in X and Y directions, but do show variation along a 45° slope, which further indicates Na₂O alteration.

Thus, along with K₂O alteration, Na₂O is modified in some of the samples. The relative immobility of SiO₂, Al₂O₃, Fm elements and CaO shown in Figure 9 is supported by Figure 10.

The distributions of the Queensborough ultramafic samples on the LMPR plots (Figures 9 and 10) are not susceptible to consistent interpretations. This is because the fields on the LMPR plots were defined using unaltered mafic to felsic volcanic rock suites [Beswick and Soucie, 1978] and did not include ultramafic, komatiitic volcanics. The ultramafic samples are therefore plotted on molecular proportion ratio plots (MPR plots) specifically designed by Beswick [1982] to describe the fractionation trends and alteration of komatiitic rocks. These plots have axes of; SiO₂:TiO₂ vs. FM²:TiO₂, SiO₂:Al₂O₃ vs. FM:Al₂C₃, SiO₂:CaO vs. FM:CaO, SiO₂:Na₂O vs. FM:Na₂O, and SiO₂:K₂O vs. FM:K₂O. SiO₂ and FM are the main components in olivine and calcic clinopyroxene, which are the dominant minerals in komatiites and komatiitic basalts. The denominators in each plot are elements which are not extensively present in olivine [Beswick, 1982], and thus will show if the rocks have had any chemical modifications. The ratio

² FM equals MgO + FeO* [Beswick, 1982].

of FM:SiO₂ in olivine is 2:1, and defines a komatiite trend as komatiites are dominantly olivine fractionated. Conversely, FM:SiO₂ of 1:2 is the oxide ratio of calcic clinopyroxene, which is the dominant mineral fractionating in komatiitic basalts [Beswick, 1982]. Thus, suites of komatiites or komatiitic basalts, which have no major mobilization of SiO₂, TiO₂, Al₂O₃, CaO, Na₂O, K₂O or FeO* + MgO, should plot along the appropriate ratio line [Beswick, 1982].

The Queensborough ultramafic samples are plotted on the MPR plots (Figure 11). They are divided into the four mineralogical assemblages discussed in Chapter 3 (section 3-5). The five plots can be separated into two groups; group one consisting of Figures 11A, 11B and 11C; and group two consisting of Figures 11D and 11E.

The first group all show the ultramafic samples to lie in a broad linear zone between the two ratio lines. Within this zone, each assemblage has a linear trend, with minimal scatter. Assemblages I and II have the greatest slope, assemblage III has a slightly shallower slope, and assemblage IV has the lowest slope (Figure 11). Much of the scatter in the ultramafic suite is attributed to the modal mineralogy of each assemblage. Assemblages I and II consist of plagioclase and actinolite, and actinolite and talc respectively. These assemblages were interpreted to be originally dominated by pyroxene, and this is indicated, as the slopes near that of the 1:2 ratio line of calcic clinopyroxene (Figure 11). Assemblage III is mainly talc and carbonate, and

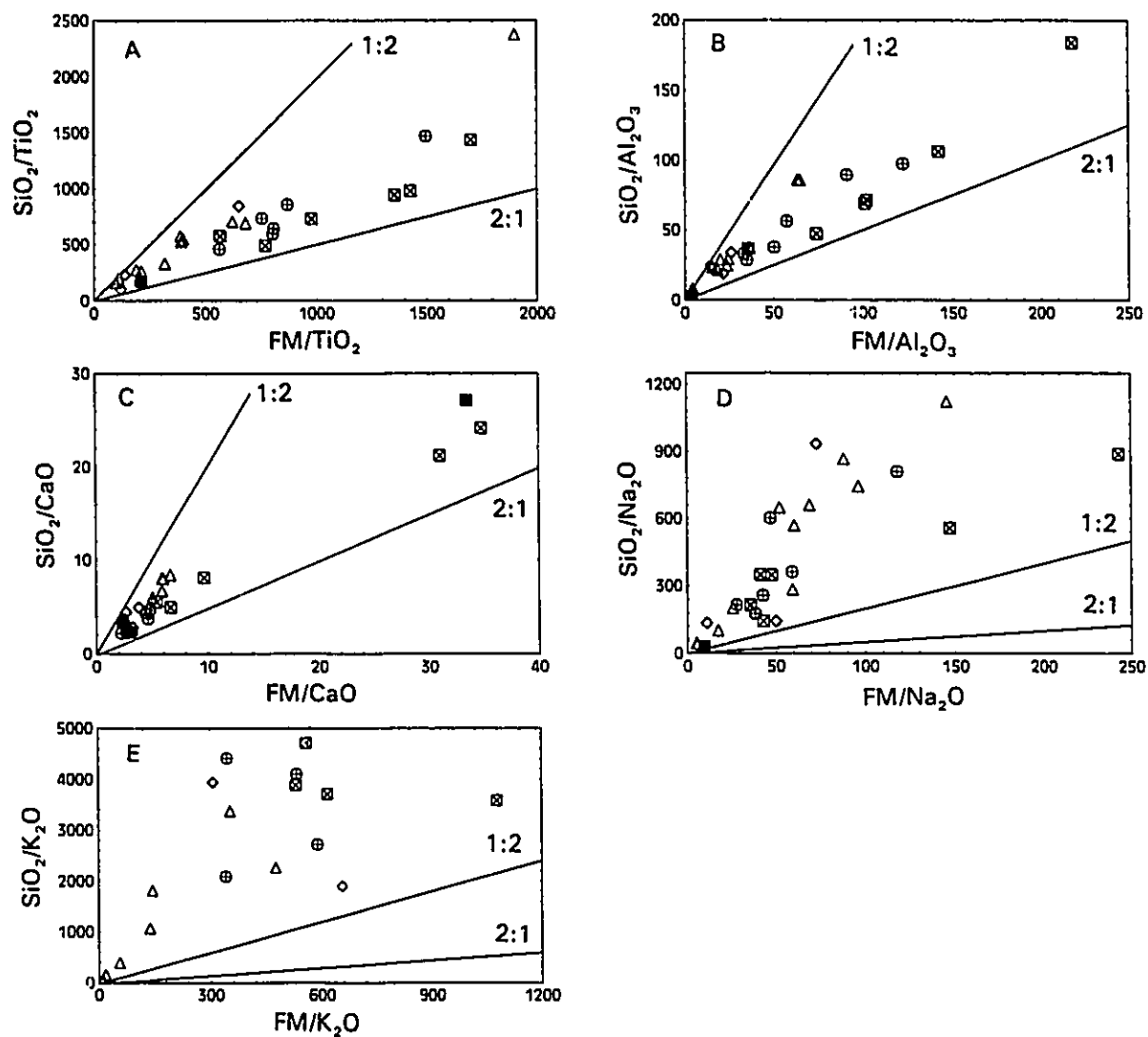


Figure 11 - Molecular Proportion Plots for ultramafic rocks from Beswick [1982]. Symbols are; triangles - assemblage I; diamonds - assemblage II; circles with crosses - assemblage III; squares with crosses - assemblage IV; filled square - chlorite schist.

is considered to have been a mixture of pyroxene and olivine, and thus would lie on a lower slope than assemblages one and two. Assemblage IV consists of serpentine and talc, and thought to be originally dominated by olivine, which is shown as the slope nears the 2:1 olivine ratio line (Figure 11). The amount of X and Y scatter from each of the assemblage's trend line is minimal, which suggests that is little alteration of total $\text{FeO} + \text{MgO}$, TiO_2 , Al_2O_3 , and CaO . Although linear trends are present for each of the assemblages, SiO_2 is not completely immobile. This is shown by the high concentrations of SiO_2 for some of the ultramafic samples (Figure 12) which suggests that silicification may be present. This is a common feature of ultramafic and mafic rocks undergoing deformation and alteration [W.H. Blackburn, pers. comm, 1994].

The second group of graphs, Figures 11D and 11E show wide scatter not only within the ultramafic suite but also within each assemblage. As SiO_2 and the FM elements are inferred to be relatively immobile from Figures 11A through 11C, K_2O and Na_2O must be the mobile elements. This is consistent with the interpretation of the mafic rocks, where K_2O and Na_2O were shown to be modified. This consistency is not surprising as the mafic and ultramafic rocks should have the same metasomatic and metamorphic histories.

4.3 - Major Element Data

The major elements are plotted on variation diagrams versus MgO, for each rock suite (Figure 12). As K_2O and Na_2O have been shown to be modified by metamorphism, they are not discussed. The most prominent feature of all the diagrams is the five percent gap (from approximately 10 to 15%), where no samples plot, and that separates the mafic rocks from the ultramafic rocks. Also noticeable, are the differences in chemical trends of the mafic rocks compared to the ultramafic rocks.

There are only a few samples of meta-volcanic rocks which show limited range in major element contents (Figure 12; Appendix C). The meta-volcanic samples plot as high-Fe tholeiitic basalts on the Jensen Cation Plot (Figure 13).

The meta-gabbroic samples have a range of MgO (3 to 10 wt. %), with relatively wide ranges (compared to the other rock suites) of SiO_2 (42 - 58 wt. %), TiO_2 (0.1 - 3.0 wt. %), Fe_2O_3 (5 - 22 wt. %) and MnO (0.05 - 0.4 wt. %). The other elements show a more limited range; Al_2O_3 (12 - 17 wt. %), except for one sample (22 wt. %); CaO (6 - 13 wt. %); and P_2O_5 (0.05 - 0.4 wt. %). They show increasing trends of SiO_2 , Al_2O_3 , Fe_2O_3 , MnO, and P_2O_5 and decreasing trends of TiO_2 and CaO versus decreasing MgO (Figure 12).

The mafic dykes have a range of MgO (4 - 9 wt. %), with relatively wide ranges of SiO_2 (47 - 55 wt. %), TiO_2 (0.2 - 3 wt. %), Fe_2O_3 (10 - 19

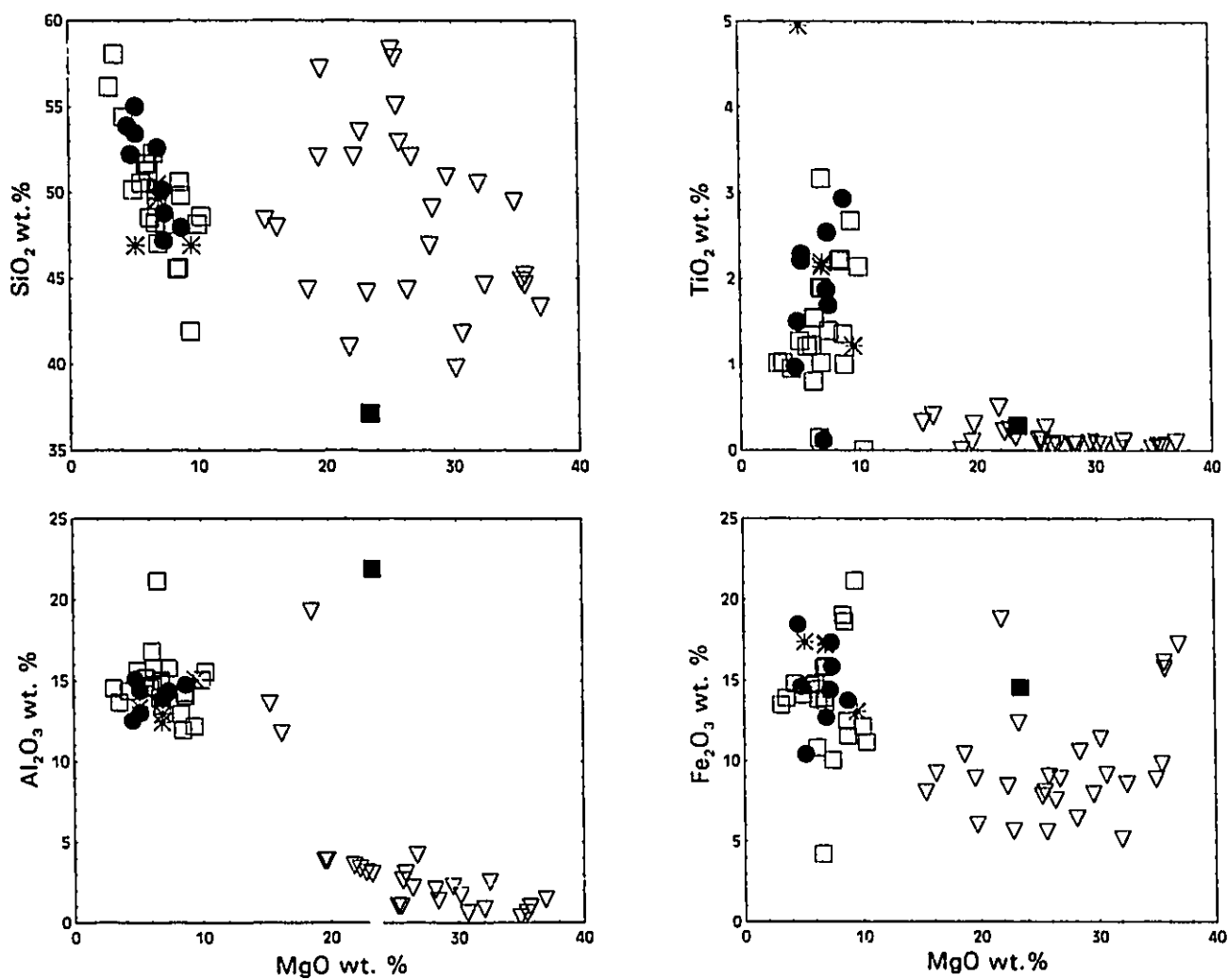


Figure 12 - Major element variation plots versus MgO. Symbols are; inverted triangles - ultramafics; filled circles - mafic dykes; open squares - meta-gabbros; asteriks - meta-volcanics; filled squares - chlorite schists.

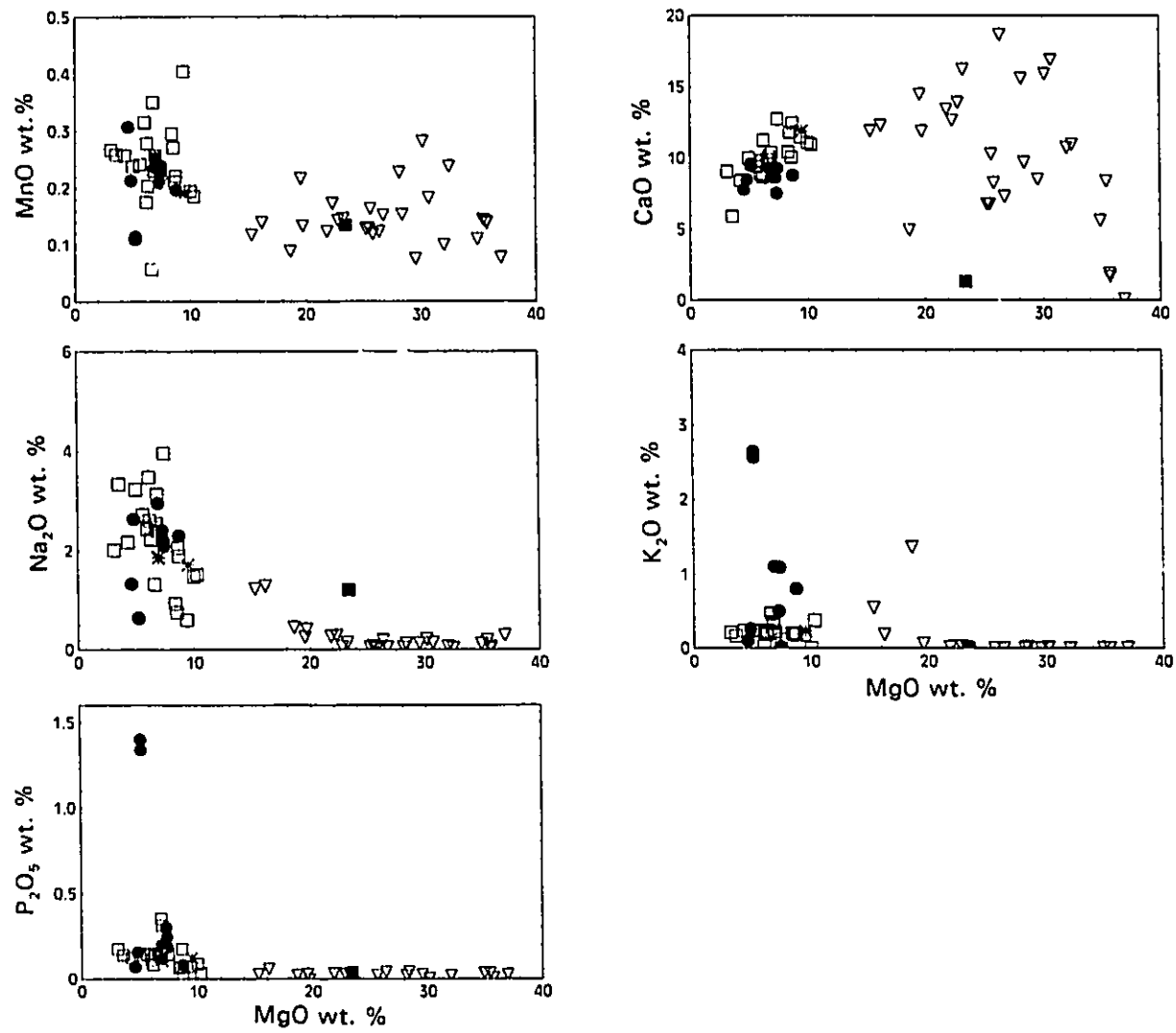


Figure 12 - ... continued

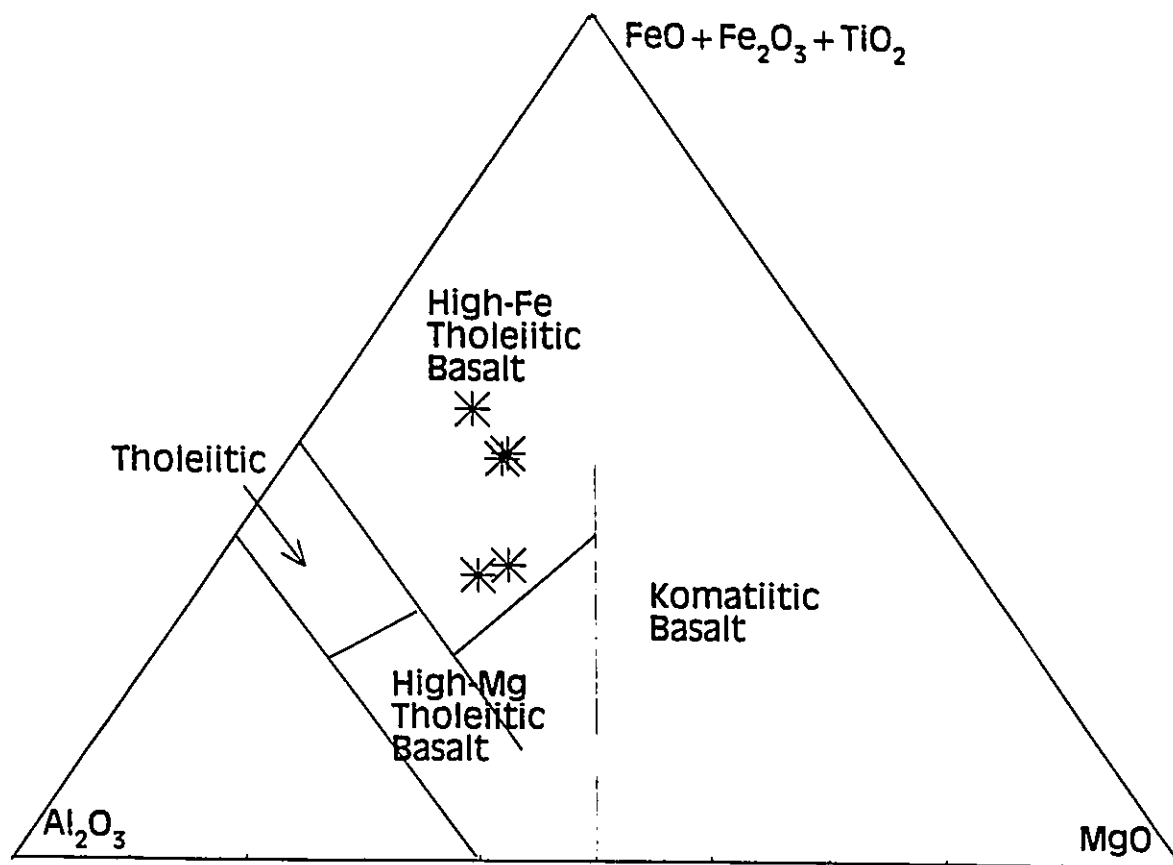


Figure 13 - Jensen Cation Plot of the meta-volcanic samples of the Queensborough area.

wt. %), and P_2O_5 (0.1 - 1.4 wt. %). The other major elements have more limited ranges; Al_2O_3 (12 - 15 wt. %); MnO (0.1 - 0.3 wt. %); CaO (7 - 10 wt. %); and P_2O_5 (0.1 - 0.4 wt. %) except for two samples near 1.4 wt. %. The mafic dykes show increasing trends of SiO_2 , Fe_2O_3 , MnO, and P_2O_5 , and decreasing trends of TiO_2 , and Al_2O_3 with decreasing MgO. Although most of the samples plot in a general trend, a few of the mafic dykes plot as outliers from the trends. For example, on the P_2O_5 vs. MgO and the MnO vs. MgO graphs, two samples plot well above and below the majority of the samples, respectively. This may be explained by the presence of more than one dyke suite. This is not an unreasonable assumption; in the neighbouring Belmont Domain, Smith and Holm [1987, 1990a, 1990b] have identified seven suites of dykes.

The similar trends in many of the plots (ie. SiO_2 vs. MgO, Fe_2O_3 vs. MgO; Figure 12), shown by the three mafic suites support the interpretation that they are petrogenetically related and were formed during the same geologic event. These trends are typical of rocks which have formed by mineral-melt equilibria processes (ie. fractional crystallization or partial melting).

The ultramafics have a wide range and high contents of MgO (Figure 12; Appendix C), which vary systematically among the four mineralogical assemblages within the suite (Chapter 3). Assemblages I and II have between 15 and 28 weight percent MgO, and assemblages III and IV have

between 26 and 38 weight percent MgO (Appendix C). The difference between the two groups can be related to the presence of serpentine in assemblages III and IV (Appendix B). Assemblages I and II show increasing trends of TiO_2 and Al_2O_3 , and decreasing trends of CaO with decreasing MgO. Assemblages III and IV show increasing trends of Al_2O_3 , MnO and CaO and decreasing trends of Fe_2O_3 with decreasing MgO. The ultramafic suite has on the average, very low contents of TiO_2 , Al_2O_3 , Fe_2O_3 , and P_2O_5 as compared to the averages of the mafic rocks (Figure 12; Appendix C), while SiO_2 , MnO, and CaO averages are similar. The chemical variations within the ultramafic suite can be attributed to the original mineralogy. Assemblages I and II, which contain the lower contents of MgO for the ultramafic suite, comprise mostly of actinolite/tremolite, chlorite and plagioclase, and actinolite, carbonate and talc respectively. Assemblages III and IV comprise talc and carbonate, and serpentine, talc and carbonate respectively. The ultramafics in Figure 12 show increasing TiO_2 and Al_2O_3 with decreasing MgO, and evenly distributed Fe_2O_3 , MnO and P_2O_5 . These trends suggest assemblages I and II were originally dominated by pyroxene, while olivine dominated assemblages III and IV.

As discussed in section 3.7, the chlorite schists are zones of intense deformation and appear to be principle locations of fluid movement. Their chemistry generally plots within the fields occupied by the ultramafic suite (at MgO = 23 wt. %). TiO_2 , MnO, and P_2O_5 contents in the chlorite schists

are similar to the average contents of the ultramafics but the chlorite schists have more Al_2O_3 , Fe_2O_3 and less SiO_2 and CaO than the ultramafics. The presence of plagioclase and chlorite within the schists account for the Al_2O_3 increase, while the greater proportion of chlorite, amphibole and opaque minerals in the schists compared to the ultramafics account for the higher contents of Fe_2O_3 . The SiO_2 and CaO decrease may be attributed to the mobility of these elements during deformation and metasomatism.

4.4 - Trace Element Data

All trace element data can be found in Appendix C, and are plotted in Figure 14 versus MgO . With the erratic distribution of Ba, Rb, and Sr in Figure 14, and the indication of their mobility in the Belmont Domain [Smith and Holm, 1987], which has had a similar metamorphic history as the Grimsthorpe Domain, they are not discussed.

The meta-volcanic samples have relatively large ranges of Cr (100 - 450 ppm), Nb (5 - 23 ppm), V (20 - 50 ppm) and Zr (60 - 280 ppm). They show more limited ranges of; Co (40 - 70 ppm), and Ni (70 - 120 ppm). The meta-volcanics show increasing trends of Nb, Y, and Zr, and decreasing trends of Co, Cr, and Ni against decreasing MgO (Figure 14).

The meta-gabbros have relatively large ranges of Co (20 - 80 ppm), Cr (30 - 600 ppm), Nb (1 - 21 ppm), Ni (10 - 240 ppm), V (20 - 1400 ppm), and Zr (0 - 200 ppm) and a more limited range of Y (0 - 40 ppm). They

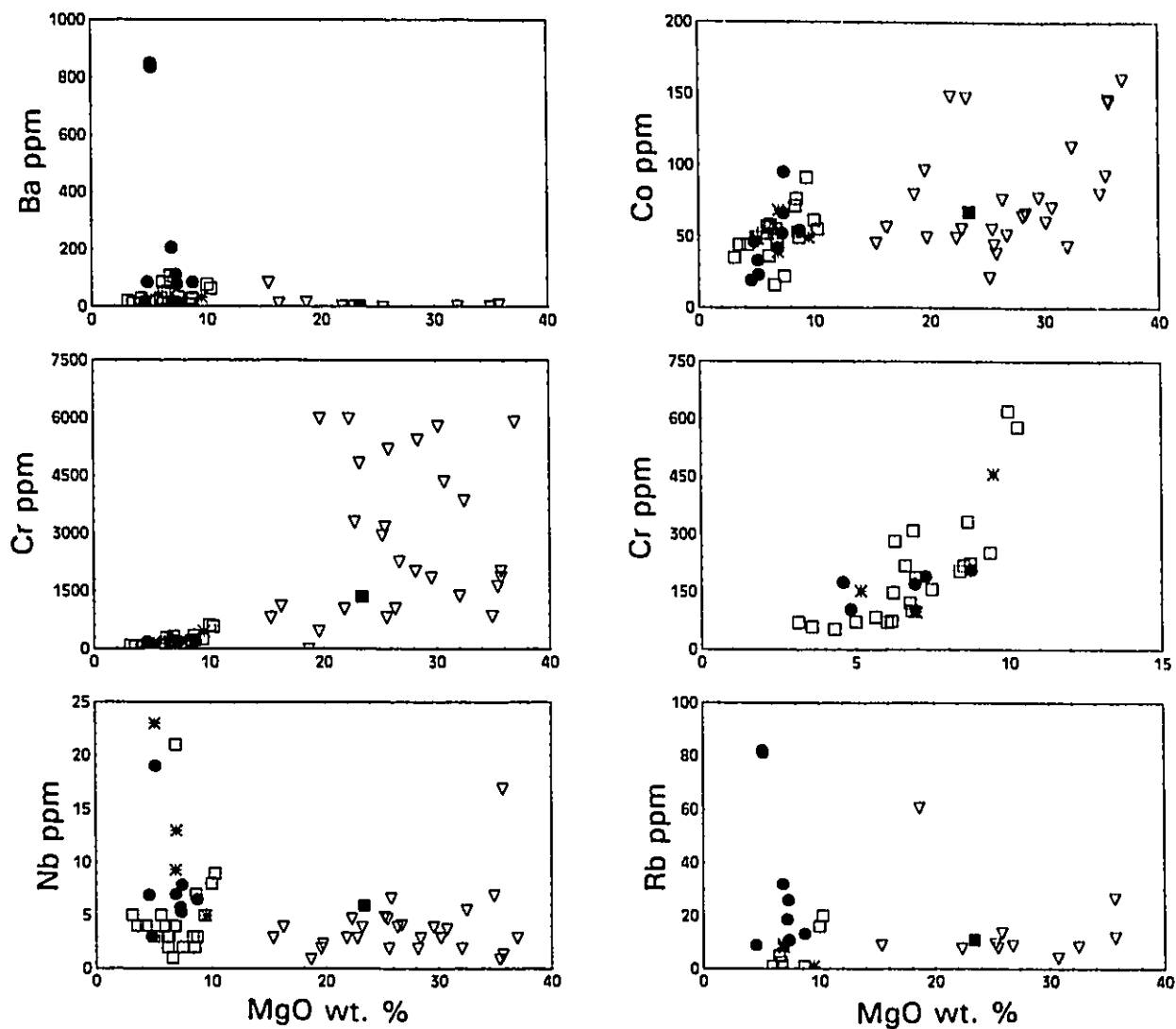


Figure 14 - Trace element variation plots versus MgO. Symbols are; inverted triangles - ultramafics; filled circles - mafic dykes; open squares - meta-gabbros; asteriks - meta-volcanics; filled squares - chlorite schists.

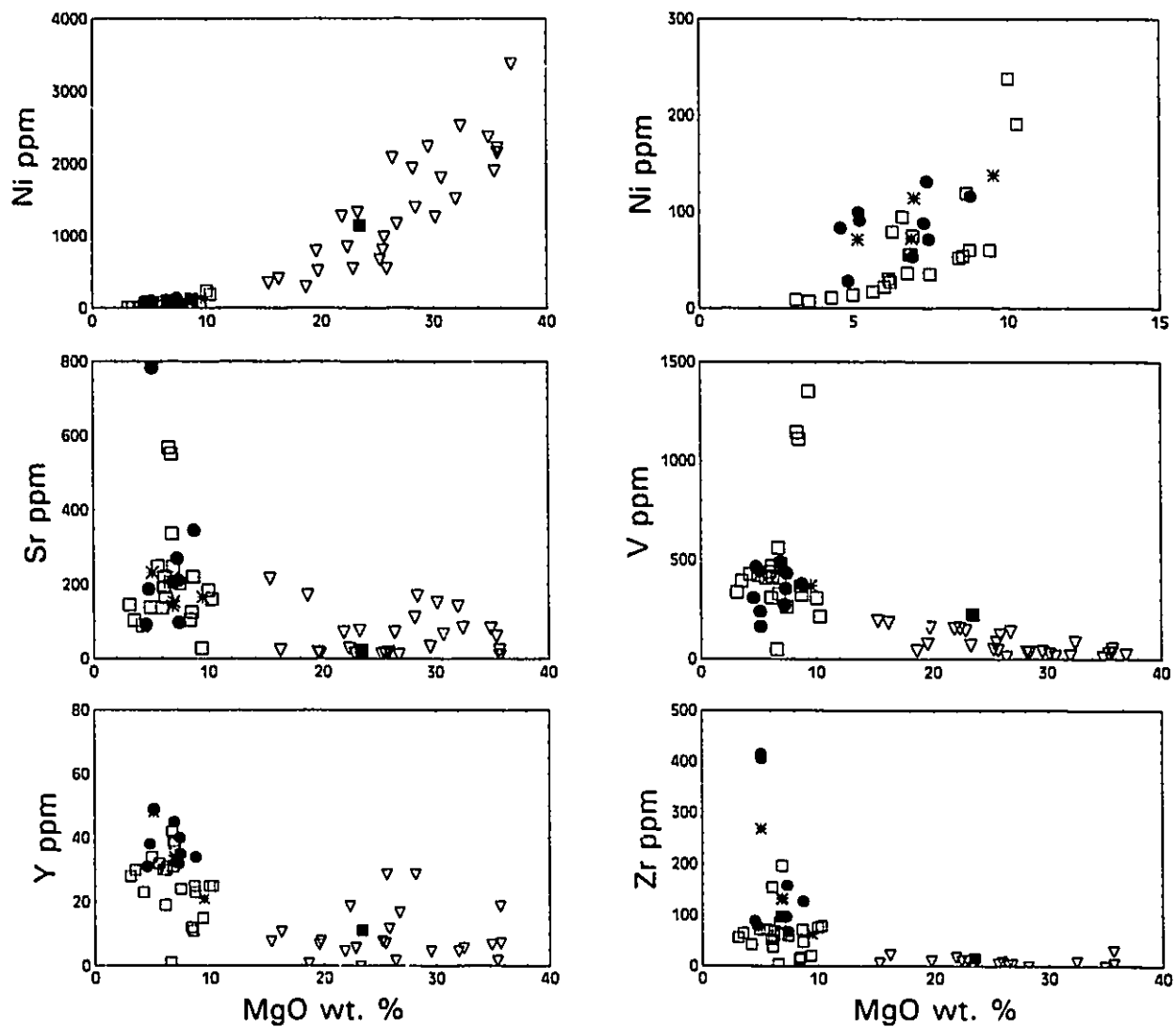


Figure 14 - ... continued.

show increasing trends of Nb and Y, and decreasing trends of Co, Cr and Ni against decreasing MgO (Figure 14).

The mafic dykes have relatively large ranges of Co (20 - 100 ppm), Nb (3 - 19 ppm), Ni (30 - 140 ppm), V (200 - 500 ppm) and Zr (50 - 400 ppm). They show more limited ranges of Cr (120 - 180 ppm) and Y (40 - 50 ppm). The dykes show increasing trends of Nb, V, Y and Zr, and decreasing trends of Co, Cr and Ni against decreasing MgO. In the plots of Nb, Ni, V, Y and Zr, the trends have some scatter to them, from the presence of more than one dyke suite, and thus variations in original concentrations. Trace element ratios suggest that three mafic dyke suites are present (Table 4). Zr/Y, V/Y and V/Zr ratios clearly define the three suites, while Nb/Y ratios can define two groups. Table 4 compares trace element ratios of the Queensborough mafic dykes with selected dyke suites from the Belmont domain. Group I dykes (TD-18, 33 and 43) of the Queensborough area can be roughly compared with the Turriff dykes on the basis of Zr/Y, V/Y and V/Zr ratios. Group II dykes (TD-48, 50, 51, and 52) can be compared with either the Low Zirconium Suite (LZS) or the Tudor dykes using all four ratios. The Group III dykes (TD-55 and 55D) do not compare with any of Smith and Holm's suites very well. The most conspicuous feature of the Group III dykes is their high contents of Zr (Figure 15). The Group I dykes have the steeper slope in the Y vs. Zr graph.

	Nb/Y	Zr/Y	V/Y	V/Zr
LZS	0.11	2.83	7.67	2.71
IZS	0.10	2.96	6.09	2.06
HZS	0.14	4.54	1.96	0.43
Turriff				
BD3	0.18	2.41	7.84	3.25
BD52	0.31	2.35	8.11	3.46
Tudor D				
BD8	0.15	3.13	6.85	2.19
BD16	0.14	2.83	7.29	2.58
BD21	0.19	2.99	7.15	2.40
Queensborough				
TD18	0.16	2.16	10.91	5.06
TD33	0.08	2.08	12.18	5.86
TD43	0.23	1.94	12.37	6.37
TD48	0.19	3.74	11.15	2.98
TD50	0.22	2.84	9.94	3.50
TD51	0.13	3.95	8.85	2.24
TD52	0.18	3.03	8.53	2.81
TD55	0.38	8.28	4.88	0.58
TD55D	0.39	8.47	3.35	0.40

Table 4 - Average trace element ratios for selected suites of dykes and volcanics from the Belmont Domain [Smith and Holm, 1990a] and from the mafic dykes in the Queensborough area.

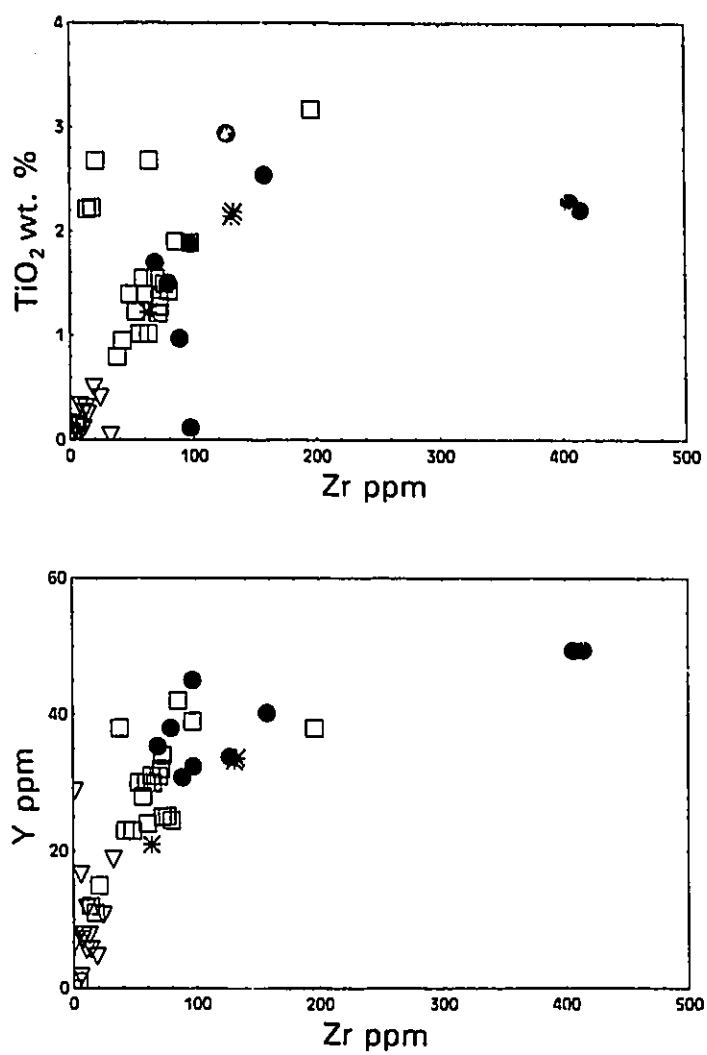


Figure 15 - TiO₂ versus Zr and Y vs. Zr plots.

Co, Cr, Ni, and Y all show similar decreasing trends with increasing MgO for the three mafic suites which are typical of rocks that have formed from mineral-melt equilibria processes. On the Y versus Zr plot (Figure 15), the meta-gabbro samples and mafic dykes have two linear trends. This can be explained by different degrees of partial melting over time. The meta-volcanics lie along the trend with the lower slope, inferring that these rocks were formed from a single melting event, thus not allowing for any chemical variation.

The ultramafic suite shows very irregular patterns in many of the elements (eg. Co, Cr, Y). They are very low in Ce, La, V and Zr and high in Co, Cr and Ni, in comparison with the mafic rock suites. Nb, V, and Zr show increasing trends, while Ni shows a decreasing trend with decreasing MgO. The chlorite schists have similar values to the averages of the ultramafic suite, with exceptions being higher Nb and V and lower Cr (Figure 14; Appendix C). As with the major element chemistry, the ultramafics have much different trace element trends compared to the mafic rocks.

4.5 - Petrogenesis

The ultramafic rocks clearly show different chemical signatures from the mafic rocks (see Figures 12 and 14). The mafic rocks show systematic increasing and decreasing major element contents versus MgO that are indicative of mineral-melt equilibria processes. The MgO-FeO diagram of Hanson and Langmuir [1978] (Figure 16) shows fields of melt and residues

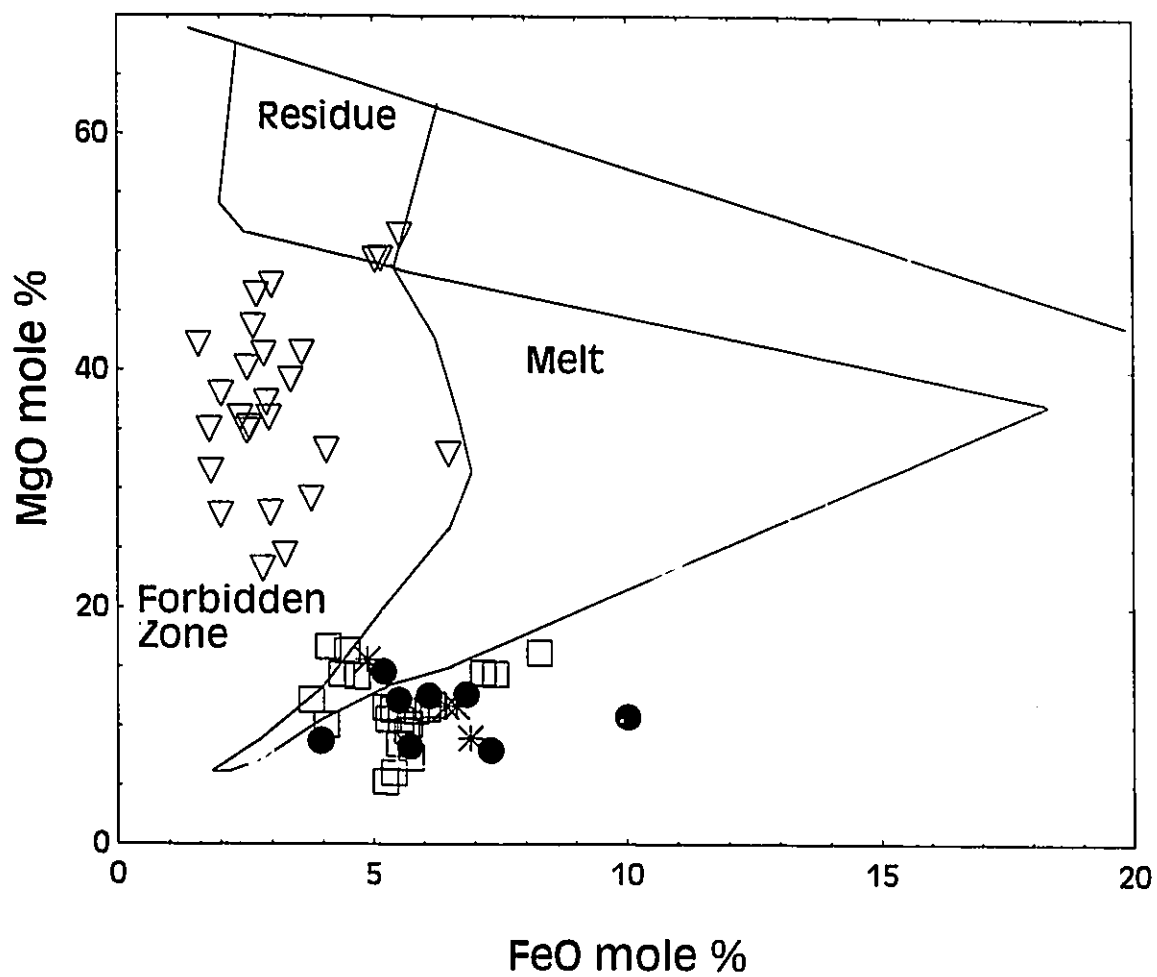


Figure 16 - MgO versus FeO sail diagram of Hanson and Langmuir [1978].
 Symbols are; inverted triangles - ultramafics; filled circles - mafic dykes; open squares - meta-gabbros; asteriks - meta-volcanics; filled squares - chlorite schists.

for batch melting³ of a pyrolite⁴ source. Samples which plot in the melt section (lower part) of the diagram are partial melts and fractional crystallization products. The residue field (upper part) is the material left over after a melt has left the magma source. The mafic samples of the Queensborough Complex all plot within or below the melt field. Thus, these suites can be explained through partial melting and fractional crystallization. In addition, the mafic rocks show fractional crystallization trends of olivine, orthopyroxene, plagioclase and clinopyroxene (Figure 17). This is in agreement with the original mineralogy inferred from their metamorphic minerals and textures discussed at the end of Chapter 3.

Rocks of the ultramafic suite do not show the partial melting-fractional crystallization trends of the mafic rocks. Rather, on the MgO-FeO diagram (Figure 16), the ultramafics plot in the forbidden zone. This strongly suggests that these samples have not formed by partial melting or fractional crystallization. In addition, they do not plot in the residue field (Figure 16), and thus are not the refractory portion of the mafic samples, suggesting that the ultramafics are cumulates. This is supported by the very low concentrations of incompatible elements such as TiO_2 , P_2O_5 , Co,

³ Batch melting is melting in which after a certain fraction of melting, the melt is removed from the solid phases and there is no further melting [Presnall, 1969].

⁴ Pyrolite is a model rock calculated by combining 83 wt. % residual harzburgite and 17 wt. % basalt [Ringwood, 1975].

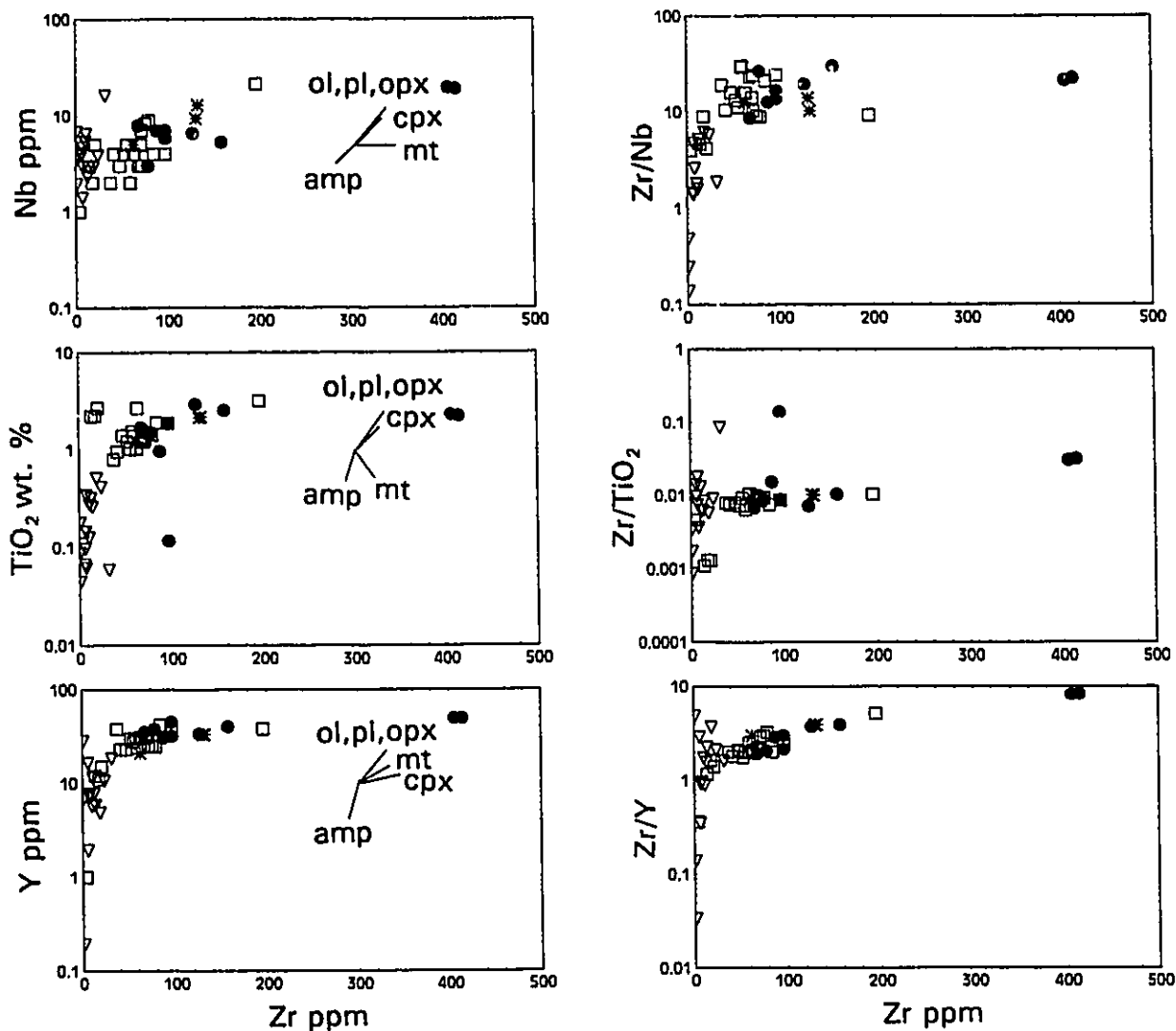


Figure 17 - Nb, TiO₂ and Y versus Zr fractional crystallization plots. Symbols are; inverted triangles - ultramafics; filled circles - mafic dykes; open squares - meta-gabbros; asteriks - meta-volcanics; filled squares - chlorite schists.

Cr, and Ni and the irregular distributions of most major elements. On the TiO_2 vs. Zr and Y vs. Zr plots (Figure 17), the trend of compositional variation of the ultramafics lead into the mafic samples. This suggests the two suites of rocks to be from the same geologic event. The ultramafic trends are also opposite the vectors shown for fractional crystallization of olivine, orthopyroxene, plagioclase and clinopyroxene, suggesting the ultramafics were accumulating these minerals. The occurrence of compositional layering and the irregular distribution of metamorphic mineral assemblages in the ultramafic suite further implies these rocks to have an accumulative origin.

4.6 - Summary of Chemistry

The meta-volcanics, meta-gabbros, and mafic dykes of the Queensborough Ophiolite Complex show minimal chemical alteration in SiO_2 , Al_2O_3 , Fe_2O_3 , MgO and CaO , but do show K_2O and Na_2O mobility. The ultramafic rocks also show alkali mobility, and are also enriched in SiO_2 . There are distinct differences in the major and trace element chemistry in the mafic rocks compared to the ultramafic rocks and chlorite schists. The mafic rocks show mineral-melt equilibrium characteristics, and have fractional crystallization trends of olivine, orthopyroxene, plagioclase and clinopyroxene. The ultramafic suite and chlorite schists do not have these characteristics, but rather show characteristics that can be explained in

terms of accumulation of olivine, orthopyroxene, (plagioclase) and clinopyroxene.

Chapter 5 - Discussion and Conclusions

5.1 - The Queensborough Ophiolite Complex

The Queensborough Complex has been shown to comprise mafic and ultramafic rocks which have a systematic rock succession typical of ophiolite complexes.

Ophiolites may form either in mid-ocean ridges (MOR) or in back-arc basins. Ophiolites formed in mid-ocean ridges generally are large in size and have predominantly mid-oceanic ridge basalt (MORB) chemistry. Those ophiolites formed in back-arc basins are much smaller, and often have their chemistry modified from that of MORB, by the subducting lithosphere. The geologic interpretations of the tectonic evolution of the Grimsthorpe and surrounding domains lie in the description of the Queensborough Ophiolite Complex. If the Queensborough Complex is formed at a mid-ocean ridge, then a large volume of ocean floor will be inferred, as suggested by Brown *et al.* [1975]. If the Complex was formed in a back-arc basin, it may have formed on attenuated continental crust as suggested by Condie and Moore [1977], Bartlett [1983], Holm *et al.* [1986], and Smith and Holm [1987, 1990a, 1990b].

The distinction between mid-ocean ridge ophiolites and back-arc ophiolites is not so simple. Convergent margins between continental and oceanic plates are extremely complex. Numerous microplates may be

formed, which may include true back-arc basins [ie. the Sulu Sea, Smith *et al.*, 1991a], or the presence of trapped oceanic crust [ie. the Celebes Sea, Smith *et al.*, 1991b].

Thus, the Queensborough Complex has three possible origins; 1) it is remnant oceanic crust, the majority of which has been subducted. In which case, the Grimsthorpe Domain may represent the suture between Laurentia on the west and the Baltic Shield to the west; 2) the Complex may be a true back-arc marginal basin, in which case, there is an offshore arc to the east, and the continental suture is even farther east; or 3) the Queensborough Complex is a fragment of trapped oceanic crust.

One discriminant between the oceanic setting and back-arc setting is the proportion of high level plutons [Pearce *et al.*, 1984]. Ophiolites formed in oceanic environments have a tiny proportion of diorites and plagiogranites. Ophiolites formed in back-arc basins may be intruded by large bodies of diorite and granodiorite. The Queensborough Complex lies alongside a large granodiorite-tonalite pluton, the Elzevir Batholith. This strongly implies the Queensborough Complex was formed in a back-arc basin.

There have been several studies to differentiate between the two ophiolites through geochemical data. Back-arc ophiolites are thought to generally contain a geochemical component from the underlying subducting slab, whereas a mid-ocean ridge ophiolite would not have this component.

This subduction component is commonly considered to be a slab-derived fluid with high concentrations of Large Ion Lithophile Elements (LILE) and Light Rare Earth Elements (LREE) and low concentrations of High Field Strength Elements (HFSE) and Heavy Rare Earth Elements (HREE) which is added to the mantle wedge. Basalts derived from this metasomatized mantle are enriched in LILE and LREE and depleted in HFSE and HREE relative to MORB [Pearce, 1983; Davidson *et al.*, 1993].

Pearce *et al.*, [1984] suggests that the two ophiolites may be distinguished using their Cr, TiO₂, and Y contents. This method leads to the conclusion that the mafic rocks of the Queensborough Complex are MORB related [Figure 18].

Figure 19b is a multi-element plot of the Queensborough meta-volcanic samples. The rocks have a relatively flat pattern, slightly more enriched than N-MORB, and have low LIL/HFS elemental ratios. These points support the conclusion that the Queensborough Complex is MORB related. However, Saunders and Tarney [1984] have shown that volcanics which erupt in back-arc basins associated with young subduction zones, as well as those erupted in wide basins, do not show the subduction chemical component [eg. Parece Vela Basin; Saunders and Tarney, 1984].

Chemically, the Queensborough Ophiolite Complex is suggested to be MORB related, but the presence of the large Elzevir Tonalite is supporting evidence that strongly suggests the Complex was formed in a back-arc

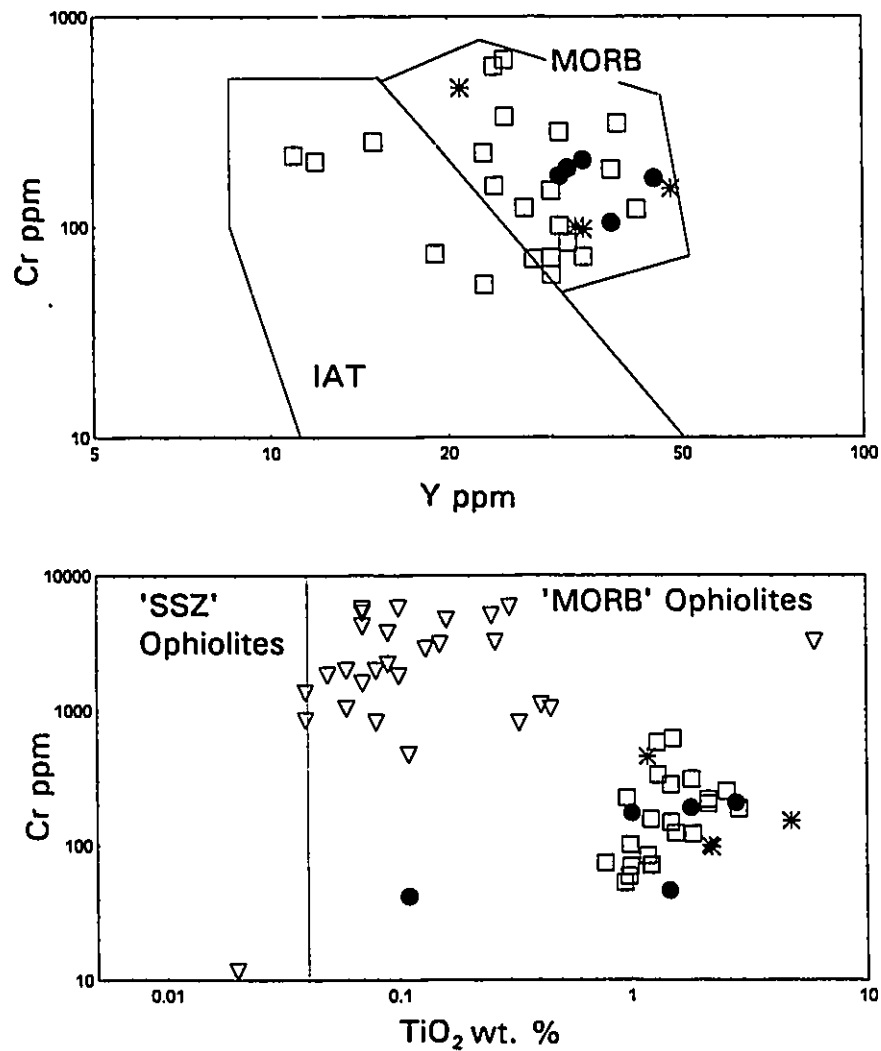


Figure 18 - Cr-Y and Cr-TiO₂ plots of Pearce *et al.* [1984] for discriminating between supra-subduction zone (SSZ) ophiolites and mid-ocean ridge (MORB) ophiolites. Symbols are; inverted triangles - ultramafics; filled circles - mafic dykes; open squares - meta-gabbros; asteriks - meta-volcanics; filled squares - chlorite schists.

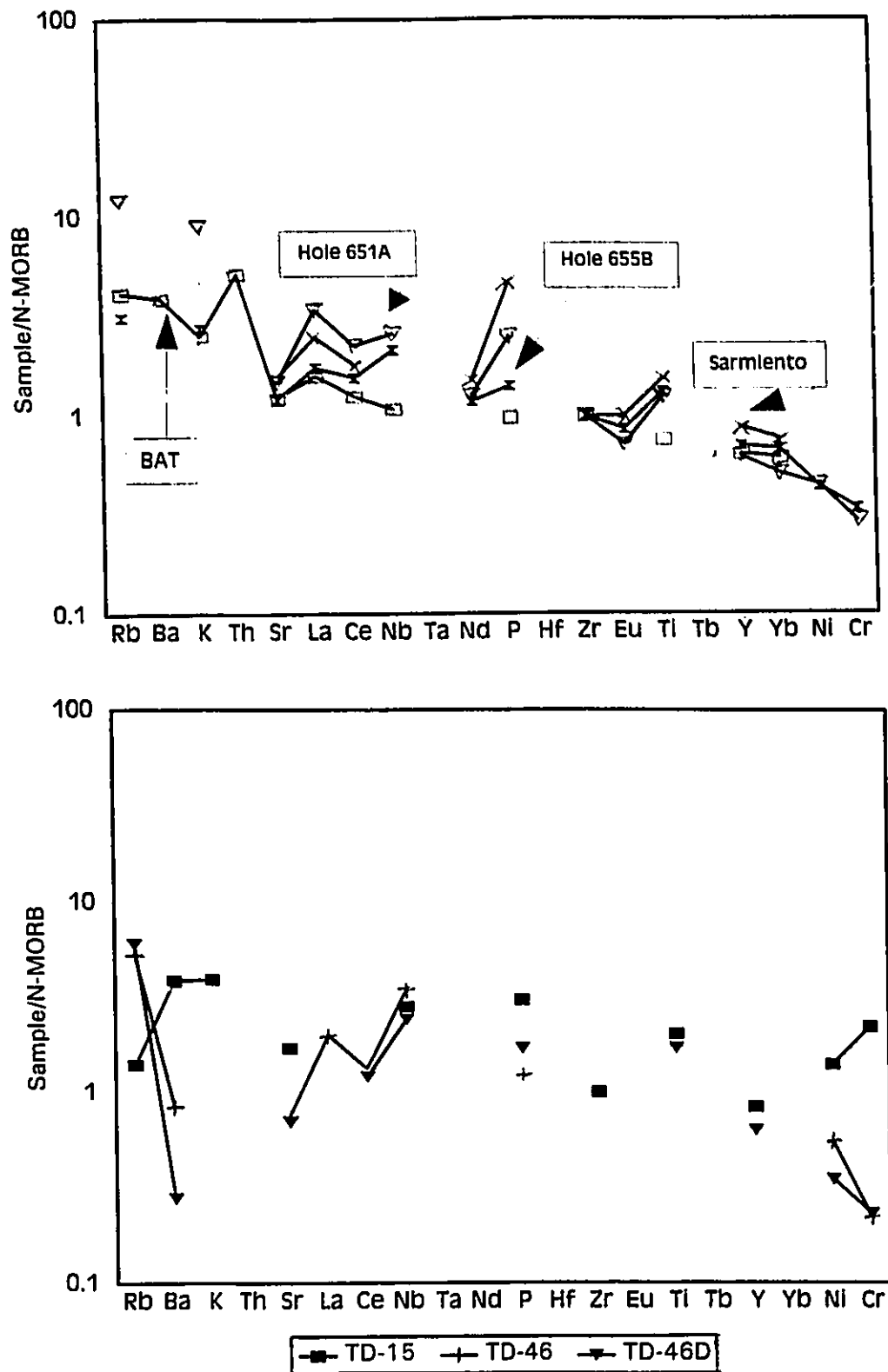


Figure 19 - Multi-element plots from Saunders and Tarney [1984]. Top diagram shows examples of back-arc basins; BAT - average of back-arc tholeiites [Holm, 1984]; Sarmiento [Stern, 1979]; and Holes 651A and 655B from the Tyrrhenian Sea [Kastens and Mascle, 1990]. Bottom diagram shows the meta-volcanics of the Queensborough Complex.

basin. The lack of a subduction component in the chemistry of the meta-volcanics suggests that the basin is associated with a young subduction zone.

5.2 - Tectonic Models

The conclusions derived from the Queensborough Complex can be used to refine the previous models of the Belmont and Grimsthorpe Domains. The island arc model of Brown *et al.*, [1975] was based on data from the Kaladar Complex. The Kaladar Complex is very similar to the Queensborough Complex, and most likely is the same body, separated by the Elzevir Tonalite. The Belmont Domain, interpreted as a back-arc basin formed on attenuated continental crust [ie. Smith and Holm, 1987] can be used in conjunction with the model of Brown *et al.*, to show that the attenuation of the continental crust reached its maximum separation in the Grimsthorpe Domain.

A modern analogue for the tectonic evolution of the Central Metasedimentary Belt can be found in the Tyrrhenian Sea, west of Italy. The Tyrrhenian Sea is a region of extensional tectonism within an overriding plate of a convergent plate margin. As such, the Tyrrhenian Sea qualifies as a species of "back-arc" basin. Rather than having one well-defined oceanic spreading axis, the Tyrrhenian has two basalt-floored sub-basins: the Marsili Basin and the Vavilov Basin [Kastens and Mascle, 1990]. In comparison,

the Queensborough area most likely has only one spreading center, although, the separation of the Queensborough and Kaladar Complexes may define a second spreading center.

Unlike the majority of back-arc basins that have formed in intra-oceanic settings, the Tyrrhenian Sea split a preexisting continent. As a result, the margins of the Tyrrhenian are passive continental margins; in particular, the eastern Sardinia margin comprises a series of fault-bounded, tilted blocks similar to those seen on classic rifted passive margins bounding major ocean basins [Kastens and Mascle, 1990]. The Grimsthorpe Domain is bounded by steeply dipping faults and shear zones. Although the nature of the Queensborough Fault Zone and Mooroton Shear Zone is not specifically known, listric faults are common to the west of the area, which are indicative of extensional tectonics [Milkereit *et al.*, 1992].

Basement rocks in the Vavilov basin are now known from drilling by the Ocean Drilling Program (ODP) [Kastens and Mascle, 1990]. Vesicular basalt, pillow basalt and basalt breccia underlie calcareous and terrigenous sediments. The basalts overlie serpentized peridotite. The depth of water in the Vavilov Basin is 3300 to 3500 metres (Hole 655 and 651 respectively). Only one hole intersected a peridotite basement, and only for 30 m. The Queensborough Complex has pillow basalts present, although only a minor component, and peridotites and pyroxenites are abundant.

Figure 19a shows the average basalt compositions for each hole drilled into the Vavilov Basin. They show enriched LIL elements, while the HFS elements are similar to N-MORB. Comparing these patterns and abundances to the Queensborough meta-volcanics (Figure 19b), there are some similarities, specifically in the range of Ta to Cr. In addition, major and trace element chemistry of serpentized peridotites of the Tyrrhenian are similar to the serpentine-bearing ultramafic rocks of the Queensborough (Table 5).

Table 5 - Average major and trace element data of serpentized peridotites of the Tyrrhenian Sea [Bonatti *et al*, 1990] and from Assemblage four of the ultramafic suite in the Queensborough Ophiolite.

	Tyrrhenian Sea Peridotites	Queensborough Ultramafics
SiO ₂	44.12	40.28
TiO ₂	0.022	0.07
Al ₂ O ₃	0.65	1.06
Fe ₂ O ₃	7.84	11.07
MnO	0.074	0.101
MgO	35.54	30.03
CaO	0.124	3.81
Na ₂ O	0.02	0.138
K ₂ O	0.012	0.02
H ₂ O	12.44	12.77
Cr	1962	2373
Ni	2002	2385

Figure 20 shows a cross-section of the eastern part of the Tyrrhenian Sea, from the lower Sardinian margin in the west, into the Vavilov Basin in

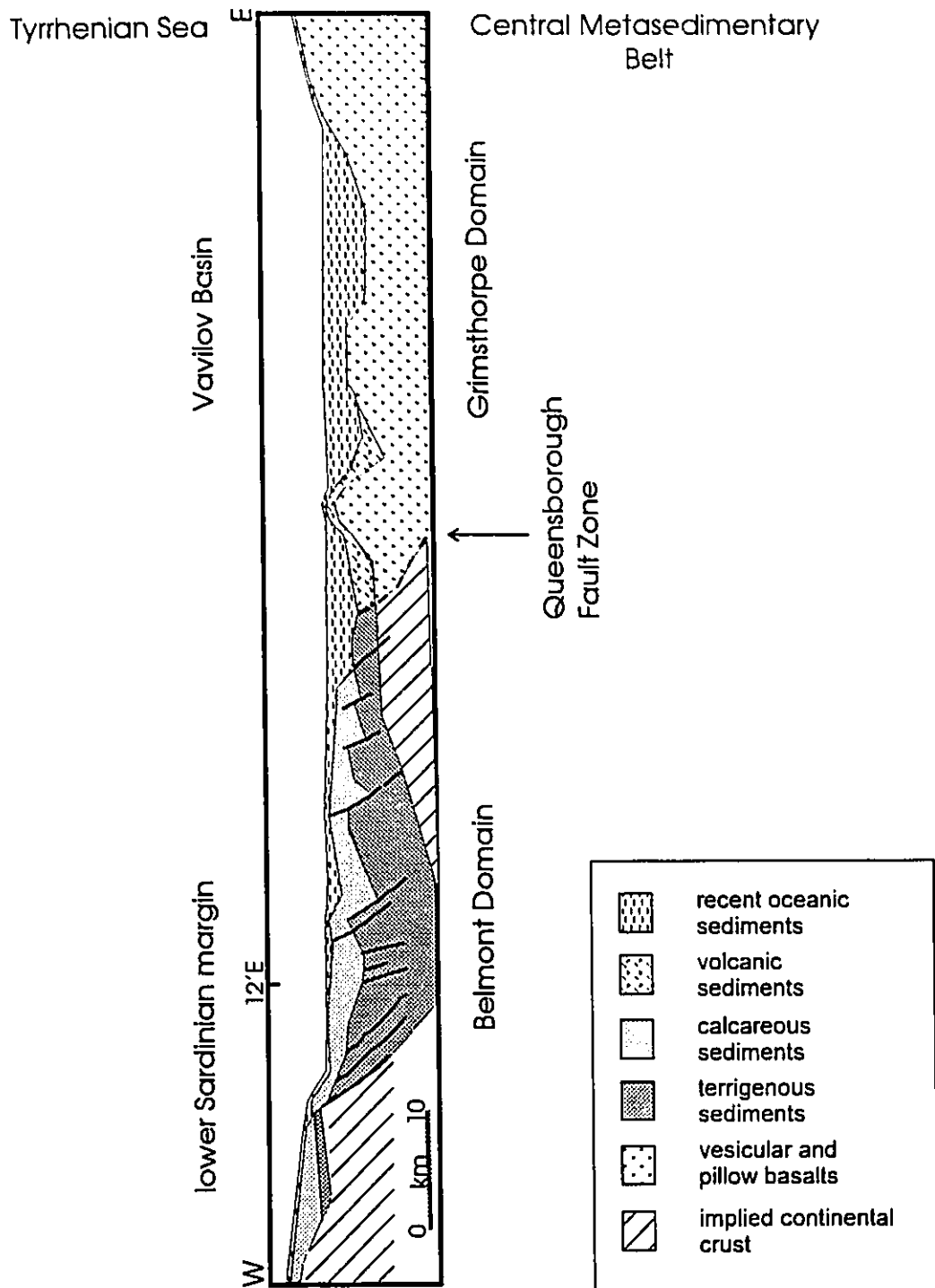


Figure 20 - Cross-section of the lower Sardinian margin and the Vavilov Basin, and the comparable portions of the Central Metasedimentary Belt, in eastern Ontario [after Mascle and Rehault, 1990].

the east [Masle and Rehault, 1990]. This section is comparable to the Belmont and Grimsthorpe Domain boundary, where the Grimsthorpe Domain is situated in the volcanic section, to the east. As the Vavilov Basin is very young [9 Ma; Kastens and Masle, 1990], it has not undergone much erosion, whereas the Grimsthorpe has been suggested to have had greater than 20 km of rock eroded from the crust. The listric faults seen in the Sardinian margin are extensional, and the same pattern is seen in the Elzevir Terrane [ie. Milkereit *et al.*, 1992]. With the later convergence during the Grenville orogeny, these fault planes became zones for thrusting.

5.3 - Conclusions

1) The Queensborough area, southern Grimsthorpe Domain, is dominated by massive to sheared meta-gabbros, not meta-volcanic and volcanoclastic rocks as previously interpreted.

2) The ultramafic-amphibolite belt west of the Elzevir Tonalite is best interpreted as part of a Mesoproterozoic ophiolite, herein named the Queensborough Ophiolite Complex.

3) The systematic rock succession and chemistry of the Queensborough Ophiolite Complex can be compared with the Eastern Papua Ophiolite Complex and the Yakuno Ophiolite.

4) The Queensborough Ophiolite Complex is interpreted as being formed in a back-arc basin rather than a mid-ocean ridge. This is supported by the presence of the Elzevir Tonalite Batholith.

5) The back-arc basin in which the Queensborough Ophiolite Complex developed is similar in its tectonic evolution to the Tyrrhenian Sea, which also formed on attenuated continental crust. Each basin contains similar rock successions including chemically similar basalts and serpentinized peridotites.

References

- Bartlett, J.R. 1983. Stratigraphy, physical volcanology and geochemistry of the Belmont Lake metavolcanic complex, southeastern Ontario; unpublished MSc Thesis, Carleton University, Ottawa, Ontario, 218 pp.
- Best, M.G. 1982. Igneous and Metamorphic Petrology. W.H. Freeman & Company, New York. 630 pp.
- Beswick, A.E. 1982. Some general aspects of alteration, and genetic relations in komatiitic suites. *in Komatiites*, ed. N.T. Arndt and E.G. Nisbet. London: Allen and Unwin. pp 283-308.
- Beswick, A.E. and Soucie, G. 1978. A correction procedure for metasomatism in an Archean greenstone belt; *Precambrian Research*, 6, pp 235-248.
- Bonatti, E., Seyler, M., Channell, J., Giraudeau, J., and Mascle, G. 1990. Peridotites drilled from the Tyrrhenian Sea, ODP Leg 107; *in Proc. ODP, Sci. Results*, 107; Kastens, K.A., Mascle, J., *et al.* College Station, TX (Ocean Drilling Program), pp 37-48.
- Boutcher, S.M.A., Davis, G.L., and Moorhouse, W.W. 1965. Potassium-argon and uranium-lead ages from two localities; *Canadian Mineralogist*, 8, pp 198-203.
- Brown, R.L., Chappell, J.F., Moore, J.M. and Thompson, P.H. 1975. An ensimatic island arc and ocean closure in the Grenville Province of southeastern Ontario, Canada; *Geoscience Canada*, 2, pp 141-144.
- Carlson, K.A., van der Pluijm, B.A. and Hanmer, S. 1990. Marble mylonites of the Bancroft Shear Zone: evidence for extension in the Canadian Grenville; *Geological Society of America, Bulletin*, 102, pp 174-181.
- Carmichael, D.M., 1969. On the mechanisms of prograde metamorphic reactions in quartz-bearing pelitic rocks. *Contrib. Mineral. Petrol.*, 20, pp 244-267.
- Coleman, R.G. 1977. Ophiolites. Springer-Verlag, New York. 229 p

- Condie, K.C. 1982. Early and Middle Proterozoic supracrustal successions and their tectonic settings; *American Journal of Science*, **282**, pp 341-357.
- Condie, K.C. and Moore, J.M. 1977. Geochemistry of Proterozoic volcanic rocks from the Grenville Province, Eastern Ontario; *in* *Volcanic Regimes in Canada*, Geological Association of Canada, Special Paper 16, pp 149-168.
- Culshaw, N.G., Davidson, A., and Nadeau, L. 1983. Structural subdivisions of the Grenville Province in the Parry Sound-Algonquin region, Ontario; *in* *Current Research, Part B*, Geological Survey of Canada, Paper 83-1B, pp 243-252.
- Davidson, A. 1986. New interpretations in the southwestern Grenville Province; *in* *The Grenville Province*, Geological Association of Canada, Special Paper 31, pp 61-74.
- Davidson, J.P., Boghossian, N.D. and Wilson, M. 1993. The geochemistry of the igneous rock suite of St. Martin, northern Lesser Antilles. *Journal of Petrology*, **34**, pp 839-866.
- Davidson, A., Culshaw, N.G. and Nadeau, L. 1982. A tectono-metamorphic framework for part of the Grenville Province, Parry Sound region, Ontario; *in* *Current Research, Part A*, Geological Survey of Canada, Paper 82-1A, pp 175-190.
- Davidson, A., Culshaw, N.G. and Nadeau, L. 1984. Grenville Traverse B: Cross-sections of part of the Central Gneiss Belt; Geological Association of Canada - Mineralogical Association of Canada, Ottawa '86, Field Trip Guidebook 9B/10B, 79 pp.
- Davies, H.L. 1971. Peridotite-gabbro-basalt complex in eastern Papua: an over-thrust plate of oceanic mantle and crust. *Australian Bur. Min. Resur. Bull.* **128**, 48pp.
- deLorraine, W.F. and Dill, D.B. 1982. Structure, stratigraphic controls, and genesis of the Balmat zinc deposits, northwest Adirondacks, New York; *in* *Precambrian Sulphide Deposits*, Geological Association of Canada, Special Paper 25, pp 571-596.
- Derry, D.R. 1950. A tectonic map of Canada; Geological Association of Canada, *Proceedings*, **3**, pp 39-53.

- DiPrisco, G. 1989. Geology of the Elzevir area, Hastings and Lennox and Addington counties; *in* Summary of Field Work and Other Activities 1989; Ontario Geological Survey, Miscellaneous Paper 146, pp 169-175.
- Easton, R.M. 1986. Geochronology of the Grenville Province; *in* The Grenville Province. Geological Association of Canada, Special Paper 31, pp 127-173.
- Easton, R.M. 1988a. Precambrian geology of the Darling area, Frontenac and Renfrew counties; Ontario Geological Survey, Open File Report 5693, 208 pp.
- Easton, R.M. 1988b. The Robertson Lake Mylonite Zone - A major tectonic boundary in the Central Metasedimentary Belt, Eastern Ontario; *in* Program with Abstracts, Geological Association of Canada - Mineralogical Association of Canada - Canadian Society of Petroleum Geologists, 13, pp A34-A35.
- Easton, R.M. 1990. Geology of the Mazinaw Lake area (31 C/14); Ontario Geological Survey, Open File Map 132, scale 1:50 000.
- Easton, R.M. 1992. The Grenville Province and the Proterozoic History of Central and Southern Ontario; *in* Geology of Ontario, Ontario Geological Survey, Special Volume 4, Part 2, pp 714-904.
- Easton, R.M. and Ford, F.D. 1990. Grimsthorpe area; *in* Summary of Field Work and Other Activities 1990, Ontario Geological Survey, Miscellaneous Paper 151, pp 99-110.
- Easton, R.M. and Ford, F.D. in preparation. Geology of the Grimsthorpe area (31 C/14 SW); Ontario Geological Survey, Open File Report.
- Fisher, G.W. 1970. The application of ionic equilibria to metamorphic differentiation: an example. *Contrib. Mineral. Petrol.*, 29, pp 91-103.
- Hall, A. 1987. Igneous Petrology. Longman Scientific & Technical, New York. 573 pp.
- Hanmer, S. 1988. Ductile thrusting at mid-crustal level, southwestern Grenville Province; *Canadian Journal of Earth Sciences*, 25, pp 1049-1059.

- Hanson, G.N. and Langmuir, C.H. 1978. Modelling of major elements in mantle-melt systems using trace element approaches. *Geochimica et Cosmochimica Acta*, **42**, pp 725-741.
- Haynes, S.J. 1986. Metallogenesis of U-Th, Grenville Supergroup, Peterborough County, Ontario; *in* The Grenville Province, Geological Association of Canada, Special Paper 31, pp 271-280.
- Heinrich, E.W. 1965. Microscopic Identification of Minerals. McGraw-Hill Book Company, Toronto. 414 pp.
- Hewitt, D.F. 1968. Geology of Madoc Township and the north part of Huntingdon Township, Hastings County; Ontario Department of Mines, Geological Report 73, 45 pp.
- Holm, P.E. 1984. The geochemical fingerprints of different tectonomagmatic environments using hygromagmatophile element abundances of tholeiitic basalts and basaltic andesites; *Chem. Geol.*, **51**, pp 303-323.
- Holm, P.E., Smith, T.E., Huang, C.H., Gerasimoff, M., Grant, B., and McLaughlin, L. 1986. Geochemistry of metavolcanic rocks and dykes from the Central Metasedimentary Belt, Grenville Province, southeastern Ontario; *in* The Grenville Province, Geological Association of Canada, Special Paper 31, pp 255-269.
- Jackson, E.D. and Thayer, T.P. 1972. Some Criteria for Distinguishing Between Stratiform, Concentric and Alpine Peridotite-Gabbro Complexes; *in* International Geological Congress Twenty-Fourth Session Section 2 - Petrology pp 289-296.
- Jaques, A.L. and Robinson, G.P. 1977. The continent/island-arc collision in northern Papua New Guinea. *BMR Journal of Australian Geology & Geophysics*, **2**, pp 289-303.
- Karig, D.E. 1971. Origin and development of marginal basins in the western Pacific. *J. Geophys. Res.* **76**, pp. 2542-2561.
- Kastens, K. and Mascle, J. 1990. The geological evolution of the Tyrrhenian Sea: An introduction to the scientific results of ODP Leg 107; *in* Proc. ODP, Sci. Results, 107; Kastens, K.A., Mascle, J., *et al.* College Station, TX (Ocean Drilling Program), pp 37-48.

- Koide, Y., Sano, S., Ishiwatari, A. and Kagami, H. 1987. Geochemistry of the Yakuno ophiolite in southwest Japan. *Jour. Fac. Sci., Hokkaido Univ., Ser. IV*, **22**, pp 297-312.
- LeBaron, P.S., MacKinnon, A. and Kingston, P.W. 1987. Komatiite-hosted talc in the Tudor Formation, Madoc and Grimsthorpe townships, southeastern Ontario; *in* Summary of Field Work and Other Activities 1987, Ontario Geological Survey, Miscellaneous Paper 137, pp 301-306.
- LeBaron, P.S., and van Haaften, S. 1989. Talc in Southeastern Ontario; Ontario Ministry of Northern Development and Mines, Open File Report 5714, 240 pp.
- Lumbers, S.B. 1967. Stratigraphy, plutonic activity and metamorphism of the Ottawa River Remnant in the Bancroft-Madoc area of the Grenville Province of southeastern Ontario; unpublished PhD thesis, Princeton University, Princeton, New Jersey, 331 pp.
- Lumbers, S.B., Heaman, L.M., Vertolli, V.M. and Wu, T.-W. 1990. Nature and timing of Middle Proterozoic magmatism in the Central Metasedimentary Belt, Ontario; *in* Mid-Proterozoic Laurentia-Baltica, Geological Association of Canada, Special Paper 38, pp 243-276.
- Mascle, J. and Rehault, J.P. 1990. A revised seismic stratigraphy of the Tyrrhenian Sea: Implications for the basin evolution. *in* Proc. ODP, Sci. Results, 107; Kastens, K.A., Mascle, J., *et al.* College Station, TX (Ocean Drilling Program), pp 617-635.
- Meen, V.B. 1944. Geology of the Grimsthorpe-Barrie area; Ontario Department of Mines, Annual Report, 1942, **51**, pt.4, pp1-50.
- Milkereit, B., Forsyth, D.A., Green, A.G., Davidson, A., Hanmer, S., Hutchinson, D.R., Hinze, W.J., and Mereu, R.F. 1992. Seismic images of a Grenvillian terrane boundary. *Geology*, **20**, pp 1027-1030.
- Moore, J.M. 1982. Stratigraphy and tectonics of the Grenville Orogen in eastern Ontario; 1982 Grenville Workshop, Rideau Ferry, Abstracts, p 7.
- Moore, J.M. 1986. Introduction: The 'Grenville Problem' then and now. *in* The Grenville Province, Geological Association of Canada, Special Paper 31, pp 1-11.

- Pearce, J.A. 1983. Role of the sub-continental lithosphere in magma genesis at active continental margins; *in* Continental Basalts and Mantle Xenoliths, ed. C.J. Hawkesworth and M.J. Norry. Shiva Publishing Limited, Cambridge, pp 230-249.
- Pearce, J.A., Lippard, S.J. and Roberts, S. 1984. Characteristics and tectonic significance of supra-subduction zone ophiolites; *in* Marginal Basin Geology, B.P. Kokelaar and M.F. Howells (editors). Blackwell Scientific Publications, Oxford, pp 77-96.
- Presnall, D.C. 1969. The geometric analysis of partial fusion. *Am. J. Sci.* **267**, pp 1178-1194.
- Ringwood, A.E. 1975. Composition and petrology of the Earth's mantle. McGraw-Hill, New York, 613 pp.
- Saunders, A.D. and Tarney, J. 1984. Geochemical characteristics of basaltic volcanism within back-arc basins; *in* Marginal Basin Geology, ed. B.P. Kokelaar and M.F. Howells. Blackwell Scientific Publications, Boston, pp 59-76.
- Smith, T.E., and Holm, P.E. 1987. The trace element geochemistry of metavolcanics and dykes from the Central Metasedimentary Belt of the Grenville Province, southeastern Ontario, Canada; *in* Geochemistry and Mineralization of Proterozoic Volcanic Suites, Geological Society of London, Special Publication 33, pp 453-470.
- Smith, T.E., and Holm, P.E. 1990a. The geochemistry and tectonic significance of pre-metamorphic minor intrusions of the Central Metasedimentary Belt, Grenville Province, Canada; *Precambrian Research*, **48**, pp 341-360.
- Smith, T.E., and Holm, P.E. 1990b. The petrogenesis of mafic minor intrusions and volcanics of the Central Metasedimentary Belt, Grenville Province, Canada; MORB and OIB sources; *Precambrian Research*, **48**, pp 361-373.
- Smith, T.E., Huang, C.H., and Sajona, F.G. 1991a. Geochemistry and petrogenesis of the volcanic rocks from Holes 768 and 769, Sulu Sea; *in* Proc. ODP, Sci. Results., 124. ed. Silver, E.A., Rangin, C., von Breyman, M.T., *et al.* College Station, TX (Ocean Drilling Program), pp 297-310.

- Smith, T.E., Huang, C.H., and Sajona, F.G. 1991b. Geochemistry and petrogenesis of basalts from Holes 767C, 770B and 770C, Celebes Sea; *in* Proc. ODP, Sci. Results., 124. ed. Silver, E.A., Rangan, C., von Breyman, M.T., *et al.* College Station, TX (Ocean Drilling Program), pp 311-320.
- Stern, C. 1979. Open and closed system igneous fractionation within two Chilean ophiolites and the tectonic implications; *Contrib. Mineral. Petrol.* **68**, pp 243-258.
- Touminen, H.W. 1964. The trends of differentiation in percentage diagrams. *J. Geol.*, **72**, pp 855-860.
- Williams, H. and Malpas, J. 1972. Sheeted dikes and brecciated dike rocks within transported igneous complexes, Bay of Islands, Western Newfoundland. *Can. J. Earth Sci.* **9**, pp 1216-1229.
- Williams, H.R., Stott, G.M., Thurston, P.C., Sutcliffe, R.H., Bennett, G., Easton, R.M., and Armstrong, D.K. 1992. Tectonic Evolution of Ontario: Summary and Synthesis; *in* Geology of Ontario, Ontario Geological Survey, Special Volume 4, Part 2, pp 1255-1335.
- Winkler, H.G.F. 1979. Petrogenesis of Metamorphic Rocks. Springer-Verlag, New York, 348 pp.
- Wolff, J.M. 1982. Geology of the Kaladar area; Ontario Geological Survey, report 215, 94 pp.
- Wynne-Edwards, H.R. 1972. The Grenville Province; *in* Variations in Tectonic Styles in Canada, Geological Association of Canada, Special Paper 11, pp 263-334.

APPENDIX A

SAMPLE LOCATIONS AND ROCK TYPE

Sample #	UTM Easting	UTM Northing	Rock Type	Location
TD - 1	308000	4933600	FD	NE of Madoc (BD)
TD - 2	308000	4933600	MV	NE of Madoc (BD)
TD - 3	308000	4933600		NE of Madoc (BD)
TD - 4	308000	4933600	MD	NE of Madoc (BD)
TD - 5	308300	4933600	MS	NE of Madoc (BD)
TD - 6	308300	4933600	MD	NE of Madoc (BD)
TD - 7	308400	4933700	MD	NE of Madoc (BD)
TD - 8	311300	4935000	FD	Black River Rd (BD)
TD - 9	311500	4934300	MG4	Black River Rd (BD)
TD - 10	311500	4934300	MD	Black River Rd (BD)
TD - 11	311400	4934300	MV	Black River Rd (BD)
TD - 12	315400	4935500	MG1	Hwy 7 & 37
TD - 13	315300	4935500	FD	Hwy 7 & 37
TD - 14	314900	4935300	MG1	Hwy 7
TD - 15	314400	4935000	MV	Hwy 7 & French Set.Rd.
TD - 16	313900	4934800	MG2	Hwy 7
TD - 17	316200	4936600	MG2	Flinton Road
TD - 18	316200	4936600	MD	Flinton Road
TD - 19	316600	4937200	UM1	Flinton Road
TD - 20	316600	4937200		Flinton Road
TD - 21	316600	4937200	UM1	Flinton Road
TD - 22	316800	4937500	UM1	Flinton Road
TD - 23	316800	4937500	UM2	Flinton Road
TD - 24	316900	4937700	UM3	Flinton Road
TD - 25	316400	4937100	UM1	Flinton Road
TD - 26	312700	4934800	MG1	County Road 20
TD - 27	312700	4935000	MG3	County Road 20
TD - 28	312700	4935000	MG1	County Road 20
TD - 29	312700	4935000	MG1	County Road 20
TD - 30	312700	4935000	MG1	County Road 20
TD - 31	312700	4935000	MG3	County Road 20
TD - 32	312700	4935100	MG1	County Road 20
TD - 33	312600	4935400	MD	County Road 20
TD - 34	312500	4935400	MG3	County Road 20
TD - 35	312500	4935400	MG2	County Road 20
TD - 36	312600	4935500	MG3	County Road 20
TD - 37	312600	4935500	MG2	County Road 20
TD - 38	312400	4935800	MG2	County Road 20
TD - 39	312400	4935800	MG2	County Road 20
TD - 40	312300	4936300	MG3	County Road 20

Sample #	Easting	Northing	Rock Type	Location
TD - 41	312300	4936400	MG3	County Road 20
TD - 42	312100	1936800	MG3	County Road 20
TD - 43	312100	4936800	MD	County Road 20
TD - 44	312100	4936800	MD	County Road 20
TD - 45	312200	4936800	MG	County Road 20
TD - 46	312200	4936800	MV	County Road 20
TD - 47	311600	4938600	MG2	County Road 20
TD - 48	311500	4938700	MD	County Road 20
TD - 49	311500	4938700	FD	County Road 20
TD - 50	311500	4938700	MD	County Road 20
TD - 51	311500	4938700	MD	County Road 20
TD - 52	311500	4938700	MD	County Road 20
TD - 53	311400	4938700	MD	County Road 20
TD - 54	311400	4938800	MG	County Road 20
TD - 55	311300	4939300	MD	County Road 20
UM - 1	317700	4937500	UM1	Hidden Valley Camp. Rd.
UM - 2	317600	4937600	UM4	Hidden Valley Camp. Rd.
UM - 3	317600	4937600	UM3	Hidden Valley Camp. Rd.
UM - 4	317600	4937600	UM4	Hidden Valley Camp. Rd.
UM - 5	317600	4937600	UM4	Hidden Valley Camp. Rd.
UM - 6	317700	4937500	UM2	Hidden Valley Camp. Rd.
UM - 7	317700	4937500	UM3	Hidden Valley Camp. Rd.
UM - 8	317000	4937400	UM1	Hidden Valley Camp. Rd.
UM - 9	317000	4937300	UM4	Hidden Valley Camp. Rd.
UM - 10	316800	4937500	UM3	Hidden Valley Camp. Rd.
UM - 11	317800	4937300	UM1	Hidden Valley Camp. Rd.
KT - 1	317600	4937500	UM2	Hidden Valley Camp. Rd.
KT - 2	317600	4937500	UM1	Hidden Valley Camp. Rd.
KT - 3	317600	4937500	UM1	Hidden Valley Camp. Rd.
KT - 4	317600	4937500	UM4	Hidden Valley Camp. Rd.
KT - 5	317600	4937500	CS	Hidden Valley Camp. Rd.
KT - 6	317600	4937500	UM4	Hidden Valley Camp. Rd.
KT - 8	317700	4937900	UM1	Hidden Valley Camp. Rd.
KT - 9	317700	4937900	UM3	Hidden Valley Camp. Rd.
KT - 10	317700	4937900	UM3	Hidden Valley Camp. Rd.
KT - 11	317700	4937900	CS	Hidden Valley Camp. Rd.
KT - 12	317700	4937900	UM4	Hidden Valley Camp. Rd.
KT - 13	317700	4938100	MV	Hidden Valley Camp. Rd.
KT - 14	317600	4937400	UM3	Hidden Valley Camp. Rd.
KT - 15	310900	4940400	CS	County Road 20

Sample #	Easting	Northing	Rock Type	Location
KT - 16	306300	4947300	UM3	East of Cooper
KT - 17	306100	4947200	MG4	East of Cooper
KT - 18	306700	4947600	CS	East of Cooper
KT - 19	305400	4948500	MG3	East of Cooper
KT - 20	305400	4948500	UM3	East of Cooper
KT - 21	305400	4948500	CS	East of Cooper
KT - 22	307500	4947200	MG3	North of Queensborough
KT - 23	307800	4941200	MS	North of Queensborough
KT - 24	311700	4938000	MG	County Road 20
KT - 25	311700	4938000	MG	County Road 20
KT - 26	311700	4938000	UM1	County Road 20
KT - 27	311700	4938000	UM	County Road 20
KT - 28	311700	4938000	MG4	County Road 20
KT - 29	312100	4939300	MG4	County Road 20
KT - 30	311100	4939900	UM1	County Road 20
KT - 31	311100	4939900	MG4	County Road 20
KT - 32	324500	4945400	UM3	Flinton Road
KT - 33	317700	4937700	UM4	Hidden Valley Camp. Rd.
KT - 34	306500	4947600	CS	East of Cooper
KT - 35	311300	4939400	MG4	County Road 20
KT - 40	312800	4934600	MS	County Road 20
KT - 41	312800	4934600	MS	County Road 20
KT - 42	312400	4936300	MG	County Road 20
KT - 43	311800	4937800	MD	County Road 20
KT - 44	311800	4937800	FD	County Road 20
KT - 45	311800	4937800	MD	County Road 20
KT - 46	312600	4935600	FD	County Road 20
KT - 47	308000	4933400	MV	Northeast of Madoc (BD)
KT - 48	307900	4933600	MV	Northeast of Madoc (BD)
KT - 49	307800	4933700	MV	Northeast of Madoc (BD)
KT - 50	307400	4934500	MG	Northeast of Madoc (BD)

Sample #	Easting	Northing	Rock Type	Location
KT - 51	307400	4934500	MG	Northeast Madoc (BD)
KT - 52	311300	4935000	FD	Northeast Madoc (BD)
KT - 53	311300	4935700	MG2	Northeast Madoc (BD)
KT - 54	303200	4949600	MS	North of Cooper
KT - 55	303200	4949600	MG2	North of Cooper
KT - 56	303100	4950200	MG1	North of Cooper
KT - 57	302400	4950700	MG4	North of Cooper
KT - 58	308700	4940300	MD	East of Queensborough
KT - 59	309000	4949400	MG4	East of Queensborough
KT - 60	309700	4940500	MG4	East of Queensborough
KT - 61	311100	4940000	MG4	County Road 20
KT - 62	311700	4938100	MG2	County Road 20
KT - 63	311700	4938100	MG4	County Road 20
KT - 64	311300	4939200	MD	County Road 20
KT - 65	311100	4939400	UM2	County Road 20
KT - 66	307300	4941600	MS	North Queensborough
KT - 67	305700	4942600	MS	North Queensborough
KT - 68	305700	4943000	MS	North Queensborough
KT - 69	305700	4943000	MS	North Queensborough
KT - 70	307000	4939600	MB	West Queensborough(BD)

APPENDIX B

MODAL MINERALOGY

MV Suite	TD 2	TD 11	TD 15	TD 46	KT 13	Averages N = 5	Standard Deviation
Quartz	10	5		10	10	8.75	2.17
Plag	25	20	15	10	15	17.00	5.10
Act/Trem	40	45	70	45	65	53.00	12.08
Biotite						0.00	0.00
Opakes	5	10	5	5	5	6.00	2.00
Chlorite	15	15	5	20		13.75	5.45
Carbonat	5	5	5	10	tr	5.00	3.16
Epidote						0.00	0.00
Serpentin						0.00	0.00
Muscovite						0.00	0.00
Titanite						0.00	0.00
Talc						0.00	0.00
Sericite						0.00	0.00
Garnet						0.00	0.00
Apatite						0.00	0.00
Zircon						0.00	0.00

MG Suite Group 1	TD 12	TD 14	TD 26	TD 28	TD 29	TD 30	TD 32	KT 56
Quartz	5	10		5		5	5	
Plagioclas	25	15	50	45	30	30	55	5
Act/Trem	30	60	35	30	50	50	30	75
Biotite								
Opakes	10	5	tr	5	5	5	5	tr
Chlorite	20	5	5	10	10	10	5	10
Carbonat	10	5	5	5	5	tr	tr	5
Epidote								5
Serpentin								
Muscovite								
Titanite			5	tr			tr	
Talc								
Sericite								
Garnet								
Apatite								
Zircon								

MG Suite Group 2	TD 16	TD 17	TD 35	TD 37	TD 38	TD 39	TD 47
Quartz		10	10			5	
Plagioclas	15	20	45	10	20	40	10
Act/Trem	65	50	25	65	55	30	75
Biotite							
Opaques	5	10	5	10	5	5	5
Chlorite	5	10		10	20	10	10
Carbonat	10	tr	15	5	tr	10	tr
Epidote							
Serpentin							
Muscovite							
Titanite					tr		tr
Talc							
Sericite							tr
Garnet							
Apatite			tr				
Zircon							

MG Suite Group 2	KT 25	KT 53	KT 55	KT 62
Quartz		10	5	15
Plagioclas	15	20	60	40
Act/Trem	80	60	25	25
Biotite				
Opaques	tr	5	tr	5
Chlorite	5	tr	5	5
Carbonat		5	5	10
Epidote			tr	
Serpentin				
Muscovite				
Titanite				
Talc				
Sericite	tr			
Garnet				
Apatite				
Zircon				

MG Suite Group 3	TD 34	TD 36	TD 40	TD 41	KT 19	KT 22	TD 27	TD 31
Quartz	tr		10	5		5	10	10
Plagioclas	10	tr	40	25	10	20	25	25
Act/Trem	60	75	35	45	40	55	45	35
Biotite								
Opaques	5	10	5	5	tr	10	5	5
Chlorite	20	10	10	20	30		10	10
Carbonat	5	5	tr			5	tr	10
Epidote					cl 20	5		
Serpentin								
Muscovite								
Titanite								
Talc								
Sericite								
Garnet								5
Apatite							5	
Zircon								

MG Suite Group 4	TD 9	TD 54	KT 17	KT 24	KT 28	KT 29	KT 31
Quartz	10	5	tr		5	5	tr
Plagioclas	30	10	10	10	15	10	tr
Act/Trem	35	55	60	55	65	70	15
Biotite							
Opaques	10	10	tr	5	5	2	
Chlorite	10	10	20	10	10	5	30
Carbonat	5	5	10	10		tr	55
Epidote		5				5	
Serpentin							
Muscovite							
Titanite					tr	3	tr
Talc							
Sericite				10			
Garnet							
Apatite							
Zircon							

MG Suite Group 4	KT 35	KT 57	KT 59	KT 61	KT 63	Averages N = 39	Standard Deviation
Quartz		15	5	5	15	4.87	4.73
Plagioclas	20	10	5	35	40	23.08	15.26
Act/Trem	70	60	75	35	20	49.23	17.78
Biotite						0.00	0.00
Opaques	tr	5	tr	tr	5	4.54	3.30
Chlorite	5	5	5	5	5	9.87	7.02
Carbonat	5	5	5	20	15	6.54	9.21
Epidote			5			0.64	1.67
Serpentine						0.00	0.00
Muscovite						0.00	0.00
Titanite						0.21	0.91
Talc						0.00	0.00
Sericite						0.38	1.75
Garnet						0.13	0.79
Apatite						0.00	0.00
Zircon						0.00	0.00

UM Suite Assem. 1	TD 19	TD 22	TD 25	UM 1	UM 8	UM 11	KT 2
Quartz							
Plag	tr	10	5			15	
Act/Trem	40	65	65	75	15	25	80
Biotite							
Opaques	5	5	tr	tr	10	5	10
Chlorite	55	10	10	20	25	15	10
Carbonat	tr	10		5	50	40	
Epidote							
Serpentin							
Muscovite							
Titanite							
Talc							
Sericite			20	tr			
Garnet							tr
Apatite							
Zircon							

UM Suite Assem. 1	KT 3	KT 8	KT 26	KT 30
Quartz				
Plag			tr	5
Act/Trem	70	70	55	60
Biotite				
Opaques	15	10	5	tr
Chlorite	10	20	20	10
Carbonat	5		20	5
Epidote				
Serpentin				
Muscovite				
Titanite				
Talc				
Sericite				
Garnet				
Apatite				
Zircon				

UM Suite Assem. 2	TD 23	UM 6	KT 1	KT 65
Quartz				
Plag				
Act/Trem	45	60	35	10
Biotite				
Opaques	15	5	tr	tr
Chlorite	10	20	5	40
Carbonat	30	5	50	40
Epidote				
Serpentin				
Muscovite				
Titanite				
Talc	tr	10	10	10
Sericite				
Garnet				
Apatite				
Zircon				

UM Suite Assem. 3	TD 24	UM 3	UM 7	UM 10	KT 9	KT 10	KT 14
Quartz							
Plag							
Act/Trem							10
Biotite							
Opagues	5	5	5	5	5	5	5
Chlorite	10	5	10	10	10	5	5
Carbonat	50	45	55	55	45	50	70
Epidote							
Serpentin							
Muscovite							
Titanite							
Talc	30	45	30	30	40	40	10
Sericite	5						
Garnet							
Apatite							
Zircon							

UM Suite Assem. 3	KT 16	KT 20	KT 32	UM Suite Assem. 4	UM 2	UM 4	UM 5
Quartz				Quartz			
Plag				Plag			
Act/Trem			65	Act/Trem			
Biotite				Biotite			
Opagues	10	5	5	Opagues	10	10	tr
Chlorite	5	tr	20	Chlorite	tr	5	15
Carbonat	55	65		Carbonat	15	25	35
Epidote				Epidote			
Serpentin				Serpentin	30	50	tr
Muscovite				Muscovite			
Titanite				Titanite			
Talc	30	30	10	Talc	40	10	50
Sericite				Sericite			
Garnet				Garnet	tr		
Apatite				Apatite			
Zircon				Zircon			

UM Suite	UM 9	KT 4	KT 12	KT 33	Averages N = 32	Standard Deviation
Quartz					0.00	0.00
Plag					1.13	3.29
Act/Trem		5			27.42	29.70
Biotite					0.00	0.00
Opaques	15	5	5	10	6.13	4.35
Chlorite	20	10	15	10	13.71	11.00
Carbonat		20	20	15	26.61	22.39
Epidote					0.00	0.00
Serpentin	60	50	50	50	9.35	19.50
Muscovite					0.00	0.00
Titanite		tr			0.00	0.00
Talc	5	10	10	15	14.03	15.50
Sericite					0.81	3.61
Garnet					0.00	0.00
Apatite					0.00	0.00
Zircon					0.00	0.00

Chlorite Schists	KT 11	KT 21	KT 18	KT 34	Averages N = 4	Standard Deviation
Quartz			25	10	17.50	7.50
Plag			30	25	27.50	2.50
Act/Trem			5		5.00	0.00
Biotite					0.00	0.00
Opaques	20	5	tr	tr	6.25	8.20
Chlorite	80	95	40	60	68.75	20.73
Carbonat			tr	tr	0.00	0.00
Epidote					0.00	0.00
Serpentin					0.00	0.00
Muscovite					0.00	0.00
Titanite	tr	tr			0.00	0.00
Talc		tr			0.00	0.00
Sericite					0.00	0.00
Garnet					0.00	0.00
Apatite					0.00	0.00
Zircon					0.00	0.00

Mafic	TD	TD	TD	TD	TD	TD	TD
Dykes	4	6	7	10	18	33	43
Quartz	5		tr		5	20	
Plag	40	25	25	35	30	15	30
Act/Trem	30	60	40	25	40	50	40
Biotite		5	10	5	5	tr	
Opaques	5	5	5	10	tr	5	10
Chlorite	20		15	15	10	10	10
Carbonat				5	5	tr	10
Epidote		5	5				
Serpentin							
Muscovite							
Titanite					5		
Talc							
Sericite							
Garnet				5			
Apatite							
Zircon							

Mafic	TD	TD	TD	TD	TD	TD	KT
Dykes	44	48	50	51	52	55	43
Quartz			10	5		5	25
Plag	25	30	15	10	25	10	25
Act/Trem	40	45	55	45	40	15	25
Biotite		5	tr	15	5	35	20
Opaques	10	10	5	10	10	5	5
Chlorite	20	10	10	15	10	20	
Carbonat	5	tr	5	tr	5	5	TR
Epidote		tr				5	TR
Serpentin							
Muscovite							
Titanite							
Talc							
Sericite					5		
Garnet			tr				
Apatite							
Zircon							

Mafic Dykes	KT 45	KT 58	KT 64	Averages N = 17	Standard Deviation	Felsic Dykes	TD 1
Quartz	15	15	10	6.76	7.66	Quartz	20
Plag	20	35	15	24.12	8.62	Plag	50
Act/Trem	20	25	50	37.94	12.37	Act/Trem	10
Biotite	10	10		7.35	8.93	Biotite	10
Opaques	5	5	TR	6.18	3.22	Opaques	5
Chlorite	TR	5	10	10.59	6.39	Chlorite	5
Carbonat		TR	5	2.65	3.03	Carbonat	
Epidote	30	5		2.94	7.08	Epidote	
Serpentin				0.00	0.00	Serpentin	
Muscovite				0.00	0.00	Muscovite	
Titanite				0.29	1.18	Titanite	
Talc				0.00	0.00	Talc	
Sericite				0.29	1.18	Sericite	
Garnet				0.29	1.18	Garnet	
Apatite				0.00	0.00	Apatite	
Zircon				0.00	0.00	Zircon	

Felsic Dykes	TD 8	TD 13	TD 53	KT 44	KT 46	KT 52	Averages N = 7	Standard Deviation
Quartz	<40	55	10	30			23.00	18.87
Plag	<40	10	70	35	75	60	42.86	26.97
Act/Trem	15					TR	8.33	6.24
Biotite	5	10	15	20	5		10.83	5.34
Opaques	10		TR	15	5	10	7.50	4.79
Chlorite	10		TR	TR	TR	TR	2.50	3.82
Carbonat	20	10	5		10	30	15.00	8.94
Epidote							0.00	0.00
Serpentin							0.00	0.00
Muscovite		15	TR		5		6.67	6.24
Titanite							0.00	0.00
Talc							0.00	0.00
Sericite							0.00	0.00
Garnet							0.00	0.00
Apatite							0.00	0.00
Zircon							0.00	0.00

MS Suite	TD 5	KT 23	KT 40	KT 41	KT 54	KT 66	KT 67
Quartz	60	5	30	35	35	35	5
Plag	20	10	5	5	40	20	15
Act/Trem	tr	40	5	25			60
Biotite	tr	5	10	20		25	
Opaques	10	10	5	5	TR	15	5
Chlorite	5	tr	5	5	10		5
Carbonat	5	25	40	5	5	5	10
Epidote		5					
Serpentin							
Muscovite					10		
Titanite							
Talc							
Sericite							
Garnet							
Apatite							
Zircon							

MS Suite	KT 68	KT 69	Averages N = 9	Standard Deviation
Quartz	10	5	24.44	18.17
Plag	10	15	15.56	10.12
Act/Trem	40	40	23.33	21.47
Biotite			6.67	9.13
Opaques	5	5	6.67	4.08
Chlorite	10	5	5.00	3.33
Carbonat	25	25	16.11	12.20
Epidote	TR	5	1.11	2.08
Serpentin			0.00	0.00
Muscovite	TR		1.11	3.14
Titanite			0.00	0.00
Talc			0.00	0.00
Sericite			0.00	0.00
Garnet			0.00	0.00
Apatite			0.00	0.00
Zircon			0.00	0.00

APPENDIX C

MAJOR AND TRACE ELEMENT

GEOCHEMISTRY

MV Suite	TD2	TD11	TD15	TD46	TD46T	Averages N = 5	Standard Deviation
SiO2	47.43	44.93	45.31	50.60	51.70	47.99	2.74
TiO2	1.34	4.75	1.18	2.23	2.19	2.33	1.28
Al2O3	14.40	12.82	14.57	13.21	12.74	13.55	0.78
Fe2O3	12.24	16.64	12.64	17.63	17.59	15.35	2.40
MnO	0.24	0.33	0.19	0.26	0.26	0.25	0.05
MgO	7.74	4.93	9.18	7.09	7.05	7.20	1.37
CaO	10.13	7.45	11.49	8.89	8.85	9.36	1.36
Na2O	3.18	3.30	1.66	1.91	1.91	2.39	0.70
K2O	0.18	0.13	0.22			0.11	0.09
P2O5	0.14	0.47	0.12	0.11	0.15	0.20	0.13
LOI	2.19			0.41	0.41	1.00	0.84
Total	99.20	95.73	96.55	102.33	102.85		
Ba	11		33	15	5	16.05	10.34
Ce				20	18	18.70	0.89
Co	47	48	49	68	39	50.14	9.47
Cr	328	152	457	97	100	226.80	142.66
La				9		9.14	0.00
Nb	4	23	5	13	9	10.82	6.86
Ni	89	71	138	114	72	96.80	25.83
Rb			1	8	9	6.17	3.69
Sc	55	48	57	337	52	109.80	113.64
Sr	120	232	166	153	142	162.60	37.84
V	313	427	370	447	482	407.80	59.71
Y	39	48	21	34	33	35.00	8.79
Zr	85	268	63	132	131	135.80	71.27

MG Suite	TD12	TD14	TD26	TD28	TD29	TD30	TD32
Group 1							
SiO2	42.88	48.98	47.94	49.11	48.48	47.67	50.23
TiO2	2.89	1.31	0.96	1.18	0.99	1.83	0.775
Al2O3	12.28	13.78	13.54	14.74	14.57	14.46	16.33
Fe2O3	14.48	12.06	11.14	14.27	13.43	13.23	10.48
MnO	0.23	0.20	0.21	0.23	0.22	0.22	0.17
MgO	6.32	8.37	8.40	5.47	6.58	6.65	5.96
CaO	9.44	9.73	11.96	9.12	9.59	9.28	9.52
Na2O	2.18	1.99	1.82	2.64	2.46	3.03	3.37
K2O	0.19	0.17	0.19	0.23	0.33	0.23	0.199
P2O5	0.29	0.14	0.08	0.14	0.12	0.34	0.081
LOI							
Total	91.18	96.74	96.25	97.13	96.77	96.94	97.115
Ba	16	28	25	21	107	83	31
Ce							
Co	52	53	49	52	44	47	36
Cr	187	333	224	84	101	309	74
La							
Nb	21	7	3	5	4	4	2
Ni	75	119	60	17	55	56	30
Rb			1		1		
Sc	46	42	69	52	55	61	48
Sr	247	221	220	248	551	336	192
V	479	368	324	409	327	408	309
Y	38	25	23	32	31	39	19
Zr	196	72	48	71	63	97	38

MG Suite Group 2	TD16	TD17	TD35	TD37	TD38	TD39	TD45	TD47	TD47D
SiO2	46.70	46.98	42.33	44.43	49.46	55.12	45.78	48.98	44.53
TiO2	1.49	1.85	1.22	2.16	1.486	0.996	1.56	1.52	1.30
Al2O3	15.21	13.56	13.90	12.64	14.16	14.26	10.64	15.31	14.26
Fe2O3	13.31	15.37	8.84	18.57	13.95	13.22	13.23	12.35	10.24
MnO	0.20	0.34	0.20	0.29	0.268	0.262	0.23	0.20	0.17
MgO	6.03	6.56	6.56	8.18	5.98	3.08	5.80	10.18	9.44
CaO	10.81	9.85	11.19	10.14	8.35	8.87	7.75	11.25	10.04
Na2O	2.15	2.41	3.48	0.91	2.51	1.97	2.01	1.50	1.39
K2O	0.21	0.34	0.10	0.19	0.174	0.205		0.38	0.27
P2O5	0.14	0.15	0.13	0.07	0.125	0.172		0.09	0.03
LOI							12.76	0.99	0.99
Total	96.24	97.41	87.95	97.57	96.463	98.155	99.75	102.75	92.66
Ba	49	14	32	9	14	19	14	77	63
Ce							13	8	6
Co	58	55	22	71	56	35	39	61	55
Cr	282	121	156	204	148	70	123	621	580
La							9	6	4
Nb	3	4	2	3	2	5	11	8	9
Ni	79	36	35	52	27	9	115	238	191
Rb		3					11	16	20
Sc	67	67	45	87	62	43	15	66	116
Sr	164	205	202	104	220	145	165	83	160
V	416	560	264	1144	470	337	385	308	213
Y	31	42	24	12	30	28	27	25	24
Zr	69	85	60	14	59	56	97	76	79

MG Suite Group 3	TD27	TD31	TD34	TD36	TD40	TD41	MG Suite Group 4	TD9	TD54	Averages N = 24	Standard Deviation
SiO2	56.00	48.57	43.93	40.32	53.55	51.05	SiO2	40.98	37.90	47.30	4.17
TiO2	0.98	1.23	2.15	2.57	0.94	1.21	TiO2	3.70	0.00	1.48	0.72
Al2O3	13.19	15.13	11.50	11.72	14.13	14.39	Al2O3	12.57	0.60	13.28	2.92
Fe2O3	13.41	13.66	17.96	20.35	14.57	14.64	Fe2O3	16.75	8.37	13.47	2.42
MnO	0.25	0.23	0.26	0.39	0.25	0.311	MnO	0.28	0.12	0.24	0.05
MgO	3.44	4.83	8.21	9.03	4.23	5.93	MgO	5.54	40.09	7.94	6.92
CaO	5.69	9.68	11.36	11.01	8.27	8.75	CaO	6.99	1.36	9.07	2.12
Na2O	3.22	3.13	0.73	0.57	2.14	2.4	Na2O	3.39	0.09	2.21	0.85
K2O	0.16	0.23	0.20	0.17	0.23	0.027	K2O	0.12		0.19	0.09
P2O5	0.14	0.14	0.07	0.07	0.12	0.109	P2O5	0.42		0.13	0.09
LOI							LOI	0.40	12.42	1.20	3.45
Total	96.48	96.83	96.36	96.20	98.43	98.817	Total	91.14	100.95		
Ba	11	14	6		27	29	Ba	20	11	31.04	25.55
Ce							Ce		34	2.62	7.23
Co	44	49	76	91	44	57	Co	56	28	50.17	11.93
Cr	59	72	218	252	53	71	Cr	84	0	182.96	151.65
La							La		16	1.51	3.75
Nb	4	3	2	5	4	4	Nb	16	10	6.07	4.62
Ni	7	14	54	60	11	22	Ni	42	0	58.70	56.40
Rb						1	Rb		7	2.61	5.38
Sc	48	56	90	107	52	56	Sc	47	84	60.47	19.66
Sr	103	137	125	28	89	136	Sr	237	238	192.65	94.78
V	392	421	1110	1352	427	438	V	481	390	461.83	217.01
Y	30	34	11	15	23	30	Y	40	66	29.91	10.69
Zr	64	72	18	21	42	53	Zr	154	335	83.52	64.47

UM Suite	TD19	TD21	TD22	TD25	UM1	UM8	UM11	KT 2	KT 3	KT 3D	KT 8
Assem. 1											
SiO2	45.96	39.14	47.58	44.99	40.52	39.16	50.94	46.00	54.02	58.32	45.84
TiO2	0.41	0.02	0.11	0.33	0.08	0.16	0.26	0.25	0.13	0.15	0.09
Al2O3	11.35	17.07	3.61	12.72	1.88	2.79	3.09	2.75	1.08	1.17	3.79
Fe2O3	8.94	9.28	8.26	7.58	5.66	11.05	5.47	7.97	7.38	8.28	7.94
MnO	0.14	0.08	0.20	0.11	0.20	0.13	0.14	0.10	0.12	0.13	0.13
MgO	15.51	16.41	17.83	14.21	24.25	20.55	21.64	22.38	23.32	25.63	23.47
CaO	11.80	4.41	13.24	11.08	13.50	14.39	13.25	7.24	6.34	6.89	6.49
Na2O	1.26	0.41	0.25	1.17	0.06	0.15	0.08	0.04	0.07	0.11	0.06
K2O	0.19	1.21	0.07	0.52	0.02	0.03	0.05				
P2O5	0.06	0.03	0.03	0.03	0.03	0.03	0.04				
LOI					14.70	11.33	4.95	4.37	3.52	3.52	16.94
Total	95.61	88.06	91.18	92.74	100.89	99.76	99.90	91.10	95.99	104.19	104.75
Ba	15	18		86			4			1	
Ce											
Co	57	80	97	46	65	148	56	39	22	56	52
Cr	1133	12	488	834	2038	4851	3320	5208	2966	3199	2284
La								1	7		
Nb	4	1	2	3	2	4	3	7	5	5	4
Ni	418	308	798	360	947	1339	560	560	679	817	1181
Rb		61		9				14	10	8	9
Sc	52	3	15	56	6	6	44	88	11	75	0
Sr	27	174	21	219	114	79	18	22	16	18	14
V	191	50	85	199	46	78	151	130	58	93	146
Y	11	1	7	8	29	0	6	12	8	7	17
Zr	24			8	1	1	14	11	0	7	6

UM Suite Assem. 2	TD23	UM6	KT 1	UM Suite Assem. 3	TD24	UM3	UM7	UM10	KT 9	KT 14T
SiO2	34.91	52.56	52.54	SiO2	40.40	42.52	37.11	31.71	31.55	31.35
TiO2	0.45	0.08	0.30	TiO2	0.07	0.04	0.06	0.07	0.09	0.07
Al2O3	3.11	2.62	3.64	Al2O3	1.22	0.81	1.91	1.44	1.87	0.55
Fe2O3	16.05	5.45	5.64	Fe2O3	8.79	4.43	6.43	9.15	6.14	6.94
MnO	0.11	0.16	0.12	MnO	0.13	0.09	0.10	0.23	0.17	0.14
MgO	18.55	24.39	18.08	MgO	23.30	26.89	22.01	23.98	22.90	22.97
CaO	11.45	9.86	10.95	CaO	8.01	9.10	15.65	12.69	7.79	12.69
Na2O	0.25	0.06	0.40	Na2O	0.12	0.07	0.18	0.18	0.04	0.13
K2O	0.03	0.02		K2O	0.03	0.02	0.01	0.02		
P2O5	0.03	0.03		P2O5	0.04	0.02	0.04	0.01		
LOI		3.77	3.94	LOI		16.62	17.99	21.49	31.68	
Total	84.93	99.00	95.62	Total	82.11	100.61	101.49	100.97	102.23	74.83
Ba	4			Ba		4				
Ce				Ce						
Co	149	45	50	Co	67	44	77	61	114	71
Cr	1059	847	6010	Cr	5453	1400	1074	5801	3878	4365
La				La						
Nb	3	2	2	Nb	3	2	4	3	6	4
Ni	1283	995	520	Ni	1404	1526	2091	1274	2528	1818
Rb			0	Rb					9	5
Sc	39	3	180	Sc	3			3	0	1125
Sr	74	15	17	Sr	172	145	74	155	86	70
V	160	53	166	V	43	26	18	35	92	22
Y	5	29	8	Y		5	2		6	
Zr	19		13	Zr			6		11	0

UM Suite Assem. 4	UM2	UM4	UM5	UM9	KT 4	KT 4T	UM Suite	Averages N = 26	Standard Deviation
SiO2	42.18	37.35	45.04	37.22	38.03	41.87	SiO2	42.64	6.97
TiO2	0.04	0.07	0.10	0.10	0.05	0.06	TiO2	0.14	0.11
Al2O3	0.39	0.60	2.09	1.34	0.93	1.00	Al2O3	3.35	3.97
Fe2O3	7.66	8.26	7.12	14.88	13.82	14.70	Fe2O3	8.03	3.67
MnO	0.10	0.12	0.07	0.07	0.12	0.13	MnO	0.89	2.70
MgO	29.71	29.42	26.07	31.63	30.33	33.01	MgO	21.97	7.65
CaO	4.85	7.03	7.57	0.12	1.67	1.62	CaO	8.07	4.80
Na2O	0.13	0.18	0.13	0.27	0.04	0.08	Na2O	0.21	0.30
K2O	0.02	0.02	0.02	0.02			K2O	0.37	1.02
P2O5	0.04	0.03	0.03	0.03		0.01	P2O5	7.23	25.48
LOI	14.47	17.23	11.72	11.19	11.01	11.01	LOI	9.61	8.40
Total	99.57	100.31	99.96	96.86	96.01	103.48	Total		
Ba	4				11		Ba	9	20
Ce							Ce	254	1140
Co	81	94	78	161	147	145	Co	76	43
Cr	874	1651	1864	5918	1886	2046	Cr	2408	1825
La					8		La	57	208
Nb	7	1	4	3	17	1	Nb	4	3
Ni	2375	1908	2244	3388	2164	2228	Ni	1283	878
Rb					27	12	Rb	7	13
Sc		1	1	6	1471	0	Sc	119	339
Sr	85	65	36		28	13	Sr	71	59
V	16	38	47	30	44	60	V	70	56
Y	7	2	5		19	8	Y	6	7
Zr	1				32	7	Zr	5	8

MD Suite	TD4	TD6	TD7	TD10	TD18	TD33	TD43	TD48
SiO2	51.48	47.83	51.39	42.62	47.83	51.23	45.87	46.55
TiO2	0.64	1.25	1.27	3.52	0.11	1.47	1.59	2.85
Al2O3	13.74	13.70	14.70	13.54	12.65	14.81	13.52	14.32
Fe2O3	12.11	12.55	13.34	15.91	11.55	14.34	14.91	13.35
MnO	0.19	0.29	0.23	0.30	0.22	0.21	0.22	0.19
MgO	6.38	9.13	6.24	3.30	6.28	4.74	6.99	8.50
CaO	6.41	7.68	6.81	6.99	8.44	8.33	8.74	8.52
Na2O	4.73	3.55	3.47	4.31	2.68	2.58	1.97	2.23
K2O	0.19	0.36	0.95	0.15	1.00	0.25	0.01	0.48
P2O5	0.07	0.14	0.15	1.16	0.18	0.15	0.18	0.08
LOI	0.77	0.85	0.57				4.04	1.81
Total	96.70	97.32	99.12	91.79	90.93	98.11	98.04	98.87
Ba	48	90	528	230	205	85	14	84
Ce							6	11
Co	45	55	49	33	42	46	95	54
Cr	102	294	103	14	170	104	0	207
La							5	3
Nb	2	4	5	39	7	3	8	7
Ni	25	64	44	12	53	28	71	116
Rb	1	4	27	3	32		11	13
Sc	55	62	57	27	55	55	0	21
Sr	107	111	138	277	206	187	97	345
V	355	362	362	132	491	463	433	379
Y	15	36	33	71	45	38	35	34
Zr	19	79	87	397	97	79	68	127

MD Suite	TD50	TD51	TD52	TD55	TD55D	Averages N=13	Standard Deviation
SiO2	56.04	48.01	48.88	52.88	56.06	49.74	3.63
TiO2	1.01	2.58	1.82	2.19	2.33	1.74	0.87
Al2O3	13.03	14.52	13.90	14.22	13.26	13.84	0.61
Fe2O3	19.19	17.64	14.04	10.29	10.63	13.83	2.42
MnO	0.32	0.23	0.20	0.11	0.12	0.22	0.06
MgO	4.78	7.50	7.08	5.12	5.31	6.26	1.50
CaO	8.09	7.65	8.41	9.47	9.59	8.09	0.89
Na2O	1.39	2.26	2.35	0.63	0.64	2.52	1.16
K2O	0.10	1.11	0.49	2.61	2.61	0.79	0.82
P2O5	0.07	0.25	0.29	1.38	1.37	0.42	0.47
LOI	3.35	0.82	13.13	13.92	1.74	3.15	4.42
Total	107.36	102.56	110.59	112.82	103.65		
Ba	18	79	110	848	834	244.08	274.83
Ce	18	12	11	228	225	39.33	77.02
Co	19	66	52	33	23	47.08	18.10
Cr	174	0	190	0	0	104.46	90.53
La	10	5	4	102	98	17.45	34.02
Nb	7	5	6	19	19	10.02	9.44
Ni	83	131	88	99	91	69.62	33.56
Rb	9	26	19	82	81	23.68	25.60
Sc	23	551	29	157	62	88.77	133.19
Sr	92	210	269	782	796	278.23	221.86
V	308	354	273	239	164	331.92	99.50
Y	31	40	32	49	49	39.08	12.06
Zr	88	158	97	415	406	162.85	131.64

FD Suite	TD1	TD8	TD13	TD53	TD53T	Averages N=5	Standard Deviation	MS Suite TD5	CS Suite KT 18c
SiO2	70.43	48.31	72.79	62.35	65.04	63.78	8.58	63.58	34.20
TiO2	0.34	1.21	0.26	0.58	0.65	0.61	0.33	0.21	0.27
Al2O3	11.67	14.31	11.84	16.29	17.18	14.26	2.25	7.54	20.16
Fe2O3	6.13	12.70	3.57	4.40	5.07	6.37	3.27	2.25	13.43
MnO	0.06	0.24	0.05	0.06	0.06	0.09	0.07	0.02	0.12
MgO	1.76	5.18	1.60	1.92	2.06	2.50	1.35	0.22	21.55
CaO	1.68	6.85	0.20	4.54	5.16	3.69	2.41	0.97	1.17
Na2O	6.32	5.98	1.12	4.05	4.35	4.36	1.85	7.78	1.11
K2O	0.43	0.13	2.88	1.64	1.84	1.39	1.00	0.06	0.04
P2O5	0.07	0.14	0.08	0.08	0.16	0.11	0.04	0.08	
LOI	0.26	5.77		1.23	1.23	2.12	2.14	0.88	
Total	99.16	100.82	94.40	97.13	102.79			83.58	92.05
Ba	156	10	523	309	347	269.00	174.38	6	2
Ce				25	33	29.19	4.22	3	67
Co	6	42	6	0	0	10.80	15.83	14	1361
Cr	12	111	14	0	0	27.40	42.21		4
La				14	15	14.86	0.47	6	6
Nb	6	3	7	9	13	7.62	3.43		1141
Ni		30	16	0	0	11.50	12.52		11
Rb	12	1	77	24	31	29.00	26.10	14	342
Sc	16	54	15	0	24	21.80	17.87	14	23
Sr	60	113	82	261	285	160.20	93.93	20	224
V	25	377	69	50	77	119.60	129.94	31	11
Y	23	27	43	8	13	22.84	12.12	132	15
Zr	121	54	184	187	207	150.60	56.27		

Vita Auctoris

NAME: Michael John Harris

PLACE OF BIRTH: Windsor, Ontario, Canada

YEAR OF BIRTH: 1968

EDUCATION: Riverside Secondary School, Windsor
1982 - 1987

University of Windsor, Windsor
1987 - 1991, B.Sc. Honours Geology
1991 - 1994, M.Sc. Geology